ISSN 2186-3644 Online ISSN 2186-361X

IRDR

Intractable & Rare Diseases Research

Volume 9, Number 1
February, 2020

IRCA BSSA

IACMHR

www.irdrjournal.com

IRDR
Intractable & Rare Diseases Research

ISSN: 2186-3644
Online ISSN: 2186-361X
CODEN: IRDRA3
Issues/Year: 4
Language: English
Publisher: IACMHR Co., Ltd.

Intractable & Rare Diseases Research is one of a series of peer-reviewed journals of the International Research and Cooperation Association for Bio & Socio-Sciences Advancement (IRCA-BSSA) Group and is published quarterly by the International Advancement Center for Medicine & Health Research Co., Ltd. (IACMHR Co., Ltd.) and supported by the IRCA-BSSA, Shandong Academy of Medical Sciences, and Shandong Rare Disease Association.

Intractable & Rare Diseases Research devotes to publishing the latest and most significant research in intractable and rare diseases. Articles cover all aspects of intractable and rare diseases research such as molecular biology, genetics, clinical diagnosis, prevention and treatment, epidemiology, health economics, health management, medical care system, and social science in order to encourage cooperation and exchange among scientists and clinical researchers.

Intractable & Rare Diseases Research publishes Original Articles, Brief Reports, Reviews, Policy Forum articles, Case Reports, News, and Letters on all aspects of the field of intractable and rare diseases research. All contributions should seek to promote international collaboration.

IRCA-BSSA Group Journals

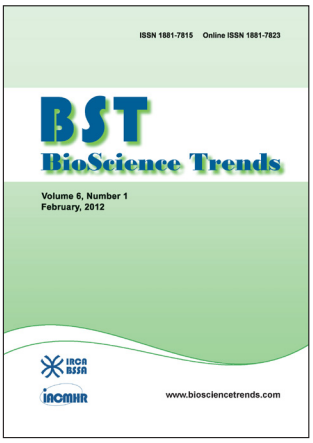

ISSN: 1881-7815
Online ISSN: 1881-7823
CODEN: BTIRCZ
Issues/Year: 6
Language: English
Publisher: IACMHR Co., Ltd.
www.biosciencetrends.com

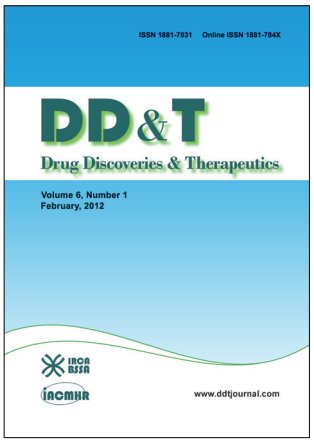

ISSN: 1881-7831
Online ISSN: 1881-784X
CODEN: DDTRBX
Issues/Year: 6
Language: English
Publisher: IACMHR Co., Ltd.
www.ddtjournal.com

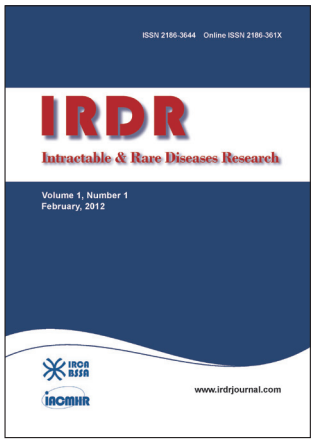

ISSN: 2186-3644
Online ISSN: 2186-361X
CODEN: IRDRA3
Issues/Year: 4
Language: English
Publisher: IACMHR Co., Ltd.
www.irdrjournal.com

Intractable & Rare Diseases Research

Editorial and Head Office

Pearl City Koishikawa 603, 2-4-5 Kasuga, Bunkyo-ku,
Tokyo 112-0003, Japan

Tel: +81-3-5840-9968, Fax: +81-3-5840-9969
E-mail: office@irdrjournal.com
URL: www.irdrjournal.com

Editorial Board

Review

Original Article

Brief Report

Case Report

Communication

Letter

Review

DOI: 10.5582/irdr.2020.01011

A basic understanding of mucopolysaccharidosis: Incidence, clinical features, diagnosis, and management

Jing Zhou[1,2,3,§], Jing Lin[1,2,3,§], Wing Ting Leung[1,2,3], Ling Wang[1,2,3,*]

[1] Laboratory for Reproductive Immunology, Hospital & Institute of Obstetrics and Gynecology, Shanghai Medical College, Fudan University, Shanghai, China;
[2] The Academy of Integrative Medicine of Fudan University, Shanghai, China;
[3] Shanghai Key Laboratory of Female Reproductive Endocrine-related Diseases, Shanghai, China.

SUMMARY Mucopolysaccharidoses (MPS) are a group of rare lysosomal storage diseases (LSD) with multi-organic and severe symptoms. MPS occur worldwide in various forms though have relative a low incidence. The prevalent type of MPS varies among different continents, indicating that it may be associated with region and ethnic background. Undegraded glycosaminoglycans (GAGs) induced by deficiency of enzymes are the primary cause of MPS. Clinical features differ depending on the specific enzyme deficiency including coarse facial features, cognitive retardation, hepatosplenomegaly, hernias, kyphoscoliosis, corneal clouding, *etc.* Symptoms of different types are usually similar especially MPS I and II, but may have distinguishable features such as severe neurological problems in MPS III and hydrops fetails in MPS VII. These clinical features contribute to diagnosis, but early and precisely diagnosis in the asymptomatic stage is imperative for better outcomes. Novel approaches including urinary and blood GAG test, enzyme assay and gene test help to diagnose MPS and to determine its subtype. Hematopoietic stem cell transplantation (HSCT) and enzyme replacement therapy (ERT) are conventional treatment for MPS, but are not effective at treating all MPS. Newer threatments, such as advanced ERT, gene therapy and substrate reduction therapy (SRT), improve therpeutic efficacy. In this review, we update information on the clinical manifestations, diagnosis, and treatment of the different forms of this disease in the hopes of stimulating further interest in MPS.

Keywords mucopolysaccharidosis, symptom, diagnosis, treatment

1. Introduction

Mucopolysaccharidoses (MPS) are a group of rare lysosomal storage diseases (LSD) caused by genetic defects. These genetic defects lead to a lack or deficiency of enzymes involved in degradation of glycosaminoglycans (GAGs) (*1*), which are long and unbranched polysaccharides functioning in processes such as cell adhesion and cellular signaling (*2*). Undegraded GAGs are considered to be the primary and direct cause of MPS, and GAG storage can lead to secondary and tertiary effects in cells, such as autophagy, apoptosis, and mitochondrial dysfunction (*1*). GAGs can accumulate in the lysosomes of cells, resulting in the dysfunction of affected tissues and causing multi-organic and severe symptoms including coarse facial features, cognitive retardation, hepatosplenomegaly, hernias, kyphoscoliosis, corneal clouding. (*3,4*).

Early diagnosis of MPS in the asymptomatic stage may be effective at preserving organic function and improving outcomes. However, delayed diagnosis is common because of insidious onset and limitations of sensitive laboratory indices (*5*). The goal of current MPS treatment is to mitigate the progression of MPS and improve quality of life.

Enzyme replacement therapy (ERT) and hematopoietic stem cell transplantation (HSCT) are two primary methods of managing MPS, but they are not sufficient to solve all of the problems with MPS (*6*). Thus, exploring new diagnostic methods and treatments based on the molecular mechanisms and pathological changes underlying MPS is imperative. The goal of this review is to update information on the clinical manifestations, diagnosis, and treatment of the different forms of this disease in the hopes of stimulating further interest in MPS.

2. Epidemiology

As a rare set of conditions, MPS account for less than

0.1% of all genetic diseases (*1*). The first reported case of MPS was described by Charles Hunter in 1917 (*7*). Two years later, MPS I was described by Hurler (*8*). MPS have a low incidence but have been reported throughout the world in various forms. Region and ethnic background may affect the phenotype of MPS. Analyzing the incidence of MPS and its types among people in different regions would help to better understand MPS.

In Asia, most patients with MPS have MPS II. In a study conducted from 1984 to 2012 in China, 506 patients with MPS were identified. MPS II accounted for nearly 50% of all cases of MPS, MPS I accounted for approximately 13.7%, MPS III accounted for 7.9%, MPS IV accounted for 24%, and MPS VI accounted for 2.6% (*9,10*). In South Korea, a total of 147 cases of MPS were reported between 1994 and 2013. MPS II was the most prevalent type of MPS (54.6%), followed by MPS III (18.4%), MPS I (15.3%), MPS IV (9.5%), and MPS VI (1.4%) (*11*). A study in Japan from 2003 to 2009 indicated that MPS II accounted for 58.1% of cases, while MPS I accounted for 16.2%, MPS III accounted for 11.1%, MPS IV accounted for 11.7%, and MPS VI accounted for 2.9% (*12*). A similar trend was also noted in the 1980s and 1990s in Japan.

MPS II is reported to have a relatively high incidence in some countries, but in Europe its incidence was lower than that of MPS I and MPS III. Data from Denmark and Norway from the 1970s to 2000s indicated that MPS I (30% in Denmark and 60% in Norway) was the most common type of MPS in both countries, followed by MPS IV (27% in Denmark and 24% in Norway) (*13*). In Germany, data on 474 patients with MPS from 1980-1995 indicated that the incidence of MPS III was 44%. The incidence of MPS I was 20%, that of MPS II was 18%, that of MPS IV was 11%, and that of MPS VI was 7%. A similar trend was noted in the Netherlands, where MPS I accounted for 25% of 331 cases of MPS, MPS II accounted for 15.5%, MPS III accounted for 47%, MPS IV accounted for 8%, and MPS VI accounted for 2% (*14*). Elsewhere in Europe, an Estonian study from 1985 to 2006 involving 15 cases of MPS reported no cases of MPS I and MPS VI (*15*). MPS II accounted for 53% of the 15 cases, MPS III accounted for 40%, and MPSIV accounted for 7%.

The incidence of MPS cannot be readily determined in the US. An American study from 1995-2005 indicated that MPS I accounted for 28.3% of cases, MPS II accounted for 24.2%, MPS III accounted for 31.7%, MPS IV accounted for 7.5%, and MPS VI accounted for 4.2% (*12*). In Canada, MPS I accounted for most (30%) of 20 cases from 1969-1996, followed by MPS IV (20%), MPS VI (15%), MPS III (15%), and MPS II (5%) (*16*).

The incidence of different types of MPS differs depending of the continent, indicating that MPS may be related to region and ethnic background. In Asia, MPS II was the most prevalent type of MPS. In Europe, MPS I and MPS III were slightly more prevalent than MPS II. Statistical studies of MPS in the US have not revealed which types are predominant, and further studies may need to be conducted to reveal trends in MPS. Some of the aforementioned data were from a specific area in a country, and different diagnostic methods were used. Given these limitations, a population-based and unified study of MPS needs to be conducted to help analyze its epidemiology and understand its pathology.

3. Clinical features

MPS are differentiated biochemically by their associated enzyme deficiency and can be classified into 7 types, designated MPS I to MPS IX (excluding MPS V and MPS VIII), and some types are further categorized into subtypes. In total, MPS are classified into 11 types and subtypes. The clinical symptoms of MPS differ depending on the specific enzyme deficiency, but major clinical features are mainly neurological symptoms, facial dysmorphism, cardiac and valvular diseases, skeletal dysfunction, respiratory problems, and ocular disorders (Table 1).

3.1. MPS I (Hurler syndrome)

Patients with MPS I have a deficiency of α-L-iduronidase (IDUA), an enzyme involved in the degradation of heparan sulphate (HS) and dermatan sulphate (DS). The accumulation of these GAGs in lysosomes triggers a cascade of cellular events and ultimately leads to organ dysfunction. MPS I is classified into three subtypes: Hurler syndrome (IH), Hurler/Scheie syndrome (IH/S), and Scheie syndrome (IS). Clinical differences between the three syndromes are not easily identified, and this is especially true for IH/S and IS. Clinically, MPS I is a continuum of phenotypes from severe (IH) to intermediate (IH/S) and milder (IS).

MPS I is a life-threatening disease that results in a severe disease burden and premature death. Striking clinical features are neurodegeneration, respiratory deterioration, cardiac diseases, and skeletal and joint disorders. Other common symptoms include ocular problems, organomegaly, deformative facies, and hearing and visual deficits (*17*). In severe cases, GAG storage usually involves the brain and bone, causing progressive neurological disease (cognitive disorders, dyslexia, thermanesthesia, *etc.*) and skeletal diseases (kyphoscoliosis, dysostosis multiplex, *etc.*) (*18*). The symptoms of IH may start in the first year of life with severe and multisystem symptoms. Without effective treatment, patients with IH may die in the first decade of life. Patients with milder symptoms can reach adulthood but also suffer multisystem syndromes.

Table 1. Classification of mucopolysaccharidosis (MPS)

Items	Subtypes	Deficient enzyme	Mutation of Gene	Locus	GAGs	Clinical features
MPS I	Hurler Syndrome	α-L-iduronidase	*IDUA*	4p16,3	HS, DS	Severe. Skeletal deformation, coarse facial features, hepatosplenomegaly, cardiac diseases, respiratory diseases, cognitive retardation, ocular disorders
	Hurler/Scheie Syndrome	α-L-iduronidase	*IDUA*	4p16,3	HS, DS	Intermediate.
	Scheie Syndrome	α-L-iduronidase	*IDUA*	4p16,3	HS, DS	Mild.
MPS II		iduronate-2-sulfatase	*IDS*	Xq28	HS, DS	Skeletal deformation, coarse facial features, hepatosplenomegaly, cardiac diseases, respiratory diseases, cognitive retardation, ocular disorders
MPS III	A	heparan-N-sulfatase	*SGSH*	17q25,3	HS	Cognitive retardation, behavioral problems
	B	α-N-acetyglucosaminidase	*NAGLU*	17q21.2	HS	
	C	α-glucosaminidase acetyltransferase	*HGSNAT*	8p11.21-p11.1	HS	
	D	N-acetylglucosamin-6-sulfatase	*GNS*	12q14,3	HS	
MPS IV	A	N-acetylgalactosamine-6-sulfate sulfatase	*GALNS*	16q24,3	KS, C6S	Skeletal deformation, corneal clouding,
	B	β-galactosidase	*GLB1*	3p22,3	KS	
MPS VI		N-acetylgalactosamine-4-sulfatse	*ARSB*	5q13-14	DS, C4S	Skeletal deformation, coarse facial features, may have normal intelligence
MPS VII		β-glucuronidase	*GUSB*	7q11,21	DS, HS, C4S, C6S	Hydrops fetalis
MPS IX		Hyaluronidase 1	*HYAL1*	3p21,3	HA	Periarticular masses, mild short stature

GAGs: glycosaminoglycans, HS: heparan sulfate, DS: dermatan sulfate, KS: keratan sulfate, C4S: chondroitin-4-sulfate, C6S: chondroitin-6-sulfate, HA: hyaluronic acid

Patients with IS have a more attenuated disease burden and longer lifespan than those with IH/S (*19*).

3.2. MPS II (Hunter syndrome)

MPS II, or Hunter syndrome, is characterized by a deficiency of a lysosomal enzyme, iduronate-2-sulfatase (I2S), that results in the deposition of HS and DS in lysosomes (*20*). MPS II is the only type of MPS that is X-linked recessive while the other types are autosomal recessive diseases. MPS II primarily affects males, though a small number of females are affected because of autosomal X-chromosomal translocation and nonrandom X-chromosome inactivation (*21*). MPS II can be subdivided into two types according to its phenotype, MPS IIA (severe) and MPS IIB (moderate).

MPS IIA has a higher incidence than MPS IIB. Its clinical features are similar to those of MPS I, including short stature, coarse face, inguinal and umbilical hernias, thickening of tissues, valvular disease, and hepatosplenomegaly (*22*). Patients with the severe form, similar to MPS I-IH, rapidly present with symptoms and tend to die in the first decade of life. Patients with the moderate form, similar to MPS I-IH/S and IS, have a longer life span and slower progression of somatic deterioration. Usually, patients have an average of life span of one or two decades, and only patients with milder forms can survive into adulthood. Neurological degeneration varies between the severe and mild forms. Patients with MPS IIA present with progressive central nervous symptoms such as a cognitive disorder, hyperactivity, and aggressiveness (*23*), while those with MPS IIB may have normal neural development.

3.3. MPS III (Sanfilippo syndrome)

MPS III is categorized into four subtypes, MPS

IIIA, IIIB, IIIC, and IIID, that are characterized by a lack of heparan-N-sulfatase (SGHS), α-N-acetylglucosaminidase (NAGLU), α-glucosaminidase acetyltransferase (HGSNAT), and N-acetylglucosamine 6-sulfatase (GNS), respectively. All of these lysosomal enzymes are involved in the degradation of HS, and any deficiency leads to HS storage. MPS IIIA and IIIB are more common than IIIC and IIID in clinical settings. Clinical features vary among the different subtypes. Progressive symptoms of central nervous system dysfunction including idiopathic developmental delay, cognitive decline, hyperactivity, and sleep disorder are prominent characteristics of MPS III. Somatic symptoms are also present in MPS III but are more subtle than in other types and are heterogeneous among patients (*24,25*).

The development of MPS III consists of three phases after a pre-symptomatic phase with normal development (*26*). The first phase starts at 1-3 years of age (may occur later in patients with mild phenotypes) with slowing or halted cognitive deterioration. Speech deterioration is usually noticeable and accompanied by behavioral problems. Physical development may be normal in the first stage (*27*).

The second phase is characterized by progressive cognitive decline, sleep disturbance, and obvious behavioral problems. Behavioral problems including aggressive behavior result from hyperactivity, anxious behavior, and autistic-like behavior. This phase occurs at the age of 3-4, while patients with the mild phenotype may have a gradual progression and longer survival.

The third phase usually starts in the teenage years and involves a decline in motor function and lack of behavioral problems due to a loss of locomotion. During this stage, severe dementia, spasticity, and swallowing difficulties start to manifest and may eventually result in patients becoming bedridden or entering a vegetative state (*28*).

3.4. MPS IV (Morquio syndrome)

MPS IV is subdivided into MPS IVA and MPS IVB depending on a deficiency in N-acetylgalactosamine-6-sulfate sulfatase (GALNS) or β-galactosidase (GLB1). A deficiency in GALNS in MPS IVA impairs the degradation of chondroitin-6-sulfate (C6S) and keratan sulfate (KS), which contributes to severe clinical symptoms. A GLB1 deficiency in MPS IVB leads to a moderate phenotype with only accumulation of KS. Unlike the other types, MPS IV involves mild cognitive impairment but more obvious systemic skeletal dysplasia. MPS IV usually starts at the age of 1-3 with skeletal dysmorphia including growth retardation, a short neck, cervical spinal cord compression, odontoid hypoplasia, hypermobile joints, pectus carinatum, and an abnormal gait (*29,30*). Other common features are corneal clouding, hearing loss, respiratory obstruction, and sleep apnea (*31,32*).

3.5. MPS VI (Maroteaux-Lamy syndrome)

MPS VI is characterized by a deficiency of N-acetylgalactosamine-4-sulfatse that results in the storage of DS and chondroitin-4-sulfate (C4S). The accumulation of GAGs in organs and tissues also leads to multisystem clinical symptoms and progressive deterioration with age. Clinical features, the age of onset, and the rate of progression vary among patients with MPS VI but are generally distributed into slowly and rapidly progressing phenotypes (*33*).

The slowly progressing phenotypes develop slowly and have attenuated symptoms but require surgical intervention and may result in a severe morbidity (*34*). Bones and joints are commonly affected, and skeletal malformation is also a noticeable feature in MPS VI. Relevant skeletal diseases include dysostosis multiplex, scoliosis, joint stiffness, joint contractures, pectus carinatum, and spinal cord compression. Other somatic features are coarse facies, an enlarged tongue, teeth abnormalities, hirsutism, corneal clouding, umbilical hernia, and hepatomegaly (*35,36*). Patients with MPS VI usually have a low quality of life and die before the second decade of life because of cardiac and valvular diseases, pulmonary infection, or restrictive lung diseases (*37,38*). Mental retardation used to be considered unrelated to MPS VI, but central nervous pathological manifestation including communicating hydrocephalus, cerebral atrophy, and a low IQ have been found in patients with MPS VI (*39,40*).

3.6. MPS VII (Sly syndrome)

MPS VII is a rare type of MPS. The pathology of MPS VII is a lack of the β-D-glucuronidase enzyme that causes an accumulation of DS, HS, C4S, and C6S in tissues. MPS VII has a phenotypic heterogeneity and multiple systematic clinical features including a short stature, coarse facial features, corneal clouding, hydrocephalus, skeletal deformation, and cardiac diseases, resembling MPS I and II. However, hydrops fetalis, an abnormal accumulation of body fluids in several tissues, is a distinguishing feature of MPS VII (*41*). The time of onset ranges from infancy to childhood, but few patients survive into adulthood. Most fetuses with hydrops fetalis are stillborn or die shortly after birth. Others may begin to display clinical symptoms during early childhood and have a short life expectancy (*41,42*). Heart disease and airway obstruction are major causes of death in people with MPS VII (*42*).

3.7. MPS IX (Natowicz syndrome)

MPS IX is an extremely rare type of MPS caused by

a deficiency in the lysosomal enzyme hyaluronidase, resulting in the accumulation of hyaluronan. Hyaluronan is a high-molecular-weight polymer that modulates cell proliferation, migration, and differentiation, that regulates extracellular water and protein homeostasis, that is involved in cartilage composition, and that acts as a lubricant in joints (*43-45*). The first patient with MPS IX was described in 1996 with periarticular soft-tissue masses and nodular hyperplasia, a short stature, and acetabular erosions (*46*). In 2011, Imundo *et al.* described 3 siblings of Middle Eastern descent presenting with a phenotype limited to the joints that was evident as juvenile idiopathic arthritis (*47*). Skeletal and joint manifestations are common in MPS IX in accordance with the biological function of hyaluronan. Other symptoms may include a short stature, cysts, frequent ear infections, and a cleft palate (*12*).

4. Diagnosis

MPS is an inherited progressive LSD with early onset ranging from the fetal period to adolescence. Patients with MPS often have a low quality of life and short life expectancy and require timely treatment. However, the diagnosis of MPS is usually delayed until irreversible clinical features manifest (*48*). Thus, reliable and pre-symptomatic diagnosis is imperative to improving outcomes for patients with MPS.

Careful attention should be paid to the medical history of patients and their families because MPS are autosomal recessive inherited diseases except for MPS II, which is linked to a recessive X chromosome. Close attention to the same clinical symptoms in other family members could help to diagnose MPS. Clinical signs are important evidence for diagnosing MPS and distinguishing MPS phenotypes (Table 2). The age of onset, a chronological order of symptoms, the rate of progression, and complications are essential information leading to a diagnosis (*49*).

Radiographic findings including X-rays and computed tomography (CT) and magnetic resonance imaging (MRI) are frequently used diagnostic methods. Kyphosis often appears as the first sign of MPS, and of MPS IVA in particular (*50*). It can be detected in the lumbar vertebral bodies on X-rays (*32*). Patients, and especially those with MPS I, II, or III, often have central nervous symptoms that may be evident on brain CT or MRI. Sight, hearing, the oral cavity, and the respiratory system also need to be examined to assess somatic symptoms (*3,21*).

A definitive diagnosis relies on molecular tests, such as identification of the type of GAG, and genetic testing should be performed. Due to deficiencies in specific lysosomal enzymes, GAGs accumulate in various tissues and are partially eliminated in urine. Determining the type of GAG in urine can help to distinguish the enzyme that is deficient. However, diagnosis of MPS is often delayed since the majority of patients appear normal in the early stages and since their total GAG levels in urine may be normal and thus yield a false negative (*51*). Therefore, newborn screening and sensitive new biochemical markers for MPS are needed to diagnose MPS in a timely and precise manner. The genotype is correlated with the phenotype and can be used to predict the incidence and type of MPS. An enzyme assay and genetic testing of prenatal samples can be accomplished by testing chorionic villi, amniocytes, *etc.* Enzymes can also be determined in fibroblasts, leukocytes, and plasma. If there are initial suspicions based on medical history and clinical features, then screening and subsequent confirmatory studies need to be conducted to diagnose MPS and determine its subtype.

5. Treatment

Once a diagnosis of MPS is confirmed, specific treatment should be provided in a timely manner.

Table 2. Recognition of mucopolysaccharidosis (MPS)

Clinical features	MPS I	MPS II	MPS III	MPS IV	MPS VI	MPS VII	MPS IX
Coarse facial features	+	+	-/+	-/+	+	+	-/?
Cognitive retardation	-/+	-/+	+	-	-/?	+	-
Epilepsy	+	+	+	+	+	-	-
Hepatosplenomegaly	+	+	+	-/+	+	+	-
Valve disease	+	+	+	+	+	+	-
Inguinal and umbilical hernias	+	+	+	+	+	+	-
Corneal clouding	+	+	+	+	+	+	-
Short stature	+	+	-/?	+	+	+	+
Kyphoscoliosis	+	+	+	+	+	+	-
Joints stiffness	+	+	-/?	-	+	+	+
Hearing loss	+	+	+	+	+	+	-/?
Teeth abnormalities	+	+	+	+	+	+	-
Enlarged tongue	+	+	+	+	+	+	-
Hydrops fetalis	-	-	-	-	-	+	-

+: positive; -: negative; -/+: normal or positive; -/?: negative but suspicious in some cases.

Management of MPS means slowing disease progression and improving quality of life. Palliative treatment, surgery, and disease-specific treatments are the main options for patients with MPS. Palliative treatment and surgery are intended to mitigate symptoms to reduce suffering. At present, disease-specific treatments for MPS include HSCT and ERT.

HSCT is based on the assumption that transplanted cells from bone marrow, peripheral blood or umbilical cord blood can penetrate to various tissues and organs and then produce enough of an enzyme to alleviate symptoms (*1*). Since the donor cells continuously secrete enzymes in the body, HSCT is considered to be a permanent treatment. Clinical trials have demonstrated the efficacy of HSCT for MPS I, II, IV, VI, and VII but not for MPS III (*41,52-55*). However, the main limitation of HSCT are the rarity of matching donors and transplant rejection.

ERT directly introduces a functional enzyme into the body to decrease or normalize GAG levels. Like with HSCT, clinical trials of ERT have noted positive results with MPS I, II, IV, VI, and VII (*56-60*). Both HSCT and ERT have proven unsatisfactory in patients with MPS III because MPS III is a special type of MPS that mainly involves central nervous diseases (*25*). Adverse effects of ERT have been reported, and anti-ERT antibodies are observed in most patients (*61*). Moreover, its efficacy is reduced by its low level of blood-brain barrier penetration and inefficient delivery to avascular tissues (*6*). Advanced forms of ERT including intracerebroventricular and intrathecal administration have been explored. Normal GAG storage and neurological improvement were noted in a murine model of MPS with intracerebroventricular administration (*62*). However, indications and the risk of site-specific injections are unsolved challenges, and clinical efficacy is uncertain. Therefore, novel approaches such as gene therapy and substrate reduction therapy (SRT) are important therapeutic options for MPS to improve outcomes.

Gene therapy refers to introducing a therapeutic gene into a patient's cells. This novel therapy is permanent and does not require a matching donor like HSCT or have blood-brain barrier restrictions like ERT. Gene therapy can be *in vivo* or *ex vivo*. *In vivo* gene therapy directly delivers gene products into the body *via* systematic or in situ administration (*63*). *Ex vivo* gene therapy involves modifying a patient's stem cells externally and then infusing them back into the body. Thus, an immune response to a vector or gene products could occur. Although clinical trials are already underway, gene therapy is still in development since its long-term effects are not known (*64*).

SRT seeks to reduce an excess of a substrate, thus slowing GAG synthesis, instead of increasing GAG degradation. Generally, small molecules that inhibit substrate synthesis are administrated orally. These facilitate SRT and penetrate the blood-brain barrier. Genistein, a soy-derived isoflavone, was first identified as a potential drug for SRT; it acts as a tyrosine kinase inhibitor and alleviates neurological manifestations (*65*). However, a sequent clinical trial of SRT failed to find any significant neurological benefit as a result of a decline in urinary GAGs (*66*). Therefore, novel inhibitors of GAG synthesis need to be identified as therapeutic targets. A point worth noting is that the combination of HSCT and ERT has proved to be associated with better outcomes (*67*), indicating that the management of MPS requires combined and multidisciplinary treatment.

6. Conclusion

MPS was first described in 1917; since then, thousands of cases have been reported worldwide. Although MPS are rare inherited diseases of LSD, their high mortality and expensive treatment make them a major medical and social problem. Due to their severe and progressive symptoms, MPS require intensive care for patients and keen awareness among physicians. Recognizing the onset and characteristic features of different subtypes of MPS will facilitate early diagnosis. However, symptoms of different subtypes are often similar and not easily differentiated. Greater emphasis is placed on treating severe and mild forms of MPS. Common clinical features such as a short stature and mental retardation often lead to misdiagnosis. Early diagnosis is imperative to preserve organic functions and improve quality of life.

This review has concisely summarized the characteristic features of different MPS and described diagnostic methods as well as therapeutic options. HSCT and ERT are widely used in clinical practice but are ineffective in some patients with MPS because of unsolved challenges. Novel treatments including intrathecal ERT, gene therapy, and combined therapy have emerged to compensate for the disadvantages of conventional therapies. Guidelines for management of MPS should be drafted in light of the type of MPS, clinical development, disease stage, medical history, and socioeconomic status of the patient in order to standardize the diagnosis and treatment of MPS.

Acknowledgements

This work was supported by the National Natural Science Foundation of China (grant nos. 31571196 and 30801502 to Ling Wang), the 2018 Program to Guide Medicine ("Yixue Yindao") of the Shanghai Municipal Science and Technology Commission (grant no.18401902200 to Ling Wang), the 2015 Program to Guide Medicine ("Yixue Yindao") of the Shanghai Municipal Science and Technology Commission (grant no. 15401932200 to Ling Wang), the Shanghai

Committee of the China Democratic League (grant no. 02054 to Ling Wang), the Shanghai Pujiang Program (grant no. 11PJ1401900 to Ling Wang), the FY2008 JSPS Postdoctoral Fellowship for Foreign Researchers (P08471, Ling Wang), Special Project of the China Resources Sanjiu Medical and Pharmaceutical Co. and the Obstetrics & Gynecology Special Committee, Chinese Association for the Integration of Traditional and Western Medicine (grant no. CR1901FC01 to Ling Wang), the Shanghai Project for Development of Leading Disciplines-Integrative Medicine (grant nos. 20180101 and 20150407).

References

1. Gaffke L, Pierzynowska K, Podlacha M, Brokowska J, Wegrzyn G. Changes in cellular processes occurring in mucopolysaccharidoses as underestimated pathomechanisms of these diseases. Cell Biol Int. 2019. [Epub ahead of print]
2. Quittot N, Sebastiao M, Bourgault S. Modulation of amyloid assembly by glycosaminoglycans: From mechanism to biological significance. Biochem Cell Biol. 2017; 95:329-337.
3. Del Longo A, Piozzi E, Schweizer F. Ocular features in mucopolysaccharidosis: diagnosis and treatment. Ital J Pediatr. 2018; 44:125.
4. Barone R, Pellico A, Pittala A, Gasperini S. Neurobehavioral phenotypes of neuronopathic mucopolysaccharidoses. Ital J Pediatr. 2018; 44:121.
5. Suarez-Guerrero JL, Gomez Higuera PJ, Arias Florez JS, Contreras-Garcia GA. Mucopolysaccharidosis: Clinical features, diagnosis and management. Rev Chil Pediatr. 2016; 87:295-304.
6. Sawamoto K, Stapleton M, Almeciga-Diaz CJ, Espejo-Mojica AJ, Losada JC, Suarez DA, Tomatsu S. Therapeutic options for mucopolysaccharidoses: Current and emerging treatments. Drugs. 2019; 79:1103-1134.
7. Hunter C. A Rare Disease in Two Brothers. Proc R Soc Med. 1917; 10:104-116.
8. Grupo de Trabajo Enfermedades poco f, Sociedad Argentina de Pediatria Subcomisiones CyGdT. Consensus on mucopolysaccharidosis type I diagnosis and treatment. Arch Argent Pediatr. 2008; 106:361-368.
9. Lin HY, Lin SP, Chuang CK, Niu DM, Chen MR, Tsai FJ, Chao MC, Chiu PC, Lin SJ, Tsai LP, Hwu WL, Lin JL. Incidence of the mucopolysaccharidoses in Taiwan, 1984-2004. Am J Med Genet A. 2009; 149A:960-964.
10. Chen X, Qiu W, Ye J, Han L, Gu X, Zhang H. Demographic characteristics and distribution of lysosomal storage disorder subtypes in Eastern China. J Hum Genet. 2016; 61:345-349.
11. Cho SY, Sohn YB, Jin DK. An overview of Korean patients with mucopolysaccharidosis and collaboration through the Asia Pacific MPS Network. Intractable Rare Dis Res. 2014; 3:79-86.
12. Khan SA, Peracha H, Ballhausen D, Wiesbauer A, Rohrbach M, Gautschi M, Mason RW, Giugliani R, Suzuki Y, Orii KE, Orii T, Tomatsu S. Epidemiology of mucopolysaccharidoses. Mol Genet Metab. 2017; 121:227-240.
13. Malm G, Lund AM, Mansson JE, Heiberg A. Mucopolysaccharidoses in the Scandinavian countries: Incidence and prevalence. Acta Paediatr. 2008; 97:1577-1581.
14. Poorthuis BJ, Wevers RA, Kleijer WJ, Groener JE, de Jong JG, van Weely S, Niezen-Koning KE, van Diggelen OP. The frequency of lysosomal storage diseases in the Netherlands. Hum Genet. 1999; 105:151-156.
15. Krabbi K, Joost K, Zordania R, Talvik I, Rein R, Huijmans JG, Verheijen FV, Ounap K. The live-birth prevalence of mucopolysaccharidoses in Estonia. Genet Test Mol Biomarkers. 2012; 16:846-849.
16. Lowry RB, Applegarth DA, Toone JR, MacDonald E, Thunem NY. An update on the frequency of mucopolysaccharide syndromes in British Columbia. Hum Genet. 1990; 85:389-390.
17. Muenzer J. The mucopolysaccharidoses: A heterogeneous group of disorders with variable pediatric presentations. J Pediatr. 2004; 144:S27-34.
18. Martins AM, Lindstrom K, Kyosen SO, Munoz-Rojas MV, Thibault N, Polgreen LE. Short stature as a presenting symptom of attenuated mucopolysaccharidosis type I: Case report and clinical insights. BMC Endocr Disord. 2018; 18:83.
19. Parini R, Deodato F, Di Rocco M, Lanino E, Locatelli F, Messina C, Rovelli A, Scarpa M. Open issues in mucopolysaccharidosis type I-Hurler. Orphanet J Rare Dis. 2017; 12:112.
20. Yamanishi R, Nakamura N, Tsunoda K. Recovery of vision following enzyme replacement therapy in a patient with mucopolysaccharidosis type II, Hunter syndrome. Case Rep Ophthalmol. 2019; 10:186-194.
21. Guillen-Navarro E, Domingo-Jimenez MR, Alcalde-Martin C, Cancho-Candela R, Couce ML, Galan-Gomez E, Alonso-Luengo O. Clinical manifestations in female carriers of mucopolysaccharidosis type II: A Spanish cross-sectional study. Orphanet J Rare Dis. 2013; 8:92.
22. Chinawa J, Adimora G, Obu H, Tagbo B, Ujunwa F, Onubogu I. Clinical presentation of mucopolysaccharidosis type II (Hunter's syndrome). Ann Med Health Sci Res. 2012; 2:87-90.
23. Wraith JE, Scarpa M, Beck M, Bodamer OA, De Meirleir L, Guffon N, Meldgaard Lund A, Malm G, Van der Ploeg AT, Zeman J. Mucopolysaccharidosis type II (Hunter syndrome): A clinical review and recommendations for treatment in the era of enzyme replacement therapy. Eur J Pediatr. 2008; 167:267-277.
24. Nijmeijer SCM, van den Born LI, Kievit AJA, Stepien KM, Langendonk J, Marchal JP, Roosing S, Wijburg FA, Wagenmakers M. The attenuated end of the phenotypic spectrum in MPS III: from late-onset stable cognitive impairment to a non-neuronopathic phenotype. Orphanet J Rare Dis. 2019; 14:249.
25. Jakobkiewicz-Banecka J, Gabig-Ciminska M, Kloska A, Malinowska M, Piotrowska E, Banecka-Majkutewicz Z, Banecki B, Wegrzyn A, Wegrzyn G. Glycosaminoglycans and mucopolysaccharidosis type III. Front Biosci (Landmark Ed). 2016; 21:1393-1409.
26. Wijburg FA, Wegrzyn G, Burton BK, Tylki-Szymanska A. Mucopolysaccharidosis type III (Sanfilippo syndrome) and misdiagnosis of idiopathic developmental delay, attention deficit/hyperactivity disorder or autism spectrum disorder. Acta Paediatr. 2013; 102:462-470.
27. van de Kamp JJ, Niermeijer MF, von Figura K, Giesberts MA. Genetic heterogeneity and clinical variability in the Sanfilippo syndrome (types A, B, and C). Clin Genet. 1981; 20:152-160.

28. Valstar MJ, Marchal JP, Grootenhuis M, Colland V, Wijburg FA. Cognitive development in patients with mucopolysaccharidosis type III (Sanfilippo syndrome). Orphanet J Rare Dis. 2011; 6:43.
29. Xie J, Pan J, Guo D, Pan W, Li R, Guo C, Du M, Jiang W, Guo Y. Mutation analysis and pathogenicity identification of Mucopolysaccharidosis type IVA in 8 south China families. Gene. 2019; 686:261-269.
30. Khan S, Almeciga-Diaz CJ, Sawamoto K, Mackenzie WG, Theroux MC, Pizarro C, Mason RW, Orii T, Tomatsu S. Mucopolysaccharidosis IVA and glycosaminoglycans. Mol Genet Metab. 2017; 120:78-95.
31. Nagao K, Morlet T, Haley E, Padilla J, Nemith J, Mason RW, Tomatsu S. Neurophysiology of hearing in patients with mucopolysaccharidosis type IV. Mol Genet Metab. 2018; 123:472-478.
32. Tomatsu S, Yasuda E, Patel P, *et al*. Morquio A syndrome: Diagnosis and current and future therapies. Pediatr Endocrinol Rev. 2014; 12 Suppl 1:141-151.
33. Harmatz P, Shediac R. Mucopolysaccharidosis VI: Pathophysiology, diagnosis and treatment. Front Biosci (Landmark Ed). 2017; 22:385-406.
34. Thumler A, Miebach E, Lampe C, Pitz S, Kamin W, Kampmann C, Link B, Mengel E. Clinical characteristics of adults with slowly progressing mucopolysaccharidosis VI: A case series. J Inherit Metab Dis. 2012; 35:1071-1079.
35. Valayannopoulos V, Nicely H, Harmatz P, Turbeville S. Mucopolysaccharidosis VI. Orphanet J Rare Dis. 2010; 5:5.
36. Hendriksz CJ, Giugliani R, Harmatz P, Lampe C, Martins AM, Pastores GM, Steiner RD, Leao Teles E, Valayannopoulos V, Group CSPS. Design, baseline characteristics, and early findings of the MPS VI (mucopolysaccharidosis VI) Clinical Surveillance Program (CSP). J Inherit Metab Dis. 2013; 36:373-384.
37. Lin SP, Shih SC, Chuang CK, Lee KS, Chen MR, Niu DM, Chiu PC, Lin SJ, Lin HY. Characterization of pulmonary function impairments in patients with mucopolysaccharidoses--Changes with age and treatment. Pediatr Pulmonol. 2014; 49:277-284.
38. Lin HY, Chuang CK, Chen MR, Lin SM, Hung CL, Chang CY, Chiu PC, Tsai WH, Niu DM, Tsai FJ, Lin SJ, Hwu WL, Lin JL, Lin SP. Cardiac structure and function and effects of enzyme replacement therapy in patients with mucopolysaccharidoses I, II, IVA and VI. Mol Genet Metab. 2016; 117:431-437.
39. Azevedo AC, Artigalas O, Vedolin L, Komlos M, Pires A, Giugliani R, Schwartz IV. Brain magnetic resonance imaging findings in patients with mucopolysaccharidosis VI. J Inherit Metab Dis. 2013; 36:357-362.
40. Borlot F, Arantes PR, Quaio CR, Franco JF, Lourenco CM, Bertola DR, Kim CA. New insights in mucopolysaccharidosis type VI: Neurological perspective. Brain Dev. 2014; 36:585-592.
41. Montano AM, Lock-Hock N, Steiner RD, *et al.* Clinical course of sly syndrome (mucopolysaccharidosis type VII). J Med Genet. 2016; 53:403-418.
42. Genetics Home Reference, National Institutes of Health. Mucopolysaccharidosis type VII. *https://ghr.nlm.nih.gov/condition/mucopolysaccharidosis-type-vii#* (accessed Feb. 6, 2020)
43. Nathanson MA. Hyaluronates in developing skeletal tissues. Clin Orthop Relat Res. 1990;275-289.
44. Toole BP. Hyaluronan in morphogenesis. Semin Cell Dev Biol. 2001; 12:79-87.
45. Triggs-Raine B, Salo TJ, Zhang H, Wicklow BA, Natowicz MR. Mutations in HYAL1, a member of a tandemly distributed multigene family encoding disparate hyaluronidase activities, cause a newly described lysosomal disorder, mucopolysaccharidosis IX. Proc Natl Acad Sci U S A. 1999; 96:6296-6300.
46. Natowicz MR, Short MP, Wang Y, Dickersin GR, Gebhardt MC, Rosenthal DI, Sims KB, Rosenberg AE. Clinical and biochemical manifestations of hyaluronidase deficiency. N Engl J Med. 1996; 335:1029-1033.
47. Imundo L, Leduc CA, Guha S, Brown M, Perino G, Gushulak L, Triggs-Raine B, Chung WK. A complete deficiency of Hyaluronoglucosaminidase 1 (HYAL1) presenting as familial juvenile idiopathic arthritis. J Inherit Metab Dis. 2011; 34:1013-1022.
48. Brusius-Facchin AC, Rojas Malaga D, Leistner-Segal S, Giugliani R. Recent advances in molecular testing to improve early diagnosis in children with mucopolysaccharidoses. Expert Rev Mol Diagn. 2018; 18:855-866.
49. Colmenares-Bonilla D, Colin-Gonzalez C, Gonzalez-Segoviano A, Esquivel Garcia E, Vela-Huerta MM, Lopez-Gomez FG. Diagnosis of mucopolysaccharidosis based on history and clinical features: Evidence from the Bajio Region of Mexico. Cureus. 2018; 10:e3617.
50. Northover H, Cowie RA, Wraith JE. Mucopolysaccharidosis type IVA (Morquio syndrome): A clinical review. J Inherit Metab Dis. 1996; 19:357-365.
51. Peracha H, Sawamoto K, Averill L, *et al.* Molecular genetics and metabolism, special edition: Diagnosis, diagnosis and prognosis of Mucopolysaccharidosis IVA. Mol Genet Metab. 2018; 125:18-37.
52. Lum SH, Miller WP, Jones S, Poulton K, Ogden W, Lee H, Logan A, Bonney D, Lund TC, Orchard PJ, Wynn RF. Changes in the incidence, patterns and outcomes of graft failure following hematopoietic stem cell transplantation for Hurler syndrome. Bone Marrow Transplant. 2017; 52:846-853.
53. Warkentin PI, Dixon MS, Jr., Schafer I, Strandjord SE, Coccia PF. Bone marrow transplantation in Hunter syndrome: A preliminary report. Birth Defects Orig Artic Ser. 1986; 22:31-39.
54. Chinen Y, Higa T, Tomatsu S, Suzuki Y, Orii T, Hyakuna N. Long-term therapeutic efficacy of allogenic bone marrow transplantation in a patient with mucopolysaccharidosis IVA. Mol Genet Metab Rep. 2014; 1:31-41.
55. Krivit W, Pierpont ME, Ayaz K, Tsai M, Ramsay NK, Kersey JH, Weisdorf S, Sibley R, Snover D, McGovern MM, *et al.* Bone-marrow transplantation in the Maroteaux-Lamy syndrome (mucopolysaccharidosis type VI). Biochemical and clinical status 24 months after transplantation. N Engl J Med. 1984; 311:1606-1611.
56. Kakkis ED, Muenzer J, Tiller GE, Waber L, Belmont J, Passage M, Izykowski B, Phillips J, Doroshow R, Walot I, Hoft R, Neufeld EF. Enzyme-replacement therapy in mucopolysaccharidosis I. N Engl J Med. 2001; 344:182-188.
57. Muenzer J, Beck M, Eng CM, *et al.* Long-term, open-labeled extension study of idursulfase in the treatment of Hunter syndrome. Genet Med. 2011; 13:95-101.
58. Harmatz P, Ketteridge D, Giugliani R, Guffon N, Teles EL, Miranda MC, Yu ZF, Swiedler SJ, Hopwood JJ, Group MVS. Direct comparison of measures of

endurance, mobility, and joint function during enzyme-replacement therapy of mucopolysaccharidosis VI (Maroteaux-Lamy syndrome): Results after 48 weeks in a phase 2 open-label clinical study of recombinant human N-acetylgalactosamine 4-sulfatase. Pediatrics. 2005; 115:e681-689.
59. Fox JE, Volpe L, Bullaro J, Kakkis ED, Sly WS. First human treatment with investigational rhGUS enzyme replacement therapy in an advanced stage MPS VII patient. Mol Genet Metab. 2015; 114:203-208.
60. Hendriksz CJ. Elosulfase alfa (BMN 110) for the treatment of mucopolysaccharidosis IVA (Morquio A syndrome). Expert Rev Clin Pharmacol. 2016; 9:1521-1532.
61. Schweighardt B, Tompkins T, Lau K, Jesaitis L, Qi Y, Musson DG, Farmer P, Haller C, Shaywitz AJ, Yang K, O'Neill CA. Immunogenicity of elosulfase alfa, an enzyme replacement therapy in patients with Morquio A syndrome: Results from MOR-004, a phase III trial. Clin Ther. 2015; 37:1012-1021 e1016.
62. Wolf DA, Lenander AW, Nan Z, Belur LR, Whitley CB, Gupta P, Low WC, McIvor RS. Direct gene transfer to the CNS prevents emergence of neurologic disease in a murine model of mucopolysaccharidosis type I. Neurobiol Dis. 2011; 43:123-133.
63. Penati R, Fumagalli F, Calbi V, Bernardo ME, Aiuti A. Gene therapy for lysosomal storage disorders: Recent advances for metachromatic leukodystrophy and mucopolysaccaridosis I. J Inherit Metab Dis. 2017; 40:543-554.
64. Braun SE, Pan D, Aronovich EL, Jonsson JJ, McIvor RS, Whitley CB. Preclinical studies of lymphocyte gene therapy for mild Hunter syndrome (mucopolysaccharidosis type II). Hum Gene Ther. 1996; 7:283-290.
65. Piotrowska E, Jakobkiewicz-Banecka J, Baranska S, Tylki-Szymanska A, Czartoryska B, Wegrzyn A, Wegrzyn G. Genistein-mediated inhibition of glycosaminoglycan synthesis as a basis for gene expression-targeted isoflavone therapy for mucopolysaccharidoses. Eur J Hum Genet. 2006; 14:846-852.
66. Delgadillo V, O'Callaghan Mdel M, Artuch R, Montero R, Pineda M. Genistein supplementation in patients affected by Sanfilippo disease. J Inherit Metab Dis. 2011; 34:1039-1044.
67. Dubot P, Sabourdy F, Plat G, Jubert C, Cances C, Broue P, Touati G, Levade T. First report of a patient with MPS type VII, due to novel mutations in GUSB, who underwent enzyme replacement and then hematopoietic stem cell transplantation. Internatl J of Molec Sciences. 2019; 20.

Received January 31, 2020; Revised February 7, 2020; Accepted February 10, 2020.

[§]These authors contributed equally to this work.
**Address correspondence to:*
Ling Wang, Obstetrics & Gynecology Hospital of Fudan University, 419 Fangxie Road, Shanghai 200011, China.
E-mail: Dr.wangling@fudan.edu.cn

Released online in J-STAGE as advance publication February 16, 2020.

Mini-Review

DOI: 10.5582/irdr.2019.01130

Advances in stem cell therapy for the treatment of Peyronie's disease

Mohamad Moussa[1], Mohamad Abou Chakra[2,*], Yasmin Moussa[3]

[1] Department of Urology, Zahraa Hospital, University Medical Center, Lebanese University, Beirut, Lebanon;
[2] Department of Urology, Faculty of Medical Sciences, Lebanese University, Beirut, Lebanon;
[3] Clinic of Dermatology, Dr. Brinkmann, Schult & Samimi-Fard, Gladbeck, Germany.

SUMMARY Peyronie's disease (PD) is a connective tissue disorder of the penis characterized by fibrosis and plaque formation within the tunica albuginea. PD is characterized by painful penile curvature that impairs sexual intercourse. Stem cell therapy is one of the recent non-invasive treatment options for patients with PD and it has promising results. Stem cells are undifferentiated cells that are capable of self-renewal and differentiation, promoting the repair of tissues via their immunomodulatory and anti-inflammatory action. Adipose-derived stem cells (ADSC) are used most widely due to their abundant tissue source and ease of isolation. Multiple studies have indicated the efficacy of stem cell therapy as a potential treatment for fibrotic diseases. Clearly, ADSCs may represent a way to treat and prevent PD in both rat and human models. Further clinical studies are needed to confirm the efficacy of stem cell therapy for PD in humans.

Keywords Peyronie's disease, stem cell, adipose stem cells, fibrosis, regeneration

1. Introduction

Peyronie's disease (PD) is an uncommon condition involving middle-aged men. It is caused by an inflammation in the tunica followed by scarring and penile curvature. It is considered to be a fibrotic disorder of the penis that is characterized by the formation of collagen plaques on the tunica albuginea that may cause penile curvature, narrowing, and shortening that subsequently lead to erectile dysfunction (ED) (*1,2*). The prevalence of PD varies because it is usually underreported by men. Schwarzer *et al*. conducted a large survey involving 8,000 men and noted a prevalence of 3.2% (*3*). DiBenedetti *et al*. reported a prevalence of 13% among males ages 18 years and older; this figure includes men diagnosed with, treated for, or who recently reported penile symptoms of PD (*4*).

Patients with PD present early after the onset of the disease (within 6 months) with penile pain and curvature upon erection. PD is characterized by a palpable plaque in the tunica albuginea and is usually associated with ED. It occurs in middle-aged men, most of whom are between 40 and 59 years. Penile curvature is the first symptom of the disease and develops in 94% of patients (*5*). ED is usually present in patients with PD, developing in 30-50% of those patients (*6,7*). Multiple causes can contribute to ED due to PD such as arterial insufficiency, venous insufficiency, a psychologic effect, or geometric variation (*8-11*).

One of the theories helping to explain the pathophysiology of PD is microvascular trauma. This results in edema, inflammation, and fibrin deposition within the tunica albuginea. During the acute phase of PD, transforming growth factor (TGF)-β1 is overexpressed, and this induces fibroblasts to increase collagen synthesis (*12,13*). TGF-β1 can induce its own synthesis and contributes to continuous fibrotic changes (*14*). An autoimmune theory of the pathophysiology of PD was proposed since the serology of patients with PD has detected high titers of anti-elastin antibodies (*15*). PD is associated with Dupuytren's contracture and certain human leukocyte antigen subtypes (*16,17*). Multiple genes such as matrix metalloproteinases (MMP2, MMP9) and osteoblast-specific factor 1 are overexpressed in PD and Dupuytren's contracture (*18,19*).

PD is clinically diagnosed based on a detailed history and a penile examination. Measurement of penile curvature and palpation of plaque are important elements of this examination (*19*). There are 2 phases of PD, acute and chronic. During the acute phase or inflammatory phase, there is penile pain in a flaccid or erect state and palpable plaque; this phase typically

lasts for 12-18 months after onset; this is followed by the chronic phase where pain disappears and penile curvature stabilizes (*20*).

In general, medical treatment is often used during the acute phase of the disease whereas surgery is used during the stable phase (*21*). Non-surgical treatment includes oral or intralesional pharmacotherapy. Oral therapies include vitamin E and paraaminobenzoate, colchicine, tamoxifen, and acetyl-L-carnitine. Intralesional injection therapy includes injection with interferon-alpha-2b, verapamil, or collagenase. Surgery is reserved for patients who do not respond to medical therapy or for men with severe penile curvature that affects sexual intercourse after stabilization of the disease (*21-23*). Surgical procedures are either penile shortening or penile lengthening to correct curvature; the procedure depends on penile length and the degree of curvature (*24*).

Regenerative medicine represents a novel therapy for the treatment of PD using mesenchymal stem cell therapy with both curative and preventive potential. Stem cells are self-renewing cells with a high degree of plasticity that can differentiate into multiple cell lines; they can be used to repair genetically damaged tissue or altered organs (*25*). Stem cells can be derived from embryonic, fetal, and adult tissue. They can be used in tissue engineering to repair a disrupted process (*26*). Many studies have described the use of stem cells to treat urologic conditions such as PD, incontinence, infertility, and ED (*27*).

2. Rationality behind using stem cell therapy to treat PD

Mesenchymal stem cells (MSCs) have immunomodulatory roles. Adipose-derived stem cell (ADSC) are easy to isolate and lack major histocompatibility complex-II expression, and their immunosuppressive action is mediated by prostaglandin E2 (*28*). The mechanism of ADSC therapy is not well known. After their differentiation, they can secrete growth factors promoting angiogenesis. They can act also by modulating the immune response via secretion of galectin-1 and -3, which are essential in T-cell suppression, resulting in downregulation of the inflammatory response. Thus, they promote wound repair and regeneration (*29,30*). In addition, ADSC decrease fibrosis by down-regulating profibrogenic molecules such as COL1A1 and ACTA2, thus regressing the fibrotic process in many diseases such as chronic renal fibrosis (*31*) and lung fibrosis (*32*).

Multipotent stromal cells have demonstrated efficacy in the treatment of ED due to cavernous nerve injury in multiple animal models via cell differentiation and local paracrine action (*33*). In addition, ADSCs injected into the penis of impotent type 2 diabetic rats can improve erectile function through their paracrine effect (*34*).

3. Studies corroborating the use of stem cell therapy to treat PD

In 2013, the first study used ADSCs to treat PD in an animal model; TGF-β1 was used to induce fibrosis within the tunica albuginea of rats. One day after injection of TGF-β1, human ADSCs were administered in a xenogeneic manner. Erectile function significantly improved after ADSC treatment (*35*). This is the first study to use xenogeneic cells that were transplanted into immunocompetent animals without the use of immunosuppressants, and the results were promising. ADSCs are known to have both immunomodulatory

Table1. Animal and human clinical studies corroborating the role of stem cell therapy in the treatment of PD

Study	Year	Stem cells	Studies were undertaken in humans or animals	Outcomes
Levy JA *et al*. (*39*)	2015	Placental matrix-derived mesenchymal stem cells	Humans	Peak systolic velocity and penile curvature improved significantly 6 weeks, 3 months, and 6 months after treatment. Seven of 10 fibrotic plaques in the tunica albuginea disappeared completely at 3 months.
Castiglione *et al*. (*35*)	2013	Human adipose-derived stem cells	Animals	Erectile function improved during the acute phase of PD.
Gokce *et al*. (*37*)	2014	Rat adipose-derived stem cells	Animals	Erectile function improved during the acute and chronic phase of PD.
Gokce *et al*. (*38*)	2015	Genetically modified adipose tissue-derived stem cells with human interferon α-2b	Animals	Erectile function improved during the acute and chronic phase of PD.
Castiglione *et al*. (*36*)	2019	Human adipose-derived stem cells	Animals	Tunica albuginea fibrosis decreased in a rat model of chronic PD.

PD, Peyronie's disease.

and immunosuppressive actions (*28*). In a previous study, ADSCs were injected shortly after TGF-β-induced tissue inflammation (during the acute phase), and this therapy reversed the phase of PD progression.

Another study evaluated the role of ADSC injection in the chronic phase of PD in a rat model (*36*). Rats with PD were injected with human ADSCs 1 month after injection of TGF-β1 (mimicking the chronic phase of PD), and they displayed less fibrosis on histological analysis, decreased expression of collagen III, and decreased expression of several fibrosis-related genes. All of these features are considered to be biochemical fibrotic changes. The same study also found that fibrotic plaques tended to partially regress spontaneously after 60 days. Two previous studies by Gokce *et al*. evaluated the efficacy of allogenic ADSCs and modified ADSCs expressing human interferon α-2b in the prevention and treatment of ED in a rat model of PD (*37,38*). In the first study (*37*), rats received intratunical injections of 0.5 million rat-labeled ADSCs on day 0 (prevention group) or day 30 (treatment group) after injection of TGF-β. Forty five days after treatment, both the prevention and treatment groups had better erections and less fibrosis compared to a group with untreated PD. The second study (*38*) compared the efficacy of modified ADSCs expressing human interferon α-2b and that of unmodified ADSCs using the same design as the previous study. Results indicated that modified ADSCs resulted in better recovery of erectile function.

The first study using placental matrix–derived mesenchymal stem cells (PM-MSC) to manage PD in humans involved a small sample of 5 subjects. Patients with PD with a palpable plaque received intracavernous injections of PM-MSC. Both peak systolic velocity and penile curvature improved significantly 6 weeks, 3 months, and 6 months after injection, but end diastolic velocity did not improve significantly. Seven of the 10 plaques initially evident on ultrasonography disappeared completely at 3 months (*39*). Results of animal and human trials demonstrating the possible efficacy of stem cell therapy in the treatment of PD are shown in Table 1.

4. Conclusion

Multiple studies have demonstrated the efficacy of stem cell therapy for the treatment of PD in humans and animals. Studies involving humans have been limited by their small samples and brief follow-up, but their results were promising. Randomized clinical trials in humans need to be conducted in order to prove the efficacy of stem cell therapy for the treatment of PD.

References

1. Hellstrom WJ. History, epidemiology, and clinical presentation of Peyronie's disease. Int J Impot Res. 2003; 15 Suppl 5:S91-S92.
2. Taylor FL, Levine LA. Peyronie's disease. Urol Clin North Am. 2007; 34:517-534,vi.
3. Schwarzer U, Sommer F, Klotz T, Braun M, Reifenrath B, Engelmann U. The prevalence of Peyronie's disease: Results of a large survey. BJU Int. 2001; 88:727-730.
4. Dibenedetti DB, Nguyen D, Zografos L, Ziemiecki R, Zhou X. A population-based study of Peyronie's disease: Prevalence and treatment patterns in the United States advances in urology. Adv Urol. 2011; 2011:282503.
5. Pryor JP, Ralph DJ. Clinical presentations of Peyronie's disease. Int J Impot Res. 2002; 14:414-417.
6. Deveci S, Palese M, Parker M, Guhring P, Mulhall JP. Erectile function profiles in men with Peyronie's disease. J Urol. 2006; 175:1807-1811.
7. El-Sakka AI. Prevalence of Peyronie's disease among patients with erectile dysfunction. Eur Urol. 2006; 49:564-569.
8. Pescatori ES, Drei B, Silingardi V. Advanced diagnostics in erectile dysfunction: Beyond the concept of hemodynamics. J Endocrinol Invest. 2003; 26(3 Suppl):125-126.
9. Devine CJ Jr, Somers KD, Jordan SG, Schlossberg SM. Proposal: Trauma as the cause of the Peyronie's lesion. J Urol. 1997; 157:285-290.
10. Devine CJ Jr, Horton CE. Peyronie's disease. Clin Plast Surg. 1988; 15:405-409.
11. Somers KD, Dawson DM. Fibrin deposition in Peyronie's disease plaque. J Urol. 1997; 157:311-315.
12. Border WA, Ruoslahti E. Transforming growth factor-beta in disease: The dark side of tissue repair. J Clin Invest. 1992; 90:1-7.
13. El-Sakka AI, Hassoba HM, Pillarisetty RJ, Dahiya R, Lue TF. Peyronie's disease is associated with an increase in transforming growth factor-beta protein expression. J Urol. 1997; 158:1391–1394.
14. Balza E, Borsi L, Allemanni G, Zardi L. Transforming growth factor beta regulates the levels of different fibronectin isoforms in normal human cultured fibroblasts. FEBS Lett. 1988; 228:42-44.
15. Stewart S, Malto M, Sandberg L, Colburn KK. Increased serum levels of anti-elastin antibodies in patients with Peyronie's disease. J Urol. 1994; 152:105-106.
16. Noss MB, Day NS, Christ GJ, Melman A. The genetics and immunology of Peyronie's disease. Int J Impot Res. 2000; 12 Suppl 4:S127-S132.
17. Ling RS. The genetic factor in Dupuytren's disease. J Bone Joint Surg. 1963; 45:709-718.
18. Qian A, Meals RA, Rajfer J, Gonzalez-Cadavid NF. Comparison of gene expression profiles between Peyronie's disease and Dupuytren's contracture. Urology. 2004; 64:399-404.
19. Smith JF, Walsh TJ, Lue TF. Peyronie's disease: A critical appraisal of current diagnosis and treatment. Int J Impot Res. 2008; 20:445-459.
20. Levine LA, Greenfield JM. Establishing a standardized evaluation of the man with Peyronie's disease. Int J Impot Res. 2003;15 Suppl 5:S103-S112.
21. Hellstrom WJ. Medical management of Peyronie's disease. J Androl. 2009; 30:397-405.
22. Garaffa G, Trost LW, Serefoglu EC, Ralph D, Hellstrom WJ. Understanding the course of Peyronie's disease. Int J Clin Pract. 2013; 67:781-788.
23. Kendirci M, Hellstrom WJ. Critical analysis of surgery for Peyronie's disease. Curr Opin Urol. 2004; 14:381-388.

24. Segal RL, Burnett AL. Surgical management for Peyronie's disease. World J Mens Health. 2013; 31:1-11.
25. Mimeault M, Hauke R, Batra SK. Stem cells: A revolution in therapeutics-recent advances in stem cell biology and their therapeutic applications in regenerative medicine and cancer therapies. Clin Pharmacol Ther. 2007; 82:252-264.
26. Atala A. Recent applications of regenerative medicine to urologic structures and related tissues. Curr Opin Urol. 2006; 16:305-309.
27. Alwaal A, Hussein AA, Lin CS, Lue TF. Prospects of stem cell treatment in benign urological diseases. Korean J Urol. 2015; 56:257-265.
28. Lin CS, Lin G, Lue TF. Allogeneic and xenogeneic transplantation of adipose-derived stem cells in immunocompetent recipients without immunosuppressants. Stem Cells Dev. 2012; 21:2770-2778.
29. Kokai LE, Marra K, Rubin JP. Adipose stem cells: Biology and clinical applications for tissue repair and regeneration. Transl Res. 2014; 163:399-408.
30. Hassan WU, Greiser U, Wang W. Role of adipose-derived stem cells in wound healing. Wound Repair Regen. 2014; 22:313-325.
31. Rivera-Valdés JJ, García-Bañuelos J, Salazar-Montes A, García-Benavides L, Dominguez-Rosales A, Armendáriz-Borunda J, Sandoval-Rodríguez A. Human adipose derived stem cells regress fibrosis in a chronic renal fibrotic model induced by adenine. PLoS One. 2017; 12:e0187907.
32. Llontop P, Lopez-Fernandez D, Clavo B, Afonso Martín JL, Fiuza-Pérez MD, García Arranz M, Calatayud J, Molins López-Rodó L, Alshehri K, Ayub A, Raad W, Bhora F, Santana-Rodríguez N. Airway transplantation of adipose stem cells protects against bleomycin-induced pulmonary fibrosis. J Investig Med. 2018; 66:739-746.
33. Albersen M, Kendirci M, Van der Aa F, Hellstrom WJ, Lue TF, Spees JL. Multipotent stromal cell therapy for cavernous nerve injury induced erectile dysfunction. J Sex Med. 2012; 9:385-403.
34. Garcia MM, Fandel TM, Lin G, Shindel AW, Banie L, Lin CS, Lue TF. Treatment of erectile dysfunction in the obese type 2 diabetic ZDF rat with adipose tissue-derived stem cells. J Sex Med. 2010; 7 (1 Pt 1):89-98.
35. Castiglione F, Hedlund P, Van der Aa F, Bivalacqua TJ, Rigatti P, Van Poppel H, Montorsi F, De Ridder D, Albersen M. Intratunical injection of human adipose tissue-derived stem cells prevents fibrosis and is associated with improved erectile function in a rat model of Peyronie's disease. Eur Urol. 2013; 63:551-560.
36. Castiglione F, Hedlund P, Weyne E, Hakim L, Montorsi F, Bivalacqua TJ, De Ridder D, Milenkovic U, Ralph D, Garaffa G, Muneer A, Joniau S, Albersen M; Trauma and Reconstructive Urology Working Party of the European Association of Urology Young Academic Urologists. Intratunical injection of human adipose tissue-derived stem cells restores collagen III/I ratio in a rat model of chronic Peyronie's disease. Sex Med. 2019; 7:94-103.
37. Gokce A, Abd Elmageed ZY, Lasker GF, Bouljihad M, Kim H, Trost LW, Kadowitz PJ, Abdel-Mageed AB, Sikka SC, Hellstrom WJ. Adipose tissue-derived stem cell therapy for prevention and treatment of erectile dysfunction in a rat model of Peyronie's disease. Andrology. 2014; 2:244-251.
38. Gokce A, Abd Elmageed ZY, Lasker GF, Bouljihad M, Braun SE, Kim H, Kadowitz PJ, Abdel-Mageed AB, Sikka SC, Hellstrom WJ. Intratunical injection of genetically modified adipose tissue-derived stem cells with human interferon alpha-2b for treatment of erectile dysfunction in a rat model of tunica albugineal fibrosis. J Sex Med. 2015; 12:1533-1544.
39. Levy JA, Marchand M, Iorio L, Zribi G, Zahalsky MP. Effects of stem cell treatment in human patients with Peyronie disease. J Am Osteopath Assoc. 2015; 115:e8-e13.

Received November 24, 2019; Revised January 19, 2020; Accepted January 24, 2020.

*Address correspondence to:
Mohamad Abou Chakra, Department of Urology, Faculty of Medical Sciences, Lebanese University, Beirut, Lebanon.
E-mail: mohamedabouchakra@hotmail.com

Released online in J-STAGE as advance publication February 4, 2020.

Original Article

DOI: 10.5582/irdr.2020.01018

Comprehensive bioinformatic analysis of Wnt1 and Wnt1-associated diseases

Chuanming Peng[1,2,§], Yanqin Lu[1,2,§,*], Xiuzhi Ren[3], Yanzhou Wang[4], Shie Zhang[1,2], Mei Chen[3], Junlong Liu[3], Fengling Fang[3], Tianyou Li[4], Jinxiang Han[1,2,*]

[1] School of Medicine and Life Sciences, University of Jinan, Shandong Academy of Medical Sciences, Ji'nan, China;
[2] Key Laboratory for Biotech Drugs of the National Health Commission, Key Laboratory for Rare & Uncommon Diseases of Shandong Province, Shandong Medicinal Biotechnology Centre, Shandong First Medical University & Shandong Academy of Medical Sciences, Ji'nan, China;
[3] Orthopaedic Surgery, The People's Hospital of Wuqing District, Tianjin, China;
[4] Shandong Provincial Hospital Affiliated with Shandong First Medical University, Ji'nan, China.

SUMMARY Wnt1 is the first member of the Wnt family that was identified. It is phylogenetically conserved and essential for oncogenesis and multiple developmental processes. This study has summarized diseases and mutations related to *Wnt1*. *Wnt1* is involved in various cancers, genetic type XV osteogenesis imperfecta, osteoporosis, and neurological diseases. The expression of *Wnt1* in normal tissues and different types of cancers and the potential survival of cancer were analyzed using experiment-based bioinformatic analysis. Systematic analysis indicated that abnormal expression of *Wnt1* is significantly associated with cancers, such as kidney renal carcinoma, hepatocellular carcinoma, thyroid carcinoma, head and neck squamous cell carcinoma, and uterine corpus endometrial carcinoma. GeneMANIA and STRING predicted that 32 proteins were involved with Wnt1 in Wnt signaling pathways and sorting and secretion of Wnts. These interacting molecules significantly co-occurred according to cBioPortal analysis. Thirty-three genes with an alteration frequency of more than 50% were observed in several cancers like esophageal squamous cell carcinoma, melanoma, and non-small cell lung cancer. Functional and experiment-based bioinformatics indicated that Wnt1 may act as a target of a potential biomarker for various types of human cancers. Wnt1 and other Wnt1-related proteins and signaling pathways may be ways to treat osteoporosis.

Keywords *Wnt1*, *Wnt1* mutations, *Wnt1* expression, co-occurrence, bioinformatics, type XV osteogenesis imperfecta, cancers

1. Introduction

Wnts are secreted lipid-modified glycoproteins that transmit a signal through one more of different signaling pathways including canonical Wnt-β-catenin signaling and non-canonical pathways. Aberrant components of Wnt signaling are related to various human diseases, including genetic diseases and complex diseases such as cancer (*1,2*). *Wnt1*, the first member of the Wnt family to be identified, is a gene that was activated by integration of mouse mammary tumor virus (MMTV) proviral DNA in virally induced breast tumors in 1982 (*3*). It is evolutionarily conserved and adjacent to the *Wnt10b* gene on chromosome 12 in homo sapiens (*4,5*). Wnt1 is reported to be vital for the development of the embryonic brain and central nervous system (CNS) (*6-8*). *Wnt1* expression was mapped at the dorsal p1 midline and mesencephalon (*9*). Knockout mice of the homozygous Int-1 displayed a severe phenotype, ranging from death to ataxia (*10*). Conditional knockout of *Wnt1* in mesenchymal progenitors led to severe fractures in mice resembling severe osteogenesis imperfecta (OI) (*11*). Overexpression of *Wnt1* induces duplication of the embryonic axis (*6,12*). Moreover, Wnt1 plays an essential role in osteoblast functions, bone development, and bone homeostasis (*13-15*). *Wnt1* mutations are reported to be associated with type XV OI or early-onset osteoporosis (*13,14,16,17*). The current study has summarized the expression, mutation, and functions of the Wnt1 based on a comprehensive bioinformatic analysis.

2. Materials and Methods

2.1. Phylogenetic analysis of Wnt1

The sequence of the Wnt1 protein was retrieved from an NCBI database and analyzed with the software TBtools.

Multiple sequence alignment was performed with Clustal W. A phylogenetic tree were drawn with the software Molecular Evolutionary Genetics Analysis (MEGA) and FigTree v1.4.3 using the neighbor-joining method. In total, 259 species were collected for phylogenetic analysis.

2.2. *Wnt1* and human diseases

Wnt1-related human diseases were summarized based on information from the Gene-Cloud of Biotechnology Information (GCBI) website (*https://www.gcbi.com.cn/gclib/html/index*). *Wnt1* variations were identified from St. Jude Cloud (*https://platform.stjude.cloud/requests/diseases*). *Wnt1* mutations that are responsible for type XV OI were identified from an OI mutation database (*https://oi.gene.le.ac.uk/home.php*). Mutations and copy number variations of *Wnt1* were analyzed with cBioPortal (*http://www.cbioportal.org*) (*18,19*); 46,697 samples from 44,347 patients with cancer in 176 studies were analyzed.

2.3. The expression of *Wnt1* in normal and cancer tissues and analysis of cancer survival

Wnt1 expression in different normal tissues was analyzed using a human protein atlas database (*https://www.proteinatlas.org/*). A total of 55 tissues and six different types of blood cells were analyzed along with 18 different types of blood cells and peripheral blood mononuclear cells (PBMCs). These data were normalized based on HPA, GTEx, and FANTOM5 transcriptomic analysis. The expression of *Wnt1* in human cancer was analyzed with Firebrowse (*http://firebrowse.org/*), which includes 37 different cancer types and 28 normal tissues as controls.

2.4. Prediction of the protein-protein interaction network and proteins co-occurring with Wnt1

GeneMANIA (*https://genemania.org/*) and STRING (*https://string-db.org/*) servers were used to analyze interaction proteins (*20,21*). These interactions include both physical and functional associations. cBioPortal was used to analyze the spectrum of mutations and copy number alterations of *Wnt1* and its interacting proteins in different cancers (all cancer types in TCGA data). The co-occurrence of Wnt1 and other proteins was predicted with cBioPortal.

2.5. Prediction of transcription factors and pathways involved in Wnt1

Pathways involving Wnt1 were predicted with KEGG (*http://www.kegg.jp*) and AmiGO2 (*http://amigo.geneontology.org/amigo*) and then used for gene ontology analysis (*22,23*)

3. Results

3.1. Phylogenetic analysis of the Wnt1 protein

Based on multiple sequence alignment, a phylogenetic analysis was performed to explore the likely similarities in and the relationship between the *Wnt1* protein in species from different genera and families. On the family level, hominids (*Homo sapiens, Pan paniscus, Pan troglodytes, Callithrix jacchus*) were clustered with gorillas (*Gorilla gorilla gorilla*) and Cercopithecidae (*Macaca nemestrina, Mandrillus leucophaeus*). Hamster and murine families were clustered together. These families were distinct in primates and rodents (dark blue in the figure). A total of 64 different species of mammals, which including mostly terrestrial organisms, some aquatic organisms, a few primates from Cercopithecidae, lemurids, and hominids, were cross-clustered, as represented by the light blue branch of the tree. Species from the feline family of Carnivora were grouped together. Different genera and species of ungulates, Carnivora, bats, and cetaceans were cross-clustered. Unlike species clustered in dark blue, rodents were all from the murine family; the yellow branch included other families which were predominantly squirrels, guinea pigs moles, and mole rats. Fish, birds, and amphibians are all grouped together to form two large individual branches, fish in light red were mainly bass, while Gymnotiformes, Clupeiformes, and Cyprinidae species were grouped together as a red branch (Figure 1).

3.2. *Wnt1* is related to multiple human diseases and the distribution of variants

Wnt1 mutations were found in different types of neoplasms including adenomatous polyposis coli, neoplasm metastasis, colorectal neoplasm, carcinoma, and lung neoplasms. *Wnt1* causes neurological conditions as well as OI (Figure 2A). Twelve mutations with ExAC frequencies were found in the ClinVar database (Figure 2B). The Catalogue Of Somatic Mutations In Cancer (COSMIC) database contained a total of 83 mutations, most of which were missense mutations (n = 49), followed by 24 frame shift mutations, 13 silent mutations, 4 splice region mutations, 4 nonsense mutations, and 1 splice mutation (Figure 2C). The frame shift mutation c.500delG was noted 17 times, mostly in colon and cecum cancer (Supplementary Table S1, *http://www.irdrjournal.com/action/getSupplementalData.php?ID=56*, Figure S1, *http://www.irdrjournal.com/action/getSupplementalData.php?ID=62*). A high alteration frequency was observed in ovarian cancer, colon adenocarcinoma, salivary cancer, prostate cancer, adrenocortical carcinoma, and mature T and NK neoplasms. A high percentage of *Wnt1* mutations was observed in ovarian cancer and colon adenocarcinoma. Copy number alterations of *Wnt1* were prevalent in

salivary cancer, esophageal squamous cell carcinoma, and prostate cancer (Supplementary Figure S1, *http://www.irdrjournal.com/action/getSupplementalData.php?ID=62*). OI databases worldwide contained 36 mutations (Figure 2D).

3.3. The expression of *Wnt1* in normal and cancer tissues and survival analysis for patients with cancer

Results revealed that *Wnt1* was highly expressed in the placenta, basal ganglia, cerebral cortex, lymph node, and bone marrow but less expressed in other types of blood cells, granulocytes, skin, and the rectum, parathyroid glands, fallopian tubes, and adrenal glands (Figure 3A and 3B). *Wnt1* was up-regulated (fold-change > 2) in several cancers including kidney renal clear cell carcinoma (KIRC), kidney renal papillary cell carcinoma (KIRP), pan-kidney cohort (KIPAN), and sarcoma (SARC). In contrast, down-regulation of *Wnt1* was noted in glioma (GBMLGG), skin cutaneous melanoma (SKCM), glioblastoma multiforme (GBM), pancreatic adenocarcinoma (PAAD), stomach adenocarcinoma (STAD), colon adenocarcinoma (COAD), lung squamous cell carcinoma (LUSC), and colon adenocarcinoma (COADREAD) tumor tissues (Figure 3C, Supplementary Table S2, *http://www.irdrjournal.com/action/getSupplementalData.php?ID=57*).

The average level of *Wnt1* expression was lower in tumor tissues than that in normal tissues. The association of *Wnt1* expression with survival rates ($p < 0.05$) of patients with different cancers is shown in Figure 4. In kidney renal papillary cell carcinoma and renal clear cell carcinoma, patients with a higher level of *Wnt1* expression ($n = 56$ and 249, respectively) had a significantly lower overall survival compared to those with a lower level of *Wnt1* expression ($n = 121$ and 281, respectively) (Figure 4I, 4K). This was also observed in patients with cervical squamous cell carcinoma (Figure 4B). Lower *Wnt1* expression was associated with lower survival in patients with some cancers, and especially liver hepatocellular carcinoma, thyroid carcinoma, head and neck squamous cell carcinoma, and uterine corpus

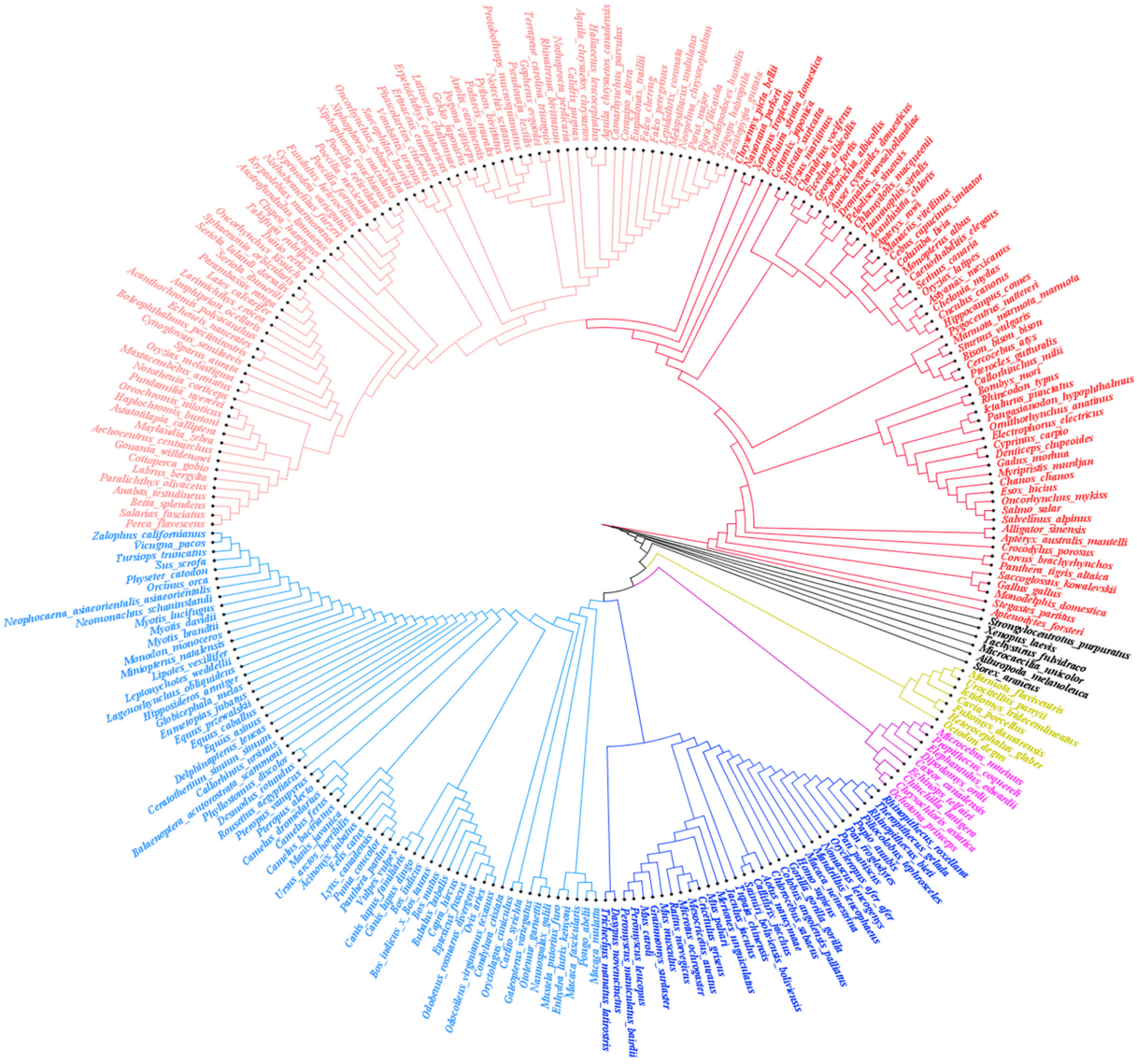

Figure 1. Phylogenetic analysis of Wnt1. In total, 259 different species were analyzed, and Wnt1 is highly conserved.

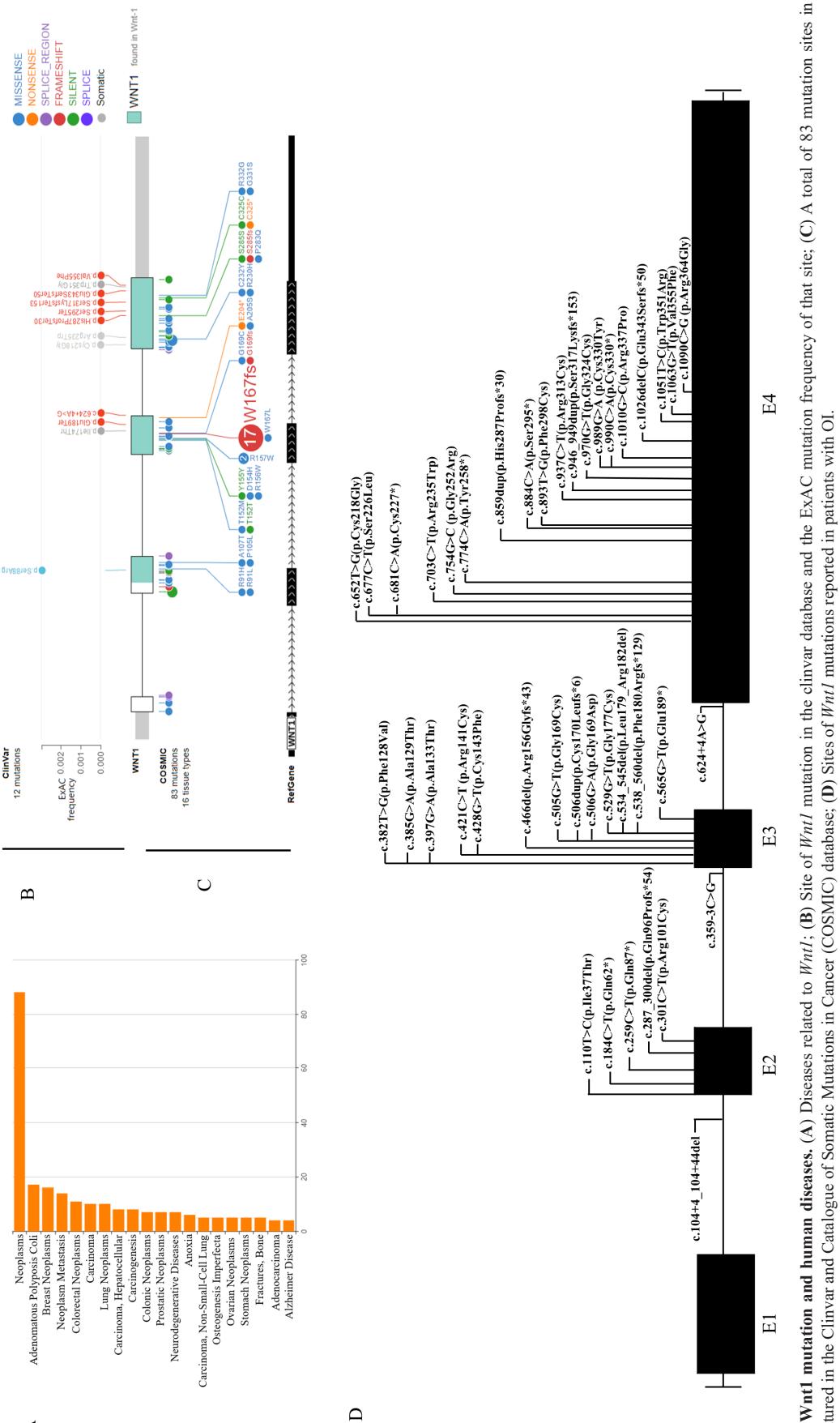

Figure 2. Wnt1 mutation and human diseases. (**A**) Diseases related to *Wntl*; (**B**) Site of *Wntl* mutation in the clinvar database and the ExAC mutation frequency of that site; (**C**) A total of 83 mutation sites in human tissues featured in the Clinvar and Catalogue of Somatic Mutations in Cancer (COSMIC) database; (**D**) Sites of *Wntl* mutations reported in patients with OI.

endometrial carcinoma (Figure 4A, 4D, 4E, and 4J).

3.4. Prediction of protein-protein interaction and cross-cancer analysis of *Wnt1* mutations and copy number alterations

GeneMANIA and String analysis of protein-protein interaction predicted a total of 21 and 25 proteins, respectively (Figure 5A, B, Supplementary Table S3, *http://www.irdrjournal.com/action/getSupplementalData.php?ID=58* and Table S4, *http://www.irdrjournal.com/action/getSupplementalData.php?ID=59*). Both programs predicted interaction with DKK1, FZD1, FzZD5, FZD8, LRP5, LRP6, PORCN, ROR2, RYK, SFRP1, WIF1, Wnt1, and Wnt3A. Most physically interacted with Wnt1, excluding MACF1, TCF4, TIMM17B, KL, FZD3, and NKD1. TIMM17B was predicted to be co-localized with Wnt1. These interacting proteins are involved in the Wnt signaling pathway except for TIMM17B and KL (Supplementary Table S4, *http://www.irdrjournal.com/action/getSupplementalData.php?ID=59*).

All 33 genes, including *CDC5L, DKK1, DVL1, FZD1, FZD10, FZD2, FZD3, FZD5, FZD6, FZD7, FZD8, KL, LRP5, LRP5L, LRP6, MACF1, NKD1, NKD2, NOTUM, PORCN, PPP2CA, PPP2R1A, ROR2, RYK, SFRP1, SFRP2, TCF4, TIMM17B, UBR3, WIF1, WLS, Wnt1*, and *Wnt3A*, were submitted to cBioPortal for alteration frequency analysis. The alteration spectrum of these 33 genes varied in 33 cancer types, including mutation, fusion, amplification, deep deletion, and multiple alteration in cancer. An alteration frequency of over 50% was observed in esophageal squamous cell carcinoma (71.58%), melanoma (68.02%), non-small cell lung cancer (64.01%), bladder urothelial carcinoma (62.77%), esophagogastric adenocarcinoma (61.26%), endometrial carcinoma (61.09%), ovarian epithelial tumor (59.76%), mature B-Cell neoplasms (52.08%), head and neck squamous cell carcinoma (51.05%), and invasive breast carcinoma (50.65%). The lowest alteration frequency (< 10%) was noted in miscellaneous neuroepithelial tumors, leukemia, and well-differentiated thyroid cancer (Figure 5C). All of these genes interacting with *Wnt1* significantly co-occurred according to co-occurrence analysis with cBioPortal (Supplementary Table S5, *http://www.irdrjournal.com/action/getSupplementalData.php?ID=60*).

3.5. Prediction of transcription factors and signaling pathways involving *Wnt1*

A total of 34 transcription factors and 10 motifs were predicted as shown in Figure 6. Some transcription factors do not have obvious annotated motifs or conserved motifs and regions. Wnt1 is involved in 14 KEGG pathways including mTOR, Wnt, Hippo, different types of cancer pathways, and signaling pathways as shown in Table 1. Gene ontology (GO) annotation annotated a total of 10 molecular functions, 19 different cellular components, and 70 biological process (Supplementary Table S6, *http://www.irdrjournal.com/action/getSupplementalData.php?ID=61*). The main molecular functions associated with Wnt1 are receptor ligand activity, morphogen activity, protein domain-specific binding, and transcription regulatory region

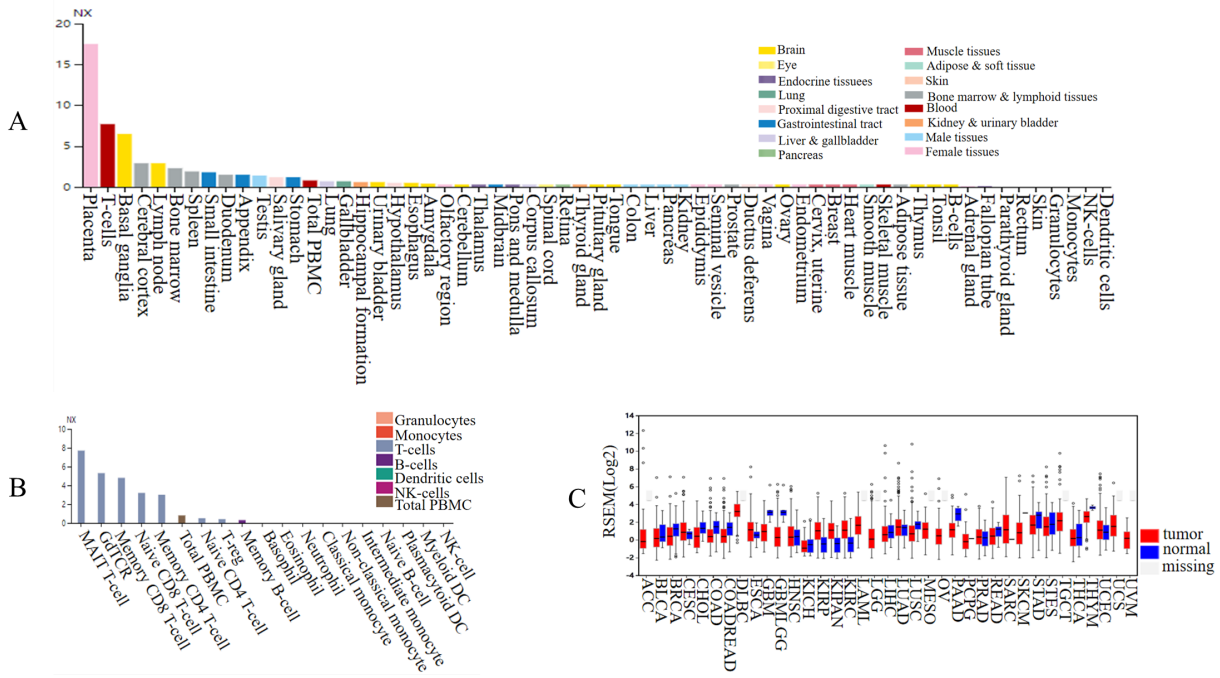

Figure 3. The level of *Wnt1* expression in different normal and cancer tissues. (**A**) A total of 55 tissues and 6 different types of blood cells; (**B**) Different types of blood cells and PBMCs; (**C**) Expression in 37 different cancer types and 28 normal tissues.

DNA binding. As a morphogen, Wnt1 is secreted as an extracellular matrix protein through the plasma membrane. Wnt1 is involved in the canonical Wnt signaling pathway and planar cell polarity pathway and it plays a role in cell fate commitment, cell proliferation, cell adhesion, cell-cell signaling, bone development, diencephalon development, embryonic brain development, and some other functions.

Table 1. KEGG pathway involved in Wnt1

KEGG ID	KEGG term
ko04150	mTOR signaling pathway
ko04310	Wnt signaling pathway
ko04390	Hippo signaling pathway
ko04391	Hippo signaling pathway – fly
ko04550	Signaling pathways regulating pluripotency of stem cells
ko04916	Melanogenesis
ko04934	Cushing syndrome
ko05165	Human papillomavirus infection
ko05200	Pathways in cancer
ko05205	Proteoglycans in cancer
ko05217	Basal cell carcinoma
ko05224	Breast cancer
ko05225	Hepatocellular carcinoma
ko05226	Gastric cancer

4. Discussion

Wnt1 is the first member of the Wnt family that was identified. It is evolutionarily conserved according to a phylogenetic analysis, and this is especially true in primates and rodents. Cross-talk among different species of fish, birds, and amphibians was observed in phylogenetic analysis. *Wnt1* is associated with various human diseases including cancers, CNS diseases, and bone diseases (early-onset osteoporosis and OI) (*15*). Altered expression of *Wnt1* and proteins it interacts with in Wnt signaling pathways and regulation were associated with oncogenesis, epithelial-to-mesenchymal transition, and the invasion of and prognosis for various cancers (*24-29*). Wnt1 is a potential prognostic factor for renal cell carcinoma and cutaneous squamous cell carcinoma (*30-32*).

OI is a genetically heterozygous disease characterized by frequently fractures and decreased bone mass. Patients with this diseases usually have blue sclera, dentinogenesis imperfecta, scoliosis, and a short stature. Type XV OI is an autosomal recessive form of OI, with biallelic mutations of Wnt1. A heterozygous mutation of Wnt1 leads to a dominant form of early on-set

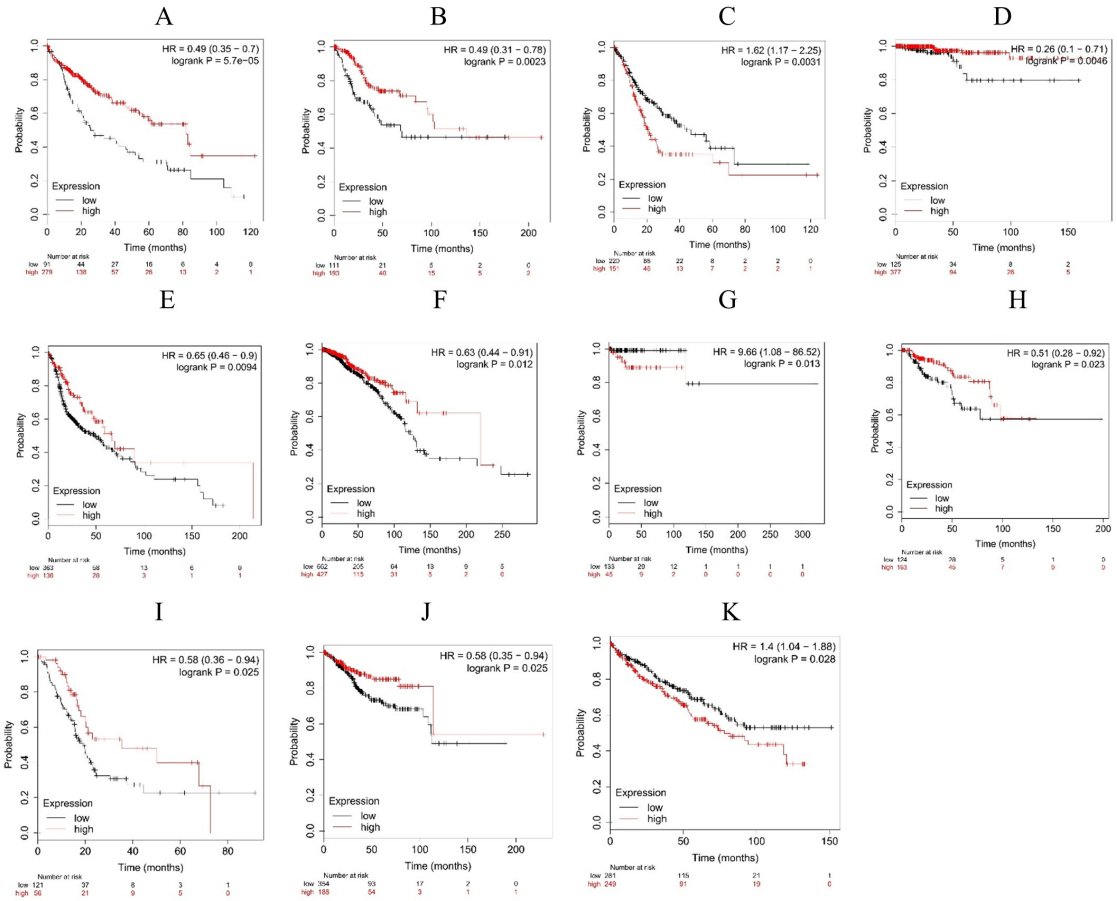

Figure 4. The survival curve of patients with high (red) and low (black)expression. (**A**) Liver hepatocellular carcinoma; (**B**) Cervical squamous cell carcinoma; (**C**) Stomach adenocarcinoma; (**D**) Thyroid carcinoma; (**E**) Head-neck squamous cell carcinoma; (**F**) Breast cancer; (**G**) Pheochromocytoma and paraganglioma; (**H**) Kidney renal papillary cell carcinoma; (**I**) Pancreatic ductal adenocarcinoma; (**J**) Uterine corpus endometrial carcinoma; (**K**) Kidney renal clear cell carcinoma.

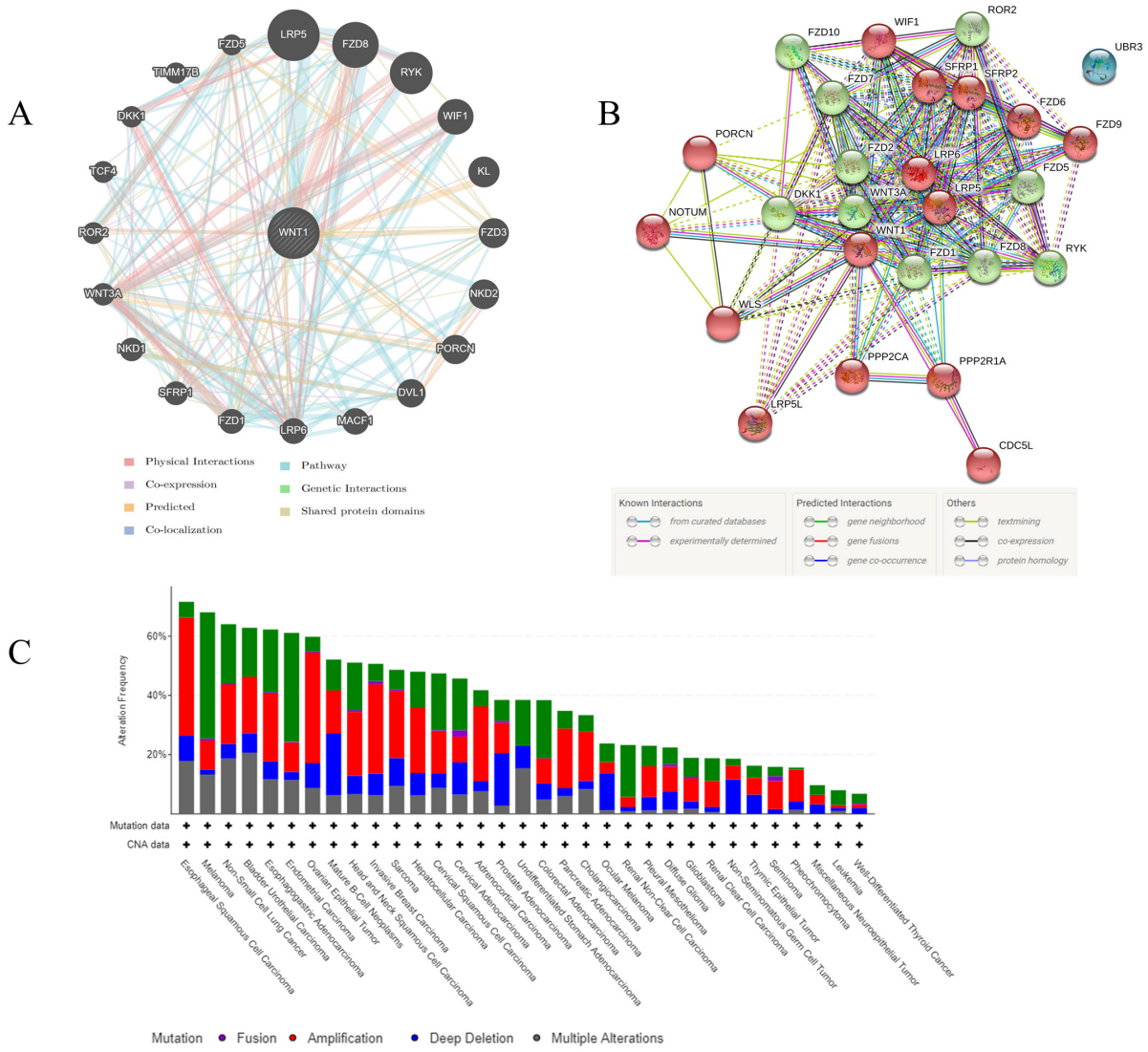

Figure 5. Proteins interacting and co-occurring with Wnt1. (A,B) Predicted proteins associated with Wnt1 according to GeneMANIA and STRING; **(C)** The alteration frequency of 33 genes as predicted in different cancers. The alteration frequency included mutations (green), fusions (violet), amplifications (red), deep deletions (deep blue), and multiple alterations (grey).

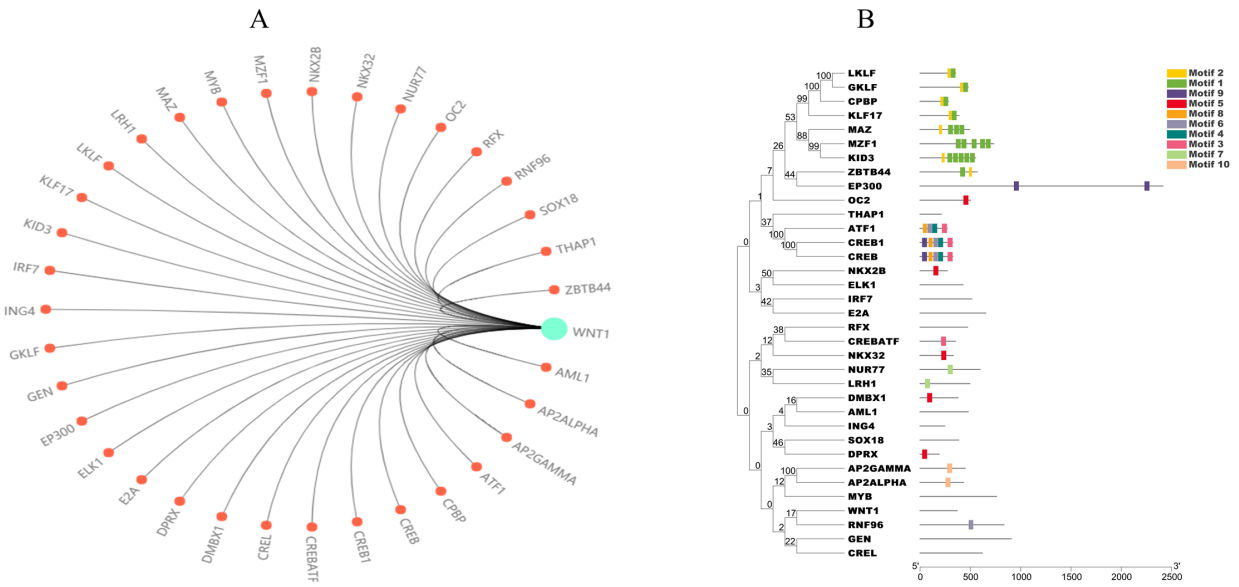

Figure 6. Prediction of Wnt1 transcription factors. (**A**) Predicted transcription factors highly associated with Wnt1; (**B**) Domain analysis of transcription factors using TBtools.

osteoporosis (*14*). Hence, some parental carriers suffer from osteoporosis (*13*). Patients with XV OI usually have severe long-bone deformities, though no fracture or deformity is noted at birth as is true in dominant forms of OI. Severe vertebral compression, developmental delay, and brain abnormalities are the main phenotypes that differ from those of other OI types (*15*). A neurological phenotype is also involved in Wnt1-induced OI (*33*). Therefore, the overlap in phenotypes between OI and other CNS diseases suggests crosstalk mechanisms related to *Wnt1* mutations.

A highly interesting finding is that the same mutation sites could lead to different diseases. G to A substitution at position 385 was found in both type XV OI in a homozygous or compound heterozygous form (*15,34*) and colorectal carcinoma (*35*). Different types of mutations in the same nucleic acids were observed in different diseases. The missense mutation c.466T was reported in stomach carcinoma. Deletion of this site led to a truncated protein with 156 amino acids found in a Chinese patient with OI whose parents were carriers (*15*). The mutations c.506dup and c.506G>A were both found in patients with XV OI (*17,34*). Deletion of this site is associated with colon and cecum carcinoma (*35,36*). *Wnt1* S88R is reported to be related to autism (*37*), though autism is also reported to be part of the phenotype for patients with type XV OI (*33*). Figure 1 shows that *Wnt1* mutations from cancers and OI are all clustered together and in the same Wnt1 domain, though most mutation sites differ. Thus, the challenge is diagnosing the condition with no obvious clinical phenotypes, especially in prenatal screening. Further research on the relationship between the phenotype and genotype could help determine the molecular mechanisms for *Wnt1*-induced diseases and guide diagnosis of the condition.

Proteins interacting with Wnt1 are related to maturation, secretion, and signaling pathways of Wnt. Like other Wnt proteins, Wnt1 is a protein that depends on O-acyltransferase porcupine (PORCN) and Wntless (WLS) for secretion (*38,39*). Notum acts as a negative regulator of Wnt signaling pathway by specifically mediating depalmitoleoylation of Wnts (*2*). Wnt1 activates canonical Wnt/β-catenin signaling *via* LRP5/6 receptors by cell-cell physical contact and regulates osteoclastogenesis with OPG in a juxtacrine manner (11). By binding to cell surface receptors, Wnt1 activates a canonical signaling pathway that increases cellular β-catenin activity. A mutation in Wnt1 or proteins it interacts with is associated with abnormal Wnt signaling and regulation; this affects oncogenesis, so Wnt1 could be a prognostic marker for cancers (*24,30,40-42*).

The current study systematically analyzed mutation, expression, and functions of Wnt1 in a number of human diseases. The expression of *Wnt1* and proteins interacting with it was involved in various cancers and is significantly related to survival in some cancers. The altered expression of *Wnt1* and proteins interacting with it may be a prognostic marker in some cancers.

Acknowledgements

This work was supported by Grants-in-Aid from the State Major Infectious Disease Research Program (Chinese Central Government, 2017ZX10103004-007) and the Shandong Government (2018WS178, 2016GSF201222).

References

1. Lu Y, Ren X, Wang Y, Han J. Wnt signaling associated human diseases. Novel Techniques in Arthritis & Bone Res. 2018; 3:555607.
2. Lu Y, Han J. Wnt Signaling and Genetic Bone Diseases. in: Osteogenesis and Bone Regeneration (Yang H, ed. IntechOpen Limited, London, UK, 2019; pp. 1-20.
3. Nusse R, Varmus HE. Many tumors induced by the mouse mammary tumor virus contain a provirus integrated in the same region of the host genome. Cell. 1982; 31:99-109.
4. Kusserow A, Pang K, Sturm C, Hrouda M, Lentfer J, Schmidt HA, Technau U, von Haeseler A, Hobmayer B, Martindale MQ, Holstein TW. Unexpected complexity of the Wnt gene family in a sea anemone. Nature. 2005; 433:156-160.
5. Nusse R. An ancient cluster of Wnt paralogues. Trends Genet. 2001; 17:443.
6. Navarro-Garberi M, Bueno C, Martinez S. Wnt1 signal determines the patterning of the diencephalic dorso-ventral axis. Brain Struct Funct. 2016; 221:3693-3708.
7. Yang J, Brown A, Ellisor D, Paul E, Hagan N, Zervas M. Dynamic temporal requirement of Wnt1 in midbrain dopamine neuron development. Development. 2013; 140:1342-1352.
8. Serbedzija GN, Dickinson M, McMahon AP. Cell death in the CNS of the Wnt-1 mutant mouse. J Neurobiol. 1996; 31:275-282.
9. Martinez-Ferre A, Navarro-Garberi M, Bueno C, Martinez S. Wnt signal specifies the intrathalamic limit and its organizer properties by regulating Shh induction in the alar plate. J Neurosci. 2013; 33:3967-3980.
10. Thomas KR, Capecchi MR. Targeted disruption of the murine int-1 proto-oncogene resulting in severe abnormalities in midbrain and cerebellar development. Nature. 1990; 346:847-850.
11. Wang F, Tarkkonen K, Nieminen-Pihala V, Nagano K, Majidi RA, Puolakkainen T, Rummukainen P, Lehto J, Roivainen A, Zhang FP, Makitie O, Baron R, Kiviranta R. Mesenchymal cell-derived juxtacrine Wnt1 signaling regulates osteoblast activity and osteoclast differentiation. J Bone and Min Res. 2019; 34:1129-1142.
12. McMahon AP, Moon RT. Ectopic expression of the proto-oncogene int-1 in Xenopus embryos leads to duplication of the embryonic axis. Cell. 1989; 58:1075-1084.
13. Keupp K, Beleggia F, Kayserili H, *et al.* Mutations in WNT1 cause different forms of bone fragility. Amer J Human Genetics. 2013; 92:565-574.
14. Laine CM, Joeng KS, Campeau PM, *et al.* WNT1 mutations in early-onset osteoporosis and osteogenesis imperfecta. N Engl J Med. 2013; 368:1809-1816.
15. Lu Y, Ren X, Wang Y, Bardai G, Sturm M, Dai Y, Riess O, Zhang Y, Li H, Li T, Zhai N, Zhang J, Rauch F, Han J. Novel WNT1 mutations in children with osteogenesis

imperfecta: Clinical and functional characterization. Bone. 2018; 114:144-149.
16. Fahiminiya S, Majewski J, Mort J, Moffatt P, Glorieux FH, Rauch F. Mutations in WNT1 are a cause of osteogenesis imperfecta. J Medical Genetics. 2013; 50:345-348.
17. Pyott SM, Tran TT, Leistritz DF, *et al.* WNT1 mutations in families affected by moderately severe and progressive recessive osteogenesis imperfecta. Amer J Human Genetics. 2013; 92:590-597.
18. Cerami E, Gao J, Dogrusoz U, *et al.* The cBio cancer genomics portal: An open platform for exploring multidimensional cancer genomics data. Cancer Discov. 2012; 2:401-404.
19. Gao J, Aksoy BA, Dogrusoz U, Dresdner G, Gross B, Sumer SO, Sun Y, Jacobsen A, Sinha R, Larsson E, Cerami E, Sander C, Schultz N. Integrative analysis of complex cancer genomics and clinical profiles using the cBioPortal. Science Signaling. 2013; 6:pl1.
20. Szklarczyk D, Franceschini A, Wyder S, Forslund K, Heller D, Huerta-Cepas J, Simonovic M, Roth A, Santos A, Tsafou KP, Kuhn M, Bork P, Jensen LJ, von Mering C. STRING v10: Protein-protein interaction networks, integrated over the tree of life. Nucleic Acids Res. 2015; 43:D447-D452.
21. Warde-Farley D, Donaldson SL, Comes O, *et al.* The GeneMANIA prediction server: Biological network integration for gene prioritization and predicting gene function. Nucleic Acids Res. 2010; 38:W214-W220.
22. Kanehisa M, Goto S. KEGG: Kyoto Encyclopedia of Genes and Genomes. Nucleic Acids Res. 2000; 28:27-30.
23. Carbon S, Ireland A, Mungall CJ, Shu S, Marshall B, Lewis S. AmiGO: Online access to ontology and annotation data. Bioinformatics (Oxford, England). 2009; 25:288-289.
24. Ruan GT, Zhu LC, Gong YZ, Liao XW, Wang XK, Liao C, Wang S, Yan L, Xie HL, Zhou X, Li YZ, Gao F. The diagnosis and prognosis values of WNT mRNA expression in colon adenocarcinoma. J Cell Biochem. 2019; doi: 10.1002/jcb.29582.
25. Brennan KR, Brown AMC. Wnt proteins in mammary development and cancer. Journal of Mammary Gland Biology and Neoplasia. 2004; 9:119-131.
26. Liu X, Giguère V. Inactivation of RARβ inhibits *Wnt1*-induced mammary tumorigenesis by suppressing epithelial-mesenchymal transitions. Nuclear Receptor Signaling. 2014; 12:e004-e004.
27. Zhang W, Sun Z, Su L, Wang F, Jiang Y, Yu D, Zhang F, Sun Z, Liang W. miRNA-185 serves as a prognostic factor and suppresses migration and invasion through Wnt1 in colon cancer. Euro J Pharmacology. 2018; 825:75-84.
28. Wang R, Geng N, Zhou Y, Zhang D, Li L, Li J, Ji N, Zhou M, Chen Y, Chen Q. Aberrant Wnt-1/beta-catenin signaling and WIF-1 deficiency are important events which promote tumor cell invasion and metastasis in salivary gland adenoid cystic carcinoma. Biomed Mater Eng. 2015; 26 Suppl 1:S2145-S2153.
29. Nakashima T, Liu D, Nakano J, Ishikawa S, Yokomise H, Ueno M, Kadota K, Huang C-L. Wnt1 overexpression associated with tumor proliferation and a poor prognosis in non-small cell lung cancer patients. Oncology Reports. 2008; 19:203-209.
30. Kruck S, Eyrich C, Scharpf M, Sievert KD, Fend F, Stenzl A, Bedke J. Impact of an altered Wnt1/beta-catenin expression on clinicopathology and prognosis in clear cell renal cell carcinoma. Int J Mol Sci. 2013; 14:10944-10957.
31. Halifu Y, Liang JQ, Zeng XW, Ding Y, Zhang XY, Jin TB, Yakeya B, Abudu D, Zhou YM, Liu XM, Hu FX, Chai L, Kang XJ. Wnt1 and SFRP1 as potential prognostic factors and therapeutic targets in cutaneous squamous cell carcinoma. Genet Mol Res. 2016; 15:10.4238/gmr.15028187.
32. Choi EJ, Yun JA, Jeon EK, Won HS, Ko YH, Kim SY. Prognostic significance of RSPO1, WNT1, P16, WT1, and SDC1 expressions in invasive ductal carcinoma of the breast. World J Surg Oncol. 2013; 11:314-314.
33. Faqeih E, Shaheen R, Alkuraya FS. WNT1 mutation with recessive osteogenesis imperfecta and profound neurological phenotype. J Med Genet. 2013; 50:491-492.
34. Liu Y, Song L, Ma D, Lv F, Xu X, Wang J, Xia W, Jiang Y, Wang O, Song Y, Xing X, Asan, Li M. Genotype-phenotype analysis of a rare type of osteogenesis imperfecta in four Chinese families with WNT1 mutations. Clin Chim Acta. 2. 2016; 461:172-180.
35. Giannakis M, Mu XJ, Shukla SA, *et al.* Genomic correlates of immune-cell infiltrates in colorectal carcinoma. Cell Reports. 2016; 15:857-865.
36. Muzny DM, Bainbridge MN, Chang K, *et al.* Comprehensive molecular characterization of human colon and rectal cancer. Nature. 2012; 487:330-337.
37. Martin PM, Yang X, Robin N, Lam E, Rabinowitz JS, Erdman CA, Quinn J, Weiss LA, Hamilton SP, Kwok PY, Moon RT, Cheyette BN. A rare WNT1 missense variant overrepresented in ASD leads to increased Wnt signal pathway activation. Transl Psychiatry. 2013; 3:e301.
38. Kadowaki T, Wilder E, Klingensmith J, Zachary K, Perrimon N. The segment polarity gene porcupine encodes a putative multitransmembrane protein involved in Wingless processing. Genes Dev. 1996; 10:3116-3128.
39. Banziger C, Soldini D, Schutt C, Zipperlen P, Hausmann G, Basler K. Wntless, a conserved membrane protein dedicated to the secretion of Wnt proteins from signaling cells. Cell. 2006; 125:509-522.
40. Zannoni GF, Angelico G, Santoro A. Aberrant non-canonical WNT pathway as key-driver of high-grade serous ovarian cancer development. Virchows Arch. 2020; doi: 10.1007/s00428-020-02760-5
41. Bodnar L, Stanczak A, Cierniak S, Smoter M, Cichowicz M, Kozlowski W, Szczylik C, Wieczorek M, Lamparska-Przybysz M. Wnt/beta-catenin pathway as a potential prognostic and predictive marker in patients with advanced ovarian cancer. J Ovarian Res. 2014; 7:16.
42. Lv J, Cao XF, Ji L, Zhu B, Wang DD, Tao L, Li SQ. Association of β-catenin, *Wnt1*, Smad4, Hoxa9, and Bmi-1 with the prognosis of esophageal squamous cell carcinoma. Med Oncol. 2012; 29:151-160.

Received February 16, 2020; Revised February 25, 2020; Accepted February 27, 2020.

[§]These authors contributed equally to this work.
**Address correspondence to:*
Yanqin Lu and Jinxiang Han, Shandong First Medical University & Shandong Academy of Medical Sciences, 18877 Jingshi Road, Ji'nan 250062, China.
E-mail: yanqinlu@yahoo.com, mls_hanjx@ujn.edu.cn

Original Article

DOI: 10.5582/irdr.2019.01139

TXNDC5 protects synovial fibroblasts of rheumatoid arthritis from the detrimental effects of endoplasmic reticulum stress

Qiqi Lu[1], Jinguang Wang[2], Xiumei Zhang[3], Ruisong Tian[4], Li Qiao[5], Luna Ge[4], Jihong Pan[4], Lin Wang[4,*]

[1] School of Medicine and Life Sciences, University of Ji'nan-Shandong Academy of Medical Sciences, Ji'nan, Shandong, China;
[2] Department of Orthopedics, Dezhou People's Hospital, Dezhou, Shandong, China;
[3] Graduate Education Centre of the Shandong Academy of Medical Sciences, Ji'nan, Shandong, China;
[4] Shandong Medicinal Biotechnology Centre, Key Laboratory for Rare and Uncommon Diseases of Shandong Province, Key Lab for Biotechnology Drugs of the Ministry of Health, Shandong First Medical University & Shandong Academy of Medical Sciences, Ji'nan, Shandong, China;
[5] College of Clinical Medicine, Shandong University, Ji'nan, Shandong, China.

SUMMARY TXNDC5 is an endoplasmic reticulum (ER)-resident chaperone that protects the endothelium from secondary effects of ER stress. Previous studies by the current authors identified TXNDC5 as a key pathological factor in promoting the inflammatory phenotype of fibroblast-like synoviocytes (FLSs) from rheumatoid arthritis (RA). However, its activity in RA FLSs under ER stress remains unclear. The current study found that TXNDC5 is responsive to ER stress in RA FLSs since its expression was induced by ER stress at both the endogenous and secretory level. A functional study indicated that silencing TXNDC5 reduced the viability of RA FLSs more markedly in the presence of ER stressors. In contrast, rhTXNDC5 attenuated a decrease in cell viability as a result of ER stress. Moreover, silencing TXNDC5 attenuated the induction of IL-6 and IL-8 from RA FLSs in response to ER stress. In addition, rhTXNDC5 induced a greater increase in VEGF production during ER stress. These findings confirm the pro-survival and pro-inflammation roles of TXNDC5 under ER stress in RA FLSs. TXNDC5 appears to act as a mediator linking ER stress and inflammation of RA.

Keywords TXNDC5, endoplasmic reticulum stress, rheumatoid arthritis

1. Introduction

Rheumatoid arthritis (RA) is an inflammatory joint disease characterized by hyperplasia of synovial tissue and formation of pannus (*1,2*). Excessive inflammatory molecules, such as cytokines and matrix metalloproteinase, are secreted and promote the destruction of cartilage and bone (*3,4*). Analyses of hyperplastic synovial tissue from patients with RA have revealed features of transformed long-living cells, such as the presence of somatic mutations, expression of oncogenes, and resistance to apoptosis (*5*). Therefore, identification of the components that are sensitive to the stimuli in the microenvironment of an inflamed joint is crucial to understanding the pathogenesis of RA and may also provide new targets for diagnosis and treatment (*6,7*).

Endoplasmic reticulum (ER) stress is a cellular danger signal, and diverse conditions including hypoxia and inflammation, which are frequently observed in joints affected by RA, can be considered inducers of ER stress (*8*). Fibroblast-like synoviocytes (FLSs) are predisposed to apoptotic resistance to ER stress and contribute to synovial hyperplasia of RA (*9*), but the mechanism of this pathology has yet to be fully clarified (*10,11*). Thioredoxin domain-containing protein 5 (TXNDC5) is a protein-disulfide isomerase located in the ER that functions as a chaperone. In vitro and in vivo studies by the current authors found that TXNDC5 was closely related to the pathological progression of RA and prostate cancer (*12,13*). Recently, the current authors found that TXNDC5 coordinated with HSC70 to exacerbate the inflammatory phenotype of RA at the endogenous level (*14*). More importantly, previous findings indicated that TXNDC5 is responsive to extracellular stimuli, such as hypoxia, pro-inflammatory factors, and androgen-deprivation, indicating that TXNDC5 may be required to adapt to extracellular changes in an inflamed joint (*15*). In addition, TXNDC5 expression was detected in synovial fluid from patients with RA, and its exact function in soluble form remains

unclear (*16*). Intriguingly, a previous study found that TXNDC5 protects endothelial cells from stress-induced cell death. However, the exact role of TXNDC5 under ER stress remains unclear (*17*).

The current study examined whether TXNDC5 expression is up-regulated when stimulated with an inducer of ER stress. TXNDC5 was knocked down to make the inhibitory effects of ER stress on the cell viability of RA FLSs more apparent, and RA FLSs were treated with recombinant human TXNDC5 (rhTXNDC5) to determine if those effects were attenuated. In addition, the expression of inflammatory factors, such as IL-6 and IL-8, was measured in response to rhTXNDC5 treatment plus ER stress. TXNDC5 was silenced to determine the response to an inducer of ER stress. This study examined whether TXNDC5 is sensitive to ER stress in RA FLSs and whether it functions as a link between ER stress and inflammation in RA.

2. Materials and Methods

2.1. Patients

Subjects were 12 patients with RA who had undergone knee joint replacement surgery. All of the patients fulfilled the 1987 American College of Rheumatology revised criteria for the diagnosis of RA. Written informed consent was obtained from every patient, and all samples were anonymized.

2.2. Stimulation assays

Primary RA FLSs were isolated and cultured as described previously (*4*), and cells passaged 3-7 times were used in this study. For stimulation, RA FLSs were plated on 24-well plates (3-5 × 10^5 cells/well) in Dulbecco's modified Eagle's medium and stimulated for the indicated times with the following agents: recombinant human TXNDC5, thapsigargin, tunicamycin, LPS, and a hypoxia inducer ($CoCl_2$).

2.3. Small interfering RNA transfection in RA FLSs

RA FLSs (2 × 10^5 cells in 100-mm-diameter dishes or 8×10^4 cells on 6-well plates) were transiently transfected with siRNA targeting TXNDC5 (#1:SI00132440; #2: SI00132447, QIAGEN, Hilden, Germany) or a negative control (QIAGEN, SI03650318) with a Hiperfect transfection reagent (QIAGEN) in accordance with the manufacturer's instructions, and all experiments were performed 24-48 h after transfection. Non-specific negative control siRNAs were also designed and synthesized (sense strand: 5'-UUCUCCGAACGUGUCACG-3' and anti-sense strand: 5'-ACGUGACACGUUCGGAGAATT-3'). Two siRNAs targeting the same gene were mixed together in equal volumes to verify the reliability of silencing efficiency and were designated siTXNDC5.

2.4. Cell viability

Briefly, 1 × 10^4 cells were seeded onto each well of 96-well plates for the indicated treatment. On the day of detection, 20 μL MTS (Promega) was added to each well. After incubation for 1 h at 37°C, the plates were shaken at room temperature for 10 min. The absorbance was measured at 495 nm, and three independent experiments were analyzed.

2.5. ELISA

Cells were cultured and stimulated as described above, and supernatants were collected as the indicated timepoints. After centrifugation to remove particulates, the release of VEGF (R&D Systems) was analyzed with ELISA in accordance with the manufacturer's instructions.

2.6. RNA extraction and real time RT-PCR (qRT-PCR)

RNA extraction and qRT-PCR were performed as previously described (*18*). Details on the primers are shown in Supplementary Table 1 (*http://www.irdrjournal.com/action/getSupplementalData.php?ID=54*). GAPDH was used as internal loading control. Relative mRNA levels were measured using the 2-Δ cycle threshold (2-ΔCT) method. Three independent experiments were completed, and each reaction was performed in triplicate.

2.7. Measurement of apoptosis using flow cytometry

Apoptosis was also assessed with Annexin V-APC/7-amino-actinomycin D staining (KeyGEN, Nanjing, China). Briefly, cells were harvested, washed with phosphate-buffered saline, resuspended in 500 μL of binding buffer, mixed with 5 μl of Annexin V-APC and 5μl of 7-ADD, and incubated for 5-15 min in the dark. Fifty thousand cells were analyzed using a FACSCalibur cytometer. Annexin V-positive cells were considered apoptotic cells and analyzed using the software ModFit. The assays were carried out in triplicate in three experiments.

2.8. Statistical analyses

Data were statistically analyzed using the software SPSS V.16 (SPSS). The *t* test was used to assess statistical differences between two groups. A P value < 0.05 was considered significant. Data are expressed as the mean ± standard deviation.

3. Results

3.1. TXNDC5 is responsive to ER stress in RA

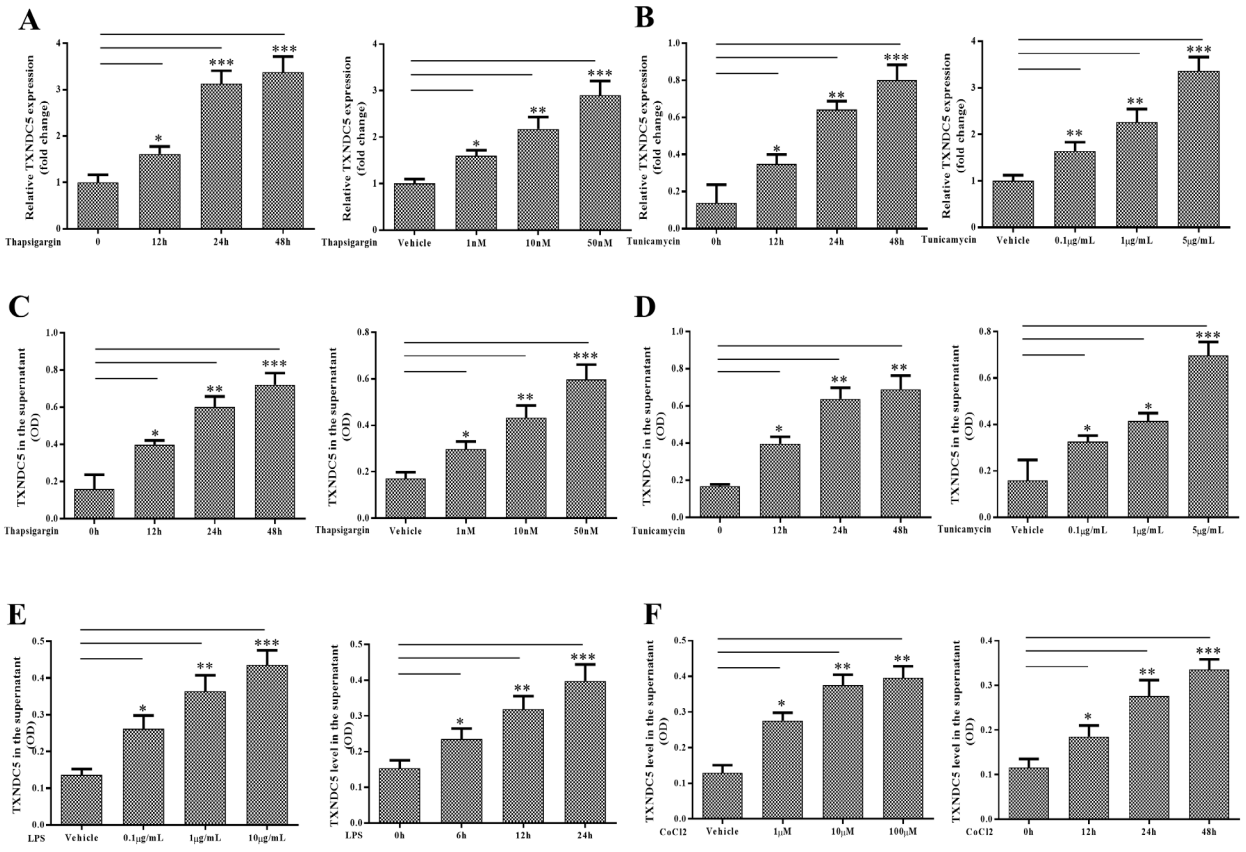

Figure 1. TXNDC5 expression is responsive to ER stress in RA. RA FLSs were exposed to inducers of ER stress, thapsigargin **(A)** and tunicamycin **(B)**, at different doses and time periods, and qRT-PCR was performed to detect the expression of TXNDC5, which was normalized to GAPDH. The expression of TXNDC5 in the supernatant of RA FLSs after treatment with thapsigargin **(C)** and tunicamycin **(D)** was analyzed with ELISA. After stimulation with LPS **(E)** and $CoCl_2$ **(F)**, the level of TXNDC5 protein in the supernatant of RA FLSs was determined with ELISA. Results are expressed as the mean ± SD of experiments performed in triplicate with culture supernatants from each of the three patients with RA. *$p < 0.05$, **$p < 0.01$, and ***$p < 0.001$.

TXNDC5 was localized in the ER, and its expression was induced under ER stress. However, its exact character in RA during ER stress remains unclear. In this study, RA FLSs were exposed to inducers of ER stress, thapsigargin and tunicamycin, and endogenous TXNDC5 expression was induced in a time- and dose-dependent manner (Figure 1A and 1B), indicating the potential involvement of TXNDC5 in RA FLSs in response to ER stress. Moreover, TXNDC5 was detected in serum from patients with RA (*12*). Interestingly, expression of TXNDC5 protein increased significantly after stimulation with thapsigargin and tunicamycin (Figure 1C and 1D). In addition, LPS and hypoxia are proven inducers of ER stress and induce endogenous TXNDC5 expression in RA FLSs (*14*). The current findings indicated that LPS or hypoxia up-regulated TXNDC5 expression in the supernatant of RA FLSs in a time- and dose-dependent manner (Figure 1E and 1F). Collectively, these results suggest that FLSs need TXNDC5 to cope with ER stress in RA, although the exact function needs to be studied in detail.

3.2. Down-regulation of endogenous TXNDC5 by siRNA increases ER-stress-induced apoptosis in RA FLSs

ER chaperones regulate cell survival, and TXNDC5 has been reported to protect endothelial cells from cell death induced by stress (*19*). However, the role of TXNDC5 in RA FLS survival under ER stress is not known. As shown in Figure 2A, tunicamycin and thapsigargin significantly increased the number of TUNEL-positive apoptotic cells among RA FLSs when TXNDC5 siRNA was introduced, in comparison to the control. Moreover, TXNDC5 siRNA-transfected cells had a more marked decrease in cell viability when treated with tunicamycin and thapsigargin (Figure 2B). These findings suggest that TXNDC5 played an important role in maintaining the survival of RA FLSs in response to proapoptotic ER stress in joints affected by RA.

3.3. Exogenous TXNDC5 protects cells from ER stress

A study has indicated that protein secreted in response to ER stress may in turn protect against ER stress-induced apoptosis (*20*). The current study investigated whether TXNDC5 in this soluble form had a similar effect on RA FLSs. Recombinant human TXNDC5 (rhTXNDC5) was used to mimic its extracellular form, and experimental doses of rhTXNDC5 used had no

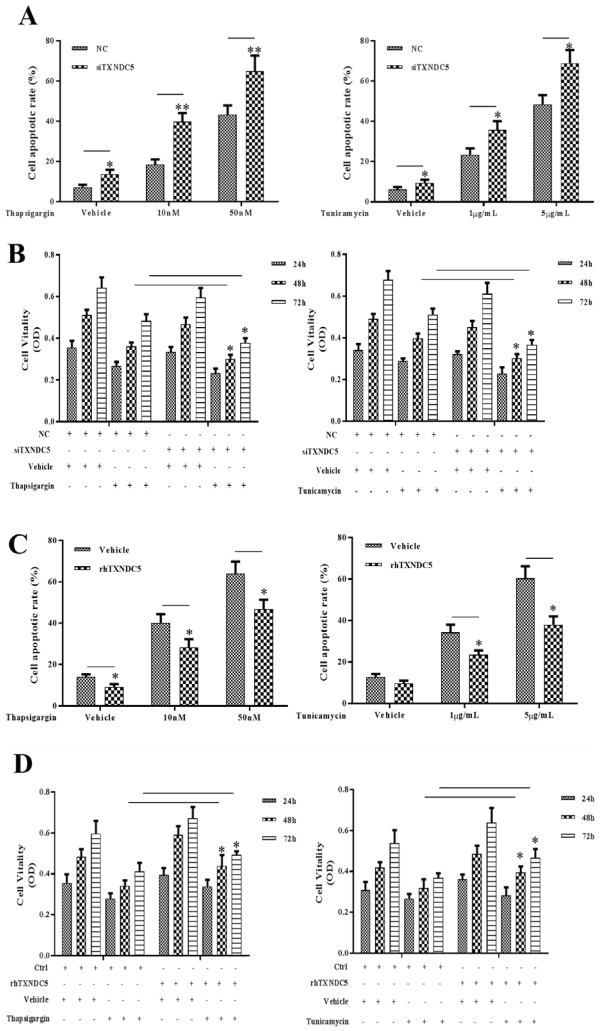

Figure 2. Effects of TXNDC5 on cell biological activity. (A) TUNEL-positive cells were analyzed in thapsigargin or tunicamycin–treated RA FLSs when TXNDC5 siRNA was introduced. Values are the mean and SD percent of TUNEL-positive cells in RA from 5 patients per group. **(B)** MTS was applied every 24 h to detect cell viability after RA FLSs were treated with thapsigargin or tunicamycin when TXNDC5 siRNA was introduced. **(C)** TUNEL-positive apoptotic cells were determined with flow cytometry in the presence of thapsigargin or tunicamycin plus rhTXNDC5. (D) MTS was applied every 24 h to detect cell viability after treatment with thapsigargin or tunicamycin plus rhTXNDC5. Data are presented from a single experiment, and each experiment was repeated three times. $*p < 0.05$ and $**p < 0.01$.

cytotoxic effect on RA FLSs (results not shown). As expected, the number of TUNEL-positive apoptotic RA FLSs induced by tunicamycin and thapsigargin decreased significantly in a dose-dependent manner when RA FLSs were preincubated with rhTXNDC5 (Figure 2C). The effect of rhTXNDC5 on cell viability following ER stress was analyzed using the MTS assay. rhTXNDC5- and vehicle-treated cells were seeded and cultured for 6 h prior to addition of tunicamycin and thapsigargin for 24, 48 and 72 h. Cell viability at each time point was evaluated using the MTS assay and normalized to the respective cell type without ER stress. As shown in Figure 2D, the number of viable rhTXNDC5-treated cells was greater than the number of control cells at all time points as a result of treatment with tunicamycin at a certain concentration (5 ug/mL). The number of cells differed significantly. Similar results were obtained when cells were treated with thapsigargin (50 nM, Figure 2D). Hence, rhTXNDC5-treated cells clearly have increased resistance to ER stress.

3.4. TXNDC5 facilitates cytokine expression and angiogenesis under ER stress

A previous study by the current authors found that cytokine production in response to pro-inflammatory stimuli was attenuated by silencing endogenous TXNDC5. A study has reported that tunicamycin can also induce cytokine production (*21*), so the current study investigated the effect of TXNDC5 on ER-stress mediated cytokine production by RA FLSs. Consistent with results of the previous study, levels of IL6 and IL-8 increased after stimulation with tunicamycin. However, silencing endogenous TXNDC5 suppressed the induction of cytokine expression in response to ER stress (Figure 3A and 3B).

The effect of rhTXNDC5 on cytokine expression in RA FLSs was examined. A qRT-PCR assay indicated that addition of rhTXNDC5 did not significantly induce the expression of IL-6 and IL-8 by RA FLSs. More interestingly, rhTXNDC5 plus LPS (Figure 3C and 3D) or hypoxia (Figure 3E and 3F) additively increased cytokine expression in a time- and concentration-dependent manner. These results indicate that TXNDC5 may act as a mediator to exacerbate inflammation under ER stress. An attempt was made to determine whether TXNDC5 affects the angiogenic process. Interestingly, the current findings indicated that rhTXNDC5 treatment induced VEGF production in RA FLSs in response to tunicamycin (Figure 3G) and thapsigargin (Figure 3H),.

4. Discussion

As a stress protein residing mainly in the ER, TXNDC5 is induced under ER stress and is involved in the regulation of ER homeostasis (*22*). RA is characterized by genes involved in ER stress (*23,24*). However, the relative contribution of TXNDC5 to RA in response to ER stress remains unclear. RA FLSs are exposed to diverse conditions including hypoxia and pro-inflammatory cytokines, and these factors act as ER stressors to exacerbate inflammation as well (*25*). A point worth noting is that previous findings indicated that TXNDC5 in RA FLSs is sensitive to proinflammatory cytokines (IL-1, TNF-α, or IL-6) and hypoxia, increasing the likelihood that TXNDC5 may be functional in RA when ER stress occurs. The current study characterized the expression of TXNDC5 in RA under ER stress, and results further confirmed that TXNDC5 expression both in the cytoplasm and

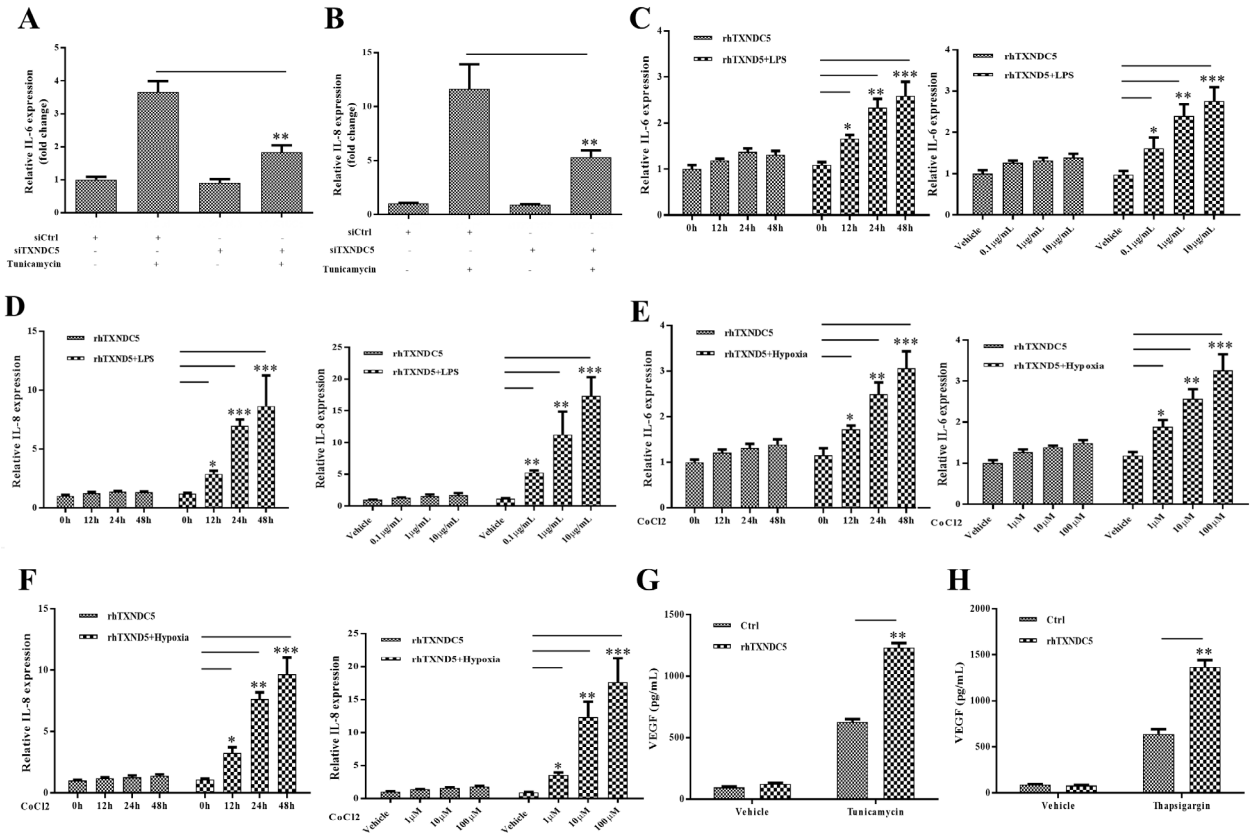

Figure 3. TXNDC5 modulates cytokine expression under ER stress. RA FLSs were exposed to tunicamycin when TXNDC5 siRNA was introduced. Then, IL-6 **(A)** and IL-8 **(B)** were analyzed with qRT-PCR. Each value represents the mean and S.D. of three independent experiments. IL-6 **(C)** and IL-8 **(D)** expression were evaluated with qRT-PCR after treatment with rhTXNDC5 and LPS at the indicated dosage or time period and normalized to GAPDH. In the presence of rhTXNDC5 and hypoxia, relative levels of IL-6 and IL-8 mRNA were evaluated with qRT-PCR **(E** and **F)**. The secretion of VEGF **(G** and **H)** was measured with ELISA. The data shown are the mean ± SD of experiments performed in triplicate. *$p < 0.05$, **$p < 0.01$, and *** $p < 0.001$.

supernatant of RA FLSs is sensitive to an inducer of ER stress, such as thapsigargin and tunicamycin. Recently, the current authors found that silencing TXNDC5 attenuated the induction of IL6 and IL8 in the presence of proinflammatory factors, such as LPS and TNF-α (*14*). The current study provides evidence that silencing TXNDC5 in RA FLSs suppresses the stimulatory effects of ER stressors on inflammatory factors. These findings clearly corroborate TXNDC5's involvement in promoting inflammation under ER stress in RA.

A previous study indicated that TXNDC5 protects endothelial cells from stress-induced apoptosis (*17*). Similar effects were also observed in RA FLSs as evinced by both cell viability and inflammatory factor expression. TXNDC5 expression is higher in RA FLSs than in osteoarthritis (OA) FLSs (*12*), so the aforementioned finding may also explain why RA FLSs were more resistant to apoptosis than OA FLSs. Indeed, a growing body of evidence suggests that the signaling pathways in ER stress and inflammation are interconnected through various mechanisms, including the production of reactive oxygen species (ROS) (*26*), the release of calcium from the ER (*27*), the activation of nuclear transcription factor NF-κB and the mitogen-activated protein kinase (MAPK) known as JUN N-terminal kinase (JNK) (*28*), and the induction of the acute-phase response. A previous study by the current authors indicated that TXNDC5 directly interacts with heat shock cognate 70 protein (HSC70) to sequester it in the cytoplasm and that HSC70 activates NF-κB signaling by destabilizing IκBβ protein (*14*). Importantly, RA has been found respond to TXNDC5 secretion by activating multiple inflammatory pathways and triggering the production of proinflammatory cytokines, suggesting that TXNDC5 is an important component of the micro-environment to mediate the pathological progression of RA. TXNDC5 may act as a mediator linking ER stress and the inflammatory response.

RA is the main source of many angiogenic factors, including VEGF, in the joints, and the level of VEGF has been proven to be highly correlated with RA disease activity (*29*). VEGF signaling is activated in response to ER stress, and activated VEGF signaling, in turn, buffers the levels of ER stress (*30*). A previous study by the current authors indicated that silencing TXNDC5 suppressed VEGF production in RA FLSs when stimulated with LPS and TNF-α. The current study

provides further evidence that rhTXNDC5 induces VEGF production during ER stress. These findings suggest that TXNDC5 may mediate angiogenesis under ER stress, and they also corroborate the close relationship between ER stress and angiogenesis during the progression of RA.

In summary, this study found that an increase in TXNDC5 as a cytoprotective response to ER stress may link ER stress and inflammation in RA. Specifically targeting TXNDC5 may be a potential treatment for RA.

Acknowledgements

This work was supported by the National Natural Science Foundation of China (grant nos. 81572544 and 81772760), the Shandong Taishan Scholarship (grant no. tsqn20161076), The Innovation Project of the Shandong Academy of Medical Sciences and the Youth Innovation Technology Plan of Shandong University (2019KJK003).

References

1. Kuo WS, Weng CT, Chen JH, Wu CL, Shiau AL, Hsieh JL, So EC, Wu PT, Chen SY. Amelioration of experimentally induced arthritis by reducing reactive oxygen species production through the intra-articular injection of water-soluble fullerenol. Nanomaterials (Basel). 2019; 9:909.
2. You S, Koh JH, Leng L, Kim WU, Bucala R. The tumor-like phenotype of rheumatoid synovium: Molecular profiling and prospects for precision medicine. Arthritis Rheumatol. 2018; 70:637-652.
3. Rana AK, Li Y, Dang Q, Yang F. Monocytes in rheumatoid arthritis: Circulating precursors of macrophages and osteoclasts and, their heterogeneity and plasticity role in RA pathogenesis. Int Immunopharmacol. 2018; 65:348-359.
4. Wang L, Song G, Zheng Y, Wang D, Dong H, Pan J, Chang X. miR-573 is a negative regulator in the pathogenesis of rheumatoid arthritis. Cell Mol Immunol. 2016; 13: 839-849.
5. Simon TA, Boers M, Hochberg M, Baker N, Skovron ML, Ray N, Singhal S, Suissa S, Gomez-Caminero A. Comparative risk of malignancies and infections in patients with rheumatoid arthritis initiating abatacept versus other biologics: A multi-database real-world study. Arthritis Res Ther. 2019; 21:228.
6. Carrión M, Frommer KW, Pérez-García S, Müller-Ladner U, Gomariz RP, Neumann E. The adipokine network in rheumatic joint diseases. Int J Mol Sci. 2019; 20:4091.
7. Asif Amin M, Fox DA, Ruth JH. Synovial cellular and molecular markers in rheumatoid arthritis. Semin Immunopathol. 2017; 39:385-393.
8. Rahmati M, Moosavi MA, McDermott MF. ER stress: A therapeutic target in rheumatoid arthritis? Trends Pharmacol Sci. 2018; 39:610-623.
9. Kurowska M, Rudnicka W, Kontny E, Janicka I, Chorazy M, Kowalczewski J, Ziółkowska M, Ferrari-Lacraz S, Strom TB, Maśliński W. Fibroblast-like synoviocytes from rheumatoid arthritis patients express functional IL-15 receptor complex: Endogenous IL-15 in autocrine fashion enhances cell proliferation and expression of Bcl-x(L) and Bcl-2. J Immunol. 2002; 169:1760-1767.
10. Shin YJ, Han SH, Kim DS, Lee GH, Yoo WH, Kang YM, Choi JY, Lee YC, Park SJ, Jeong SK, Kim HT, Chae SW, Jeong HJ, Kim HR, Chae HJ. Autophagy induction and CHOP under-expression promotes survival of fibroblasts from rheumatoid arthritis patients under endoplasmic reticulum stress. Arthritis Res Ther. 2010; 12:19.
11. Gao B, Lee SM, Chen A, Zhang J, Zhang DD, Kannan K, Ortmann RA, Fang D. Synoviolin promotes IRE1 ubiquitination and degradation in synovial fibroblasts from mice with collagen-induced arthritis. EMBO Rep. 2008; 9:480-485.
12. Chang X, Zhao Y, Yan X, Pan J, Fang K, Wang L. Investigating a pathogenic role for TXNDC5 in rheumatoid arthritis. Arthritis Res Ther. 2011; 13:124.
13. Chang X, Xu B, Wang L, Wang Y, Wang Y, Yan S. Investigating a pathogenic role for TXNDC5 in tumors. Int J Oncol. 2013; 43:1871-84.
14. Wang L, Dong H, Song G, Zhang R, Pan J, Han J. TXNDC5 synergizes with HSC70 to exacerbate the inflammatory phenotype of synovial fibroblasts in rheumatoid arthritis through NF-κB signaling. Cell Mol Immunol. 2018; 15:685-696.
15. Wang L, Song G, Chang X, Tan W, Pan J, Zhu X, Liu Z, Qi M, Yu J, Han B. The role of TXNDC5 in castration-resistant prostate cancer-involvement of androgen receptor signaling pathway. Oncogene. 2015; 34:4735-4745.
16. Chang X, Cui Y, Zong M, Zhao Y, Yan X, Chen Y, Han J. Identification of proteins with increased expression in rheumatoid arthritis synovial tissues. J Rheumatol. 2009; 36:872-880.
17. Chawsheen HA, Jiang H, Ying Q, Ding N, Thapa P, Wei Q. The redox regulator sulfiredoxin forms a complex with thioredoxin domain-containing 5 protein in response to ER stress in lung cancer cells. J Biol Chem. 2019; 294:8991-9006.
18. Wang L, Song G, Zheng Y, Tan W, Pan J, Zhao Y, Chang X. Expression of Semaphorin 4A and its potential role in rheumatoid arthritis. Arthritis Res Ther. 2015; 17:227.
19. Xu B, Li J, Liu X, Li C, Chang X. TXNDC5 is a cervical tumor susceptibility gene that stimulates cell migration, vasculogenic mimicry and angiogenesis by down-regulating SERPINF1 and TRAF1 expression. Oncotarget. 2017; 8:91009-91024.
20. Li M, Liu Y, Xia F, Wu Z, Deng L, Jiang R, Guo FJ. Progranulin is required for proper ER stress response and inhibits ER stress-mediated apoptosis through TNFR2. Cell Signal. 2014; 26:1539-1548.
21. Zhang L, Pavicic PG Jr, Datta S, Song Q, Xu X, Wei W, Su F, Rayman PA, Zhao C, Hamilton T. Unfolded protein response differentially regulates TLR4-induced cytokine expression in distinct macrophage populations. Front Immunol. 2019; 10:1390.
22. Chawsheen HA, Ying Q, Jiang H, Wei Q. A critical role of the thioredoxin domain containing protein 5 (TXNDC5) in redox homeostasis and cancer development. Genes Dis. 2018; 5:312-322.
23. Marinou I, Walters K, Dickson MC, Binks MH, Bax DE, Wilson AG. Evidence of epistasis between interleukin 1 and selenoprotein-S with susceptibility to rheumatoid arthritis. Ann Rheum Dis. 2009; 68:1494-1497.

24. Yoo SA, You S, Yoon HJ, Kim DH, Kim HS, Lee K, Ahn JH, Hwang D, Lee AS, Kim KJ, Park YJ, Cho CS, Kim WU. A novel pathogenic role of the ER chaperone GRP78/BiP in rheumatoid arthritis. J Exp Med. 2012; 209:871-886.
25. Veale DJ, Orr C, Fearon U. Cellular and molecular perspectives in rheumatoid arthritis. Semin Immunopathol. 2017; 39:343-354.
26. Lin Y, Jiang M, Chen W, Zhao T, Wei Y. Cancer and ER stress: Mutual crosstalk between autophagy, oxidative stress and inflammatory response. Biomed Pharmacother. 2019; 118:109249.
27. Barrera MJ, Aguilera S, Castro I, González S, Carvajal P, Molina C, Hermoso MA, González MJ. Endoplasmic reticulum stress in autoimmune diseases: Can altered protein quality control and/or unfolded protein response contribute to autoimmunity? A critical review on Sjögren's Syndrome. Autoimmun Rev. 2018; 17:796-808.
28. Ochoa CD, Wu RF, Terada LS. ROS signaling and ER stress in cardiovascular disease. Mol Aspects Med. 2018; 63:18-29.
29. Strunk J, Rumbaur C, Albrecht K, Neumann E, Müller-Ladner U. Linking systemic angiogenic factors (VEGF, angiogenin, TIMP-2) and Doppler ultrasound to anti-inflammatory treatment in rheumatoid arthritis. Joint Bone Spine. 2013; 80:270-273.
30. Binet F, Sapieha P. ER stress and angiogenesis. Cell Metab. 2015; 22:560-575.

Received December 21, 2019; Revised January 30, 2020; Accepted February 4, 2020.

*Address correspondence to:
Lin Wang, Shandong Medicinal Biotechnology Centre, Key Laboratory for Rare and Uncommon Diseases of Shandong Province, Key Lab for Biotechnology Drugs of Ministry of Health, Shandong First Medical University & Shandong Academy of Medical Sciences, Ji'nan 250062, China.
E-mail: wanglin.83@163.com

Released online in J-STAGE as advance publication February 16, 2020.

Original Article

DOI: 10.5582/irdr.2019.01112

Identification and clinical implications of a novel pathogenic variant in the *GJB2* gene causes autosomal recessive non-syndromic hearing loss in a consanguineous Iranian family

Mahbobeh Koohiyan*

Cancer Research Center, Shahrekord University of Medical Sciences, Shahrekord, Iran.

SUMMARY Mutations in the *GJB2* gene, which encodes the connexin26 protein and is involved in inner ear homeostasis, are the most common cause of autosomal recessive non-syndromic hearing loss (ARNSHL) in many populations. This study was aimed to determine the molecular etiology in a consanguineous Iranian family affected by profound ARNSHL. A comprehensive family history was obtained, and clinical evaluations and pedigree analysis were performed in the family with 4 affected members. After extraction of genomic DNA, the entire coding region of *GJB2* was directly sequenced in all family members. *In silico* analyses were also performed using available software tools. Sanger sequencing results showed a novel rare homozygous variant (c.109_110insG) in the *GJB2* gene. This frameshift variant in exon 2 of the *GJB2* gene fulfills the criteria of being categorized as pathogenic according to the American College of Medical Genetics and Genomics (ACMG) guideline. Confirmation was done with the co-segregation study and checking the frequency of the novel variant in 100 ethnically matched normal control subjects. The present study suggests that investigation of *GJB2* mutations may still be useful to determine the etiology of HL in Iran.

Keywords autosomal recessive non-syndromic hearing loss, *GJB2*, ACMG guideline, Iran

1. Introduction

Hearing loss (HL) is the most frequent sensory impairment, affecting 1 in 1,000 neonates worldwide (*http://hearing.screening.nhs.uk/nationalprog*). Many environmental factors, such as drug exposure, bacterial or viral infections and trauma, can cause HL; however, a significant proportion of cases is due to genetic factors. It is estimated that 70% of HL includes non-syndromic forms (NSHL), where the hearing deficit is the only clinical phenotype (*1*). Autosomal recessive mode of inheritance (ARNSHL) is highly heterogeneous, for which over 100 mapped loci are known to be involved (*http://hereditaryhearingloss.org*). Despite this, mutations in one single locus, DFNB1 (13q11-12) which contains the *GJB2* (NM_004004.5) and *GJB6* (NM_001110219.2) genes, account for 50% of the etiology in many European populations (*2*). Their identification of the first *GJB2* mutations causing hearing loss was soon followed by screenings that revealed a high frequency of *GJB2* mutations among subjects with NSHL (*3*). The gene is 5513 bp long and contains only two exons with exon 1 being untranslated. To date, 361 mutations in the *GJB2* gene have been identified with variable frequency among disparate world populations (*http://www.hgmd.cf.ac.uk*). c.35delG is the most common mutation in many populations such as Iran (*4,5*). Other mutations have a more specific origin. In Japanese, 235delC is more prevalent (*6*) and c.167delT is common in Ashkenazi Jews (*7*). Genetic diagnosis of ARNSHL is complicated, in terms of cost-effectiveness, due to the extreme genetic heterogeneity of this condition (*8-11*). So the high rate of *GJB2* related HL in most populations (*12,13*), coupled with the simple structure of the gene, which facilitated the design of different molecular tests, made screening for *GJB2* mutations the first step of genetic testing of ARNSHL (*14*). Here, we report a novel frameshift variant in a consanguineous Iranian family affected by profound ARNSHL. Our finding would be a great supplement for the *GJB2* pathogenic mutations and would make genetic counseling available for this family.

2. Methods

2.1. Participants and molecular genetic testing

Clinical examination was carried out on the four affected subjects; family CHM-1 from a village

located in southwest Iran. A comprehensive family history, including age of onset, exposure to ototoxic drugs during pregnancy and childhood infections, was obtained. Further clinical examinations such as temporal bone CT scan, thyroid ultrasound scan and thyroid hormone assays were also carried out to rule out the involvement of other body organs and syndromic HL forms (Figure 1). Air and bone conduction pure tone audiometry from 250 to 8000 Hz was obtained from all affected. All members of this family were sampled for further molecular studies. Blood samples were collected after written informed consent was obtained from all individuals or their legal guardians (if patients were under 18). Written parental consent to publish was also obtained. The study was approved by the review boards and ethics committees of the Shahrekord University of Medical Sciences.

Genomic DNA of subjects was extracted from peripheral blood lymphocytes using the standard salting out procedure (*15*). Purity and concentration of DNA samples were determined with a 1.2% agarose gel and spectrophotometer (Nanolytik, Dusseldorf, Germany). *GJB2* was screened for the coding region mutations (exon 2) using direct sequencing. The following primers were used for amplification of exon 2 of the *GJB2* gene: F1 (5′-GCTTACCCAGACTCAGAGAAG-3′) and R1 (5′-CTACAGGGGTTTCAAATGGTTGC-3′). The PCR reaction was performed as follows: 8 µL of Master Mix 2x (containing, $MgCl_2$, Taq DNA polymerase, and d NTPs (Applied Biosystems), 0.45 µL of each of the primers (10 pM), 2 µL DNA (50 ng), adjusted to 18 µL using ddH_2O. The amplification was initiated by denaturation at 95ºC for 5 minutes, followed by 30 cycles of 95ºC for 1 minute, 60ºC for 1 minute, and 72ºC for 1 minute, with a final extension cycle of 72ºC for 5 minutes. The automated Genetic Analyzer ABI 3130 XL (Applied Biosystems3130, Foster City, California, USA) was applied to directionally sequence PCR products using The Big Dye® Terminator v3.1 Cycle Sequencing Kit (Applied Biosystems3130, Foster City, California, USA).

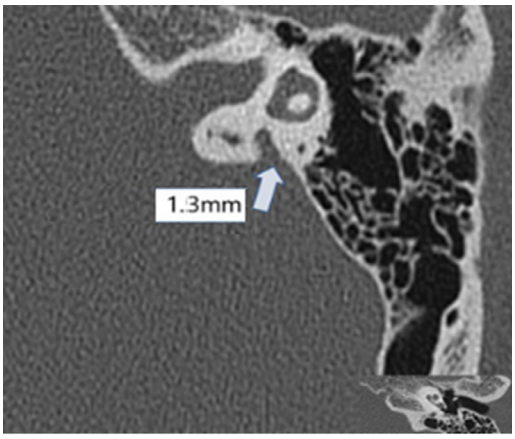

Figure 1. Temporal bone CT image of IV: 1. based on the criteria of diameter greater than 1.5 mm between the outer vestibular aqueduct and the vestibule of the total port foot or the midpoint of the isthmus is abnormal.

2.2. Computational analyses

We used Bioinformatics predictive tools including Mutation Taster, Polyphen and SIFT (*16*) to assess possible effects of mutations on the protein structure. Databases including: Connexin deafness homepage (*http://davinci.crg.es/deafness*), the Single Nucleotide Polymorphism database (dbSNP) (*http://www.ncbi.nlm.nih.gov/project/SNP*) and the 1000 Genomes Project (*http://browser.1000genomes.org*) were investigated for novel variants.

3. Results

3.1. Clinical Evaluation

In the four-generation consanguineous family CHM-1, four individuals (III-3, IV-2, IV-2, IV-3), were affected by pre-lingual bilateral profound sensorineural HL (Figure 2A). The deaf siblings had normal parents and helped to correctly define the mode of inheritance as autosomal recessive. In accordance with the subjects' interviews indicating a pre-lingual onset of deafness,

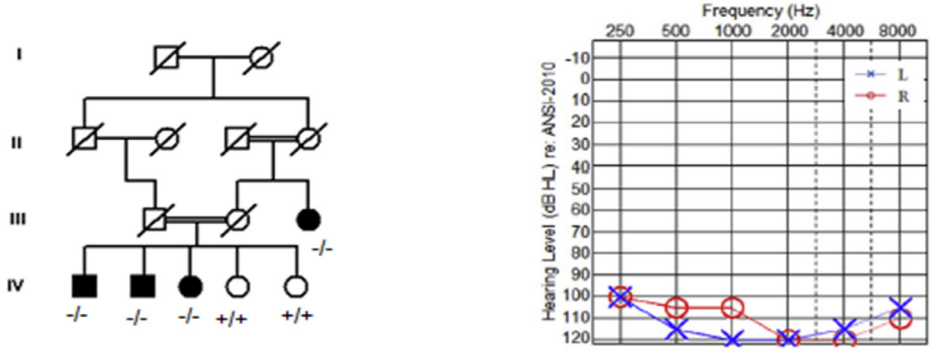

Figure 2. (A) Pedigree and segregation of the c.109_110insG variant in Iranian family CHM-1; −/−and +/+ respectively, show the homozygous (mutant) genotype and wild-type (WT) allele. (B) Right and left ear audiograms in the (IV: 2) patient.

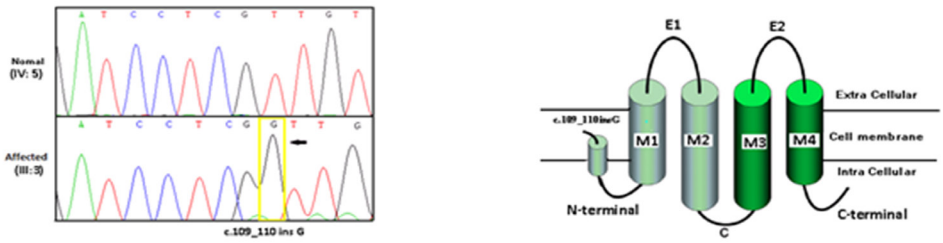

Figure 3. (A) Sequencing results of the c.109_110insG variant. (B) Schematic structure, domains and location of new variant of the Cx-26 protein in this study.

Table 1. Identified *GJB2* variant and *in silico* analyses

Mutation	Amino acid change	mutation type	Affected domain	classification	Functional effect			Segregates in the family	ACMG
					SIFT	CADD	Mutation Taster		
c.109_110insG	Val37Gly fs*11	Insertion	TM1	Trancated	Damaging	23	Disease causing	Yes	Pathogenic

Figure 4. The putative schematic representation of connexin26 protein and mutants in family CHM-1. The new variant c.109_110insG induced a frameshift mutation, caused a stop codon at position of amino acid 47, resulting in truncated connexin26 protein.

language acquisition was severely impaired in all affected individuals. More clinical examinations did not indicate any thyroid, skin, or ophthalmic abnormalities in affected members. Therefore, a syndromic form of HL was ruled out. The pedigree revealed several consanguineous marriages, suggesting ARNSHL in the offspring. Pure-tone audiometry in affected subjects showed flat audiograms characteristic of profound hearing impairment (Figure 2B).

3.2. *GJB2* Mutation Screening

Sequencing of GJB2 showed a novel homozygous variant (c.109_110insG) in the three affected siblings and their deaf aunts (Figure 3A). This variant was not found in other normal hearing family members, and was unique to those affected. Additionally, no other mutation in *GJB2* was identified in either of the subjects. c.109_110insG was not detected in 100 ethnicity-matched controls. All *in silico* programs predicted the c.109_110insG variant to have damaging effects (Table 1). Further analysis of c.109_110insG showed that the variant was not reported by 1000 genome project. This frameshift variant (p. Val37Gly*11) creates a stop codon at amino acids 47, resulting in a truncated protein with only 47 residues (versus 226 residues in the intact protein) (Figure 4). This practically means complete deletion of about 75% of the Cx26 protein. Figure 3 shows location of the variant in the first TM domain of the Cx26 protein.

4. Discussion

Various genes causing autosomal recessive non-syndromic hearing loss (ARNSHL) has been identified from Iran; but mutations related to the *GJB2* gene have been reported more frequently (*17-19*). Here, a novel homozygous variant identified by Sanger sequencing is reported within an Iranian family. The prevalence of *GJB2* mutations in Iran ranges from 4 to 38% in different ethnic groups (*14*). Such mutations are among the most frequent causes of HL in the world, and their prevalence exceeds over 50% in certain populations (*20*). *GJB2*, encodes the connexin26 (Cx26) gap-junction channel protein that underlies both intercellular communication among supporting cells and homeostasis of the cochlear fluids, endolymph and perilymph. Connexin proteins that contain one cytoplasmic domain (CL), two extracellular domains (E 1-2), and four transmembrane (TM 1-4) domains are concentrated within the membrane as connexons or hemi channels. Newly-synthesized Cx26 monomers

Figure 5. The identified variant c.109_110insG occurs at a highly conserved position (Val 37) in the Cx26 protein.

undergo conformational maturation and assembly into connexons when moving along the secretory pathway for delivery at the plasma membrane. Once there, Cx26 connexons may remain as so-called hemi channels, allowing for transport of diverse small molecules (less than 1 kDa) between the cytosol and the extracellular space. Until now, more than 100 mutations in *GJB2* have been reported to cause ARNSHL. They involve a wide spectrum of missense, nonsense, frame shift and splice site mutations (*http://davinci.crg.es/deafness*). However, one truncated mutation (c.35delG) is most frequent in the majority of the Caucasian population, with the carrier frequency as high as 2-4% (*21*). Here, we identified a novel homozygous variant, p. Val37Gly*11 in the first TM domain of the Cx26 protein, which is highly conserved in all species studied, and among different connexions (Figure 5). This frameshift variant was predicted to result in a truncated protein missing parts of the TM1-4, intervening loops and C-terminal (Figure 3B) which hampers Cx26 folding and oligomerization, leading to retention at the endoplasmic reticulum (ER) and ultimately causing a total loss of function (*22*). Interestingly, ER retention of the truncated subunits may induce in some cases the unfolded protein response, which in turn may eventually lead to apoptosis of cells expressing those *GJB2* mutant alleles (*23*). Unfortunately, there has been no in vitro functional assay to evaluate the mechanism by which *GJB2* mutations cause HL. In this case, other available lines of evidence such as those derived from segregation studies should be incorporated to pinpoint true genetic causes. The ACMG guidelines advocated our finding (*24*). The frameshift variant is a null allele leading to a truncated protein (PVS1), the variant was seen in all affected family members and was not detected in normal subjects (PS4) and bioinformatics analyses support a deleterious effect on Cx26 protein (PP3). It is located in a validated domain (TM1), this variant reduces the length of the protein (PM4) and was not reported by the dbSNP database and 1000 genome project (PM2). Thus, the variant is categorized as being pathogenic.

This study should be a great supplement for the role of *GJB2* mutations in the etiology of ARNSHL, in the Iranian population. Furthermore, our data support the view that the investigation of *GJB2* mutations is still the primary step before moving on to next-generation sequencing (NGS) (*25*). The use of Sanger sequencing for detection of *GJB2* mutations may be a faster and more economical diagnostic tool in individuals suffering with pre-lingual HL.

Acknowledgements

The author gratefully thanks all the patients who participated in this research.

References

1. Morton NE. Genetic epidemiology of hearing impairment. Ann N Y Acad Sci. 1991; 630:16-31.
2. Lucotte G, Mercier G. Meta-analysis of GJB2 mutation 35delG frequencies in Europe. Genet Test. 2001; 5:149-152.
3. Kelsell DP, Dunlop J, Stevens HP, Lench NJ, Liang JN, Parry G, Mueller RF, Leigh IM. Connexin 26 mutations in hereditary non-syndromic sensorineural deafness. Nature. 1997; 387:80-83.
4. Azadegan-Dehkordi F, Ahmadi R, Koohiyan M, Hashemzadeh-Chaleshtori M. Update of spectrum c. 35delG and c.-23+ 1G> A mutations on the GJB2 gene in individuals with autosomal recessive nonsyndromic hearing loss. Ann Hum Genet. 2019; 83:1-10.
5. Koohiyan M, Azadegan-Dehkordi F, Koohian F, Hashemzadeh-Chaleshtori M. Genetics of hearing loss in north Iran population: An update of spectrum and frequency of GJB2 mutations. J Audiol Otol. 2019; 23:175-180.
6. Abe S, Usami S, Shinkawa H, Kelley PM, Kimberling WJ. Prevalent connexin 26 gene (GJB2) mutations in Japanese. J Med Genet. 2000; 37:41-43.
7. Lerer I, Sagi M, Malamud E, Levi H, Raas-Rothschild A, Abeliovich D. Contribution of connexin 26 mutations to nonsyndromic deafness in Ashkenazi patients and the variable phenotypic effect of the mutation 167delT. Am J Med Genet. 2000; 95:53-56.
8. Zarepour N, Koohiyan M, Taghipour-Sheshdeh A, Nemati-Zargaran F, Saki N, Mohammadi-Asl J, Tabatabaiefar MA, Hashemzadeh-Chaleshtori M. Identification and Clinical Implications of a Novel MYO15A Variant in a Consanguineous Iranian Family by Targeted Exome Sequencing. Audiol Neurootol. 2019; 24:25-31.
9. Koohiyan M. A systematic review of SLC26A4 mutations causing hearing loss in the Iranian population. Int J Pediatr Otorhinolaryngol. 2019; 125:1-5.
10. Koohiyan M, Reiisi S, Azadegan-Dehkordi F, Salehi M,

Abtahi H, Hashemzadeh-Chaleshtori M, Noori-Daloii MR, Tabatabaiefar MA. Screening of 10 DFNB loci causing autosomal recessive non-syndromic hHearing loss in two Iranian pPopulations negative for GJB2 mutations. Iran J Public Health. 2019; 48:1704-1713.
11. Koohiyan M, Noori-Daloii MR, Hashemzadeh-Chaleshtori M, Salehi M, Abtahi H, Tabatabaiefar MA. A novel pathogenic variant in the CABP2 gene causes severe nonsyndromic hearing loss in a consanguineous Iranian family. Audiol Neurootol. 2019; 24:258-263.
12. Koohiyan M. Genetics of hereditary hearing loss in the Middle East: A systematic review of the carrier frequency of the GJB2 mutation (35delG). Audiol Neurootol. 2019; 24:161-165.
13. Koohiyan M, Azadegan-Dehkordi F, Koohian F, Abolhasani M, Hashemzadeh-Chaleshtori M. Genetics of hereditary hearing loss in east Iran population: A systematic review of GJB2 mutations. Intractable Rare Dis Res. 2019; 8:172-178.
14. Koohiyan M, Ahmadi A, Koohian F, Aghaei S, Amiri B, Hashemzadeh-Chaleshtori M. An update of spectrum and frequency of GJB2 mutations causing hearing loss in the south of Iran: A literature review. Int J Pediatr Otorhinolaryngol. 2019; 119:136-140.
15. Miller SA, Dykes DD, Polesky HF. A simple salting out procedure for extracting DNA from human nucleated cells. Nucleic Acids Res. 1988; 16:1215.
16. Kumar P, Henikoff S, Ng PC. Predicting the effects of coding non-synonymous variants on protein function using the SIFT algorithm. Nat Protoc. 2009; 4:1073-1081.
17. Azadegan-Dehkordi F, Bahrami T, Shirzad M, Karbasi G, Yazdanpanahi N, Farrokhi E, Koohiyan M, Tabatabaiefar MA, Hashemzadeh-Chaleshtori M. Mutations in GJB2 as major causes of autosomal recessive non-syndromic hearing loss: first report of c. 299-300delAT mutation in Kurdish population of Iran. J Audiol Otol. 2019; 23:20-26.
18. Koohiyan M, Hashemzadeh-Chaleshtori M, Salehi M, Abtahi H, Reiisi S, Pourreza MR, Noori-Daloii MR, Tabatabaiefar MA. GJB2 mutations causing autosomal recessive non-syndromic hearing loss (ARNSHL) in two Iranian populations: Report of two novel variants. Int J Pediatr Otorhinolaryngol. 2018; 107:121-126.
19. Koohiyan M, Koohian F, Azadegan-Dehkordi F. GJB2-related hearing loss in central Iran: Review of the spectrum and frequency of gene mutations. Ann Hum Genet. 2019 Sep 11. doi: 10.1111/ahg.12354.
20. Gasparini P, Rabionet R, Barbujani G, Melçhionda S, Petersen M, Brøndum-Nielsen K, Metspalu A, Oitmaa E, Pisano M, Fortina P, Zelante L, Estivill X. High carrier frequency of the 35delG deafness mutation in European populations. Eur J Hum Genet. 2000; 8:19-23.
21. Green GE, Scott DA, McDonald JM, Woodworth GG, Sheffield VC, Smith RJ. Carrier rates in the midwestern United States for GJB2 mutations causing inherited deafness. JAMA. 1999; 281:2211-2216.
22. Xiao Z, Yang Z, Liu X, Xie D. Impaired membrane targeting and aberrant cellular localization of human Cx26 mutants associated with inherited recessive hearing loss. Acta Otolaryngol. 2011; 131:59-66.
23. Lindholm D, Korhonen L, Eriksson O, Kõks S. Recent insights into the role of unfolded protein response in ER stress in health and disease. Front Cell Dev Biol. 2017; 5:48.
24. Richards S, Aziz N, Bale S, Bick D, Das S, Gastier-Foster J, Grody WW, Hegde M, Lyon E, Spector E, Voelkerding K, Rehm H; ACMG Laboratory Quality Assurance Committee. Standards and guidelines for the interpretation of sequence variants: a joint consensus recommendation of the American College of Medical Genetics and Genomics and the Association for Molecular Pathology. Genet Med. 2015; 17:405-424.
25. Koohiyan M. Next generation sequencing and genetics of hereditary hearing loss in the iranian population: New insights from a systematic review. Int J Pediatr Otorhinolaryngol. 2019; 129:109756.

Received December 3, 2019; Revised January 5, 2020; Accepted January 17, 2020

Address correspondence to:
Mahbobeh Koohiyan, Cancer Research Center, Shahrekord University of Medical Sciences, Shahrekord 8813833435, Iran.
E-mail: m_kouhiyan@yahoo.com

Released online in J-STAGE as advance publication February 3, 2020.

Original Article

DOI: 10.5582/irdr.2020.01019

Health assessment of patients with achondroplasia, pseudoachondroplasia, and rickets based on 3D non-linear diagnostics

Jian Zhang[1,2,§], Yanqin Lu[1,2,§,*], Yanzhou Wang[3], Tianyou Li[3], Chuanming Peng[1,2], Shie Zhang[1,2], Qingxia Gao[2], Wei Li[2], Chunshang Liu[2], Jinxiang Han[1,2,*]

[1] School of Medicine and Life Sciences, University of Jinan, Shandong Academy of Medical Sciences, Ji'nan, China;
[2] Key Laboratory for Biotech Drugs of the National Health Commission, Key Laboratory for Rare & Uncommon Diseases of Shandong Province, Shandong Medicinal Biotechnology Centre, Shandong First Medical University & Shandong Academy of Medical Sciences, Ji'nan, China;
[3] Shandong Provincial Hospital Affiliated with Shandong First Medical University, Ji'nan, China.

SUMMARY The goal of this study was to analyze diminishment of the functional status of the skeleton, parts of organs, regions of the brain, connective tissues, and chondrocytes in patients with achondroplasia (ACH), pseudoachondroplasia (PSACH), and rickets. Three-dimensional non-linear scanning (3D-NLS) was used to analyze the functional status of patients with genetic bone disorders, including 7 patients with ACH, 3 patients with PSACH, and 3 patients with rickets. Results indicated that the percentage of patients with long bones in the decompensatory phase did not differ depending on whether they had ACH, PSACH, or rickets. Joints in the decompensatory phase did not differ in patients with ACH except for the right hip (16.67%). Various joints were in the decompensatory phase (16.7-33.3%) in patients with rickets. The thoracic vertebrae, lumbar vertebrae, and liver were in the decompensatory phase in all 3 groups of patients. Connective tissues were in the decompensatory phase in 33.33% of patients with ACH. None of the patients with PSACH had chondrocytes in the decompensatory phase but 66.67% of patients with ACH or rickets did. Regions of the brain in the decompensatory phase were most prevalent in patients with rickets or ACH but not in patients with PSACH. In conclusion, diagnosis based on 3D-NLS was able to identify the functional status of genetic bone disorders. Some areas of decompensation were common to the 3 diseases studied but other areas were specific to a given disease.

Keywords achondroplasia, pseudoachondroplasia, rickets, health assessment, 3-D non-linear scanning technology

1. Introduction

Since three-dimensional non-linear scanning (3D-NLS) was first used in diagnostics in the late 90s, it has made significant progress thanks to the introduction of new technologies and new facilities (*1*). A clinical examination with 3D-NLS and the resulting diagnosis are based on a three-dimensional reconstruction combined with spectral-entropy analysis (SEA) of the scanned site. This technique is more visual and accurate than conventional methods in many cases, such as diagnosis of degenerative-dystrophic damage to intervertebral discs (*2*), damage to the ankle (*3*), and screening for potential vascular pathologies (*4*).

Achondroplasia (ACH, MM:100800), also known as chondrodysplasia fetalis or chondrodystrophic dwarfism, is an autosomal-dominant genetic disorder. Its incidence is between one in 77,000 and one in 15,000 (*5*). Its clinical features include an enlarged head, frontal bossing, short limbs, and trident hands. All of these features can be found at birth. Other features, such as limited elbow extension, tibial bowing, and thoracolumbar kyphosis, may also be present (*6,7*).

Pseudoachondroplasia (PSACH, MIM 177170) is another autosomal-dominant genetic disorder. It is clinically characterized by a normal head and face, lordotic lumbar spine, and epiphysis and metaphysis where epiphyseal development is delayed and metaphyses widen (*8*). It might be accompanied by symptoms of tibial bowing and early osteoarthritis due to a non-concentric load (hips and knees) (*9,10*).

Rickets is a group of heterozygous diseases caused either by a vitamin D deficiency (*11*) or dominant (*12*) or recessive genetic disorders (*13,14*). Its clinical features include delayed fontanelle closure, beading of the ribs and a pigeon chest, scoliosis, lumbar lordosis, bowed legs, muscle weakness, and metaphyseal changes that result in thickening of the wrists and ankles and even deformity of the hips (*15*).

The aim of this study was to use 3D-NLS to evaluate the functional status of the skeleton, parts of organs, regions of the brain, connective tissues, and chondrocytes in patients with ACH, PSACH, and rickets and to analyze the biochemical equilibrium between damage to organs, tissues, and cells and pathological changes.

2. Materials and Methods

2.1. Patients

This study was conducted in accordance with the Helsinki Declaration and was approved by the Ethics Committee of the Shandong Medicinal Biotechnology Centre (No. 2016-04). Informed consent was provided by all patients or their guardians. This study included 7 patients with ACH (five were 2-6 years of age, one was 23 years of age), 3 patients with PSACH (two were 3 years of age and one was 10 years of age), and 3 patients with rickets (3, 4, and 28 years of age, respectively). All patients were diagnosed clinically.

2.2. Health assessment

The functional status of target areas, including the skeleton (long bones and joints), regions of the brain (frontal lobes, parietal lobes, temporal lobes, and occipital lobes), parts of organs (heart, liver, kidneys, and lungs), connective tissues, and chondrocytes, was evaluated in patients diagnosed with ACH, PSACH and rickets using the "Metatron"-4025 system (IPP, Russia) equipped with high-frequency digital trigger sensors (4.9 GHz). The health assessment was graded according to the following functional statuses: good health, standard health, self-repair, start of decline, and excessive damage or a critical state. Whether patients with ACH, PSACH, and rickets were in a compensatory phase (good health, standard health, or self-repair) or a decompensatory phase (start of decline or excessive damage or a critical state) of their disease was analyzed and compared.

3. Results

3.1. Functional status of the skeleton

Figure 1 shows that the percentage of patients with long bones in the decompensatory phase did not differ among the 3 groups of patients. The functional status of joints (Figures 2 and 3) in the decompensatory phase did not differ for patients with ACH (66.67%) except for the right wrist or for patients with PSACH. The percentage of patients with joints in the decompensatory phase differed in patients with rickets: the shoulder was in the decompensatory phase in 33.33%, the right wrist was in the decompensatory phase in 33.33%, the right hip was in the decompensatory phase in 16.67%, and the ankle was in the decompensatory phase in 33.33%.

Figure 3 shows that the percentage of patients with cervical vertebrae in the decompensatory phase did not differ depending on whether they had ACH or PSACH, but it did differ (66.67%) in patients with rickets. The thoracic vertebrae were in the decompensatory phase in 16.67% of patients with ACH, 100% of patients with PSACH, and 33.33% of patients with rickets.

The lumbar vertebrae were in the decompensatory phase in 83.33% of patients with ACH, 50.00% of patients with PSACH, and 66.67% of patients with rickets. The sternum was in the decompensatory phase in 50.00% of patients with ACH or PSACH but did not differ in patients with rickets.

3.2. Functional status of parts of organs

The left lobe of the liver was in the decompensatory phase in 50.00% of patients with ACH, 100.00% of patients with PSACH, and 33.33% of patients with rickets while the right lobe of the liver was in the decompensatory phase in 66.67% of patients with ACH, 50.00% of patients with PSACH, and 33.33% of patients with rickets (Figures 4 and 5).

The percentage of patients with the heart or left kidney in the decompensatory phase did not differ among the 3 groups of patients, but the right kidney was in the decompensatory phase in 16.67% of patients with ACH, 0% of patients with PSACH, and 33.33% of patients with rickets. The lungs were in the decompensatory phase in 16.70% of patients with ACH but did not differ in patients with PSACH or rickets. The left hilum was in the decompensatory phase in 83.33% of patients with ACH, 50.00% of patients with PSACH, and 66.67% of patients with rickets, while the right hilum was in the decompensatory phase in 50.00% of patients with ACH, 100% of patients with PSACH, and 100% of patients with rickets.

3.3. Functional status of tissues and cells

The functional status of connective tissues and chondrocytes is shown in Figure 5. Connective tissues were in the decompensatory phase in 33.33% of patients with ACH. The percentage of patients with chondrocytes in the decompensatory phase did not differ in patients with PSACH but it did differ (66.67%) in patients with ACH or rickets.

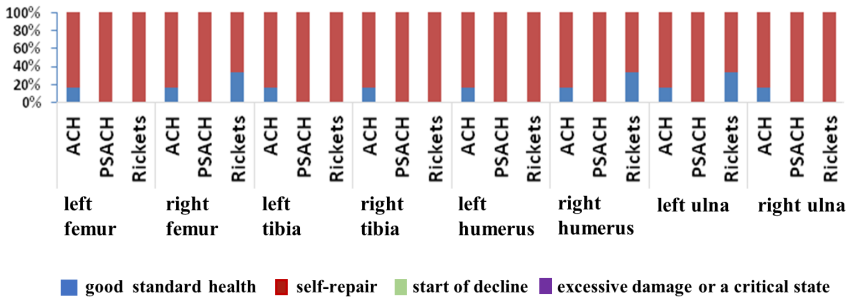

Figure 1. Functional status of long bones

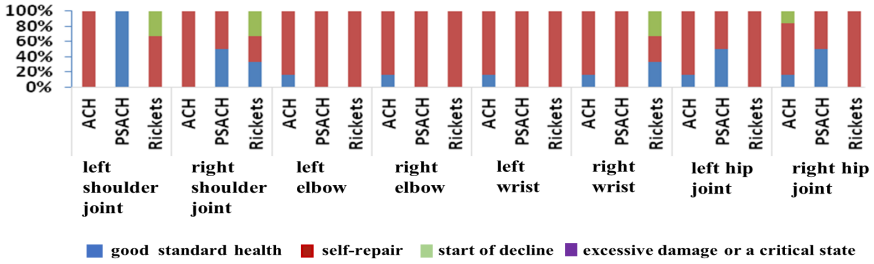

Figure 2. Functional status of joints

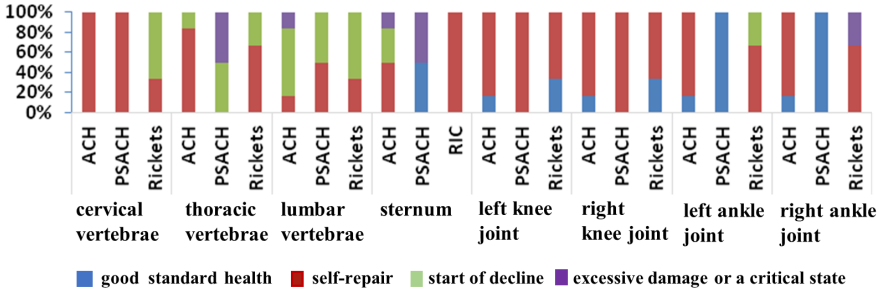

Figure 3. Functional status of parts of the spine and joints

Figure 4. Functional status of parts of organs

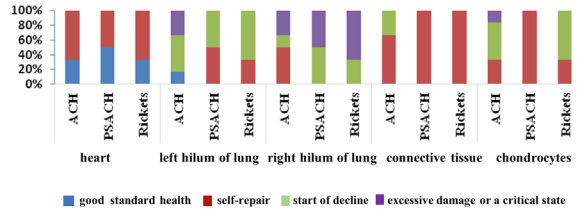

Figure 5. Functional status of parts of organs, connective tissue, and cartilage

3.4. Functional status of the brain

The functional status of regions of the brain is shown in Figure 6. The left frontal lobe and right parietal lobe were in the decompensatory phase in 33.33% of patients with rickets. The right frontal lobe, right temporal lobe, and medulla oblongata were in the decompensatory phase in 16.67% of patients with ACH. The left temporal lobe and left occipital lobe were in the decompensatory phase in 50.00% of patients with ACH, 0% of patients with PSACH, and 33.33% of patients with rickets.

The percentage of patients with the left frontal lobe and right occipital lobe in the decompensatory phase did not differ among the 3 groups of patients.

4. Discussion

Three-D NLS is able to depict pathological areas

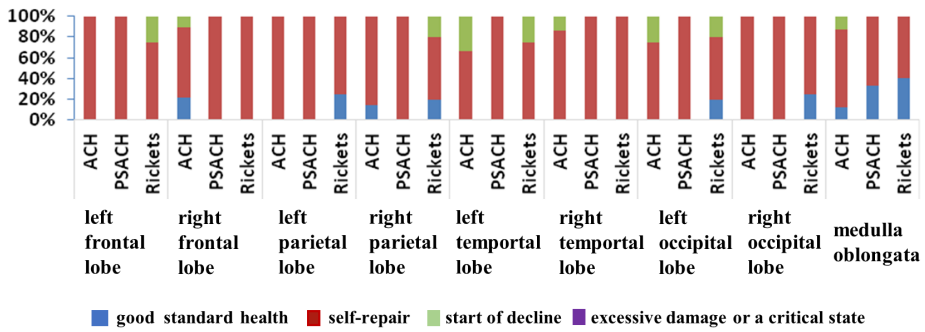

Figure 6. Functional status of cerebral regions

through reconstruction of three-dimensional high-resolution images of scanned sites. It offers accurate positioning and real-time information, and its sensitivity is comparable to that of computed tomography (CT) (*4*). In addition, it is cheap, simple, and non-invasive.

When diagnosing cholangiocarcinoma in patients with intrahepatic cholangiectasis, 3D-NLS compensates for the indistinct location according to conventional non-invasive methods such as ultrasound scanning, magnetic resonance imaging (MRI), and CT and it avoids injury to the human body by an invasive examination, such as endoscopic retrograde cholangiopancreatography (*16*).

The current study graded and quantitatively analyzed the functional status of the skeleton, regions of the brain, parts of organs, connective tissues, and chondrocytes. The percentage of patients with long bones in the decompensatory phase did not differ depending on whether they had ACH, PSACH, or rickets. The percentage of patients with the shoulder, right wrist, or ankle in the decompensatory phase differed in patients with rickets. The results agreed with clinical features such as swelling of joints like the wrists and ankles (*17*). The right hip was in the decompensatory phase only in patients with ACH, which might be related with the square-shaped ileum, small sacroiliac notches, or other clinical features of ACH (*17*). A markedly higher percentage of patients with ACH had thoracic vertebrae and lumbar vertebrae in the decompensatory phase compared to the other 2 groups. This was consistent with the thoracolumbar kyphosis characteristic of ACH (*18,19*). Decompensation in the thoracic spine of patients with PSACH was correlated with abnormal spine development (*20*). A relatively high percentage of patients with ACH had connective tissues and chondrocytes in the decompensatory phase; this is presumably related to the clinical manifestations of muscle hypotonia and soft tissue laxity, which might be responsible for thoracolumbar kyphosis. The liver was in the decompensatory phase in over 1/3 of patients with ACH, PSACH, or rickets. The hilum of the lungs was in the decompensatory phase in over half of the patients with ACH, PSACH, or rickets. The long bones were normal while the thoracic and lumbar vertebrae were affected in all the groups of patients. Abnormalities of the wrists and ankles in patients with rickets differed from those in patients with ACH or PSACH. The hips of patients with ACH differed from those in patients with the other two diseases.

In conclusion, all 3 of the diseases studied involved skeletal dysplasia with similar clinical features. As described here, 3D-NLS offers a new avenue to accurate differential diagnosis. A limitation of this study was the small sample of patients with PSACH or rickets. Therefore, these 3 diseases need to be studied further. In summary, 3D-NLS is potentially an alternative method with which to diagnose genetic bone disorders.

Acknowledgements

This work was supported by a grant from the Shandong Government (2016GSF201222, 2015ZRC03171, 2016ZDJS07A10). The authors wish to thank all of the patients who participated in this study.

References

1. Nesterov V. Main tendencies of non-linear technology development. Acta Medica Medianae. 2013; 52:41-44.
2. Nesterov VI. CT and 3D NLS-diagnostics of degenerative-dystrophic damages of intervertebral discs. Kerala Journal of Orthopaedics. 2013; 26:110-112.
3. Nesterov V. MRI and NLS-diagnostics of ankle joint damages. Kerala Journal of Orthopaedics. 2013; 26:67-69.
4. Vagulin VM, Patrushev SM, Nesterov VI. 3D NLS-method in vascular pathology diagnosis. CorSalud. 2013; 5:237-239. (in Spanish)
5. Baujat G, Legeai-Mallet L, Finidori G, Cormier-Daire V, Le Merrer M. Achondroplasia. Best Pract Res Clin Rheumatol. 2008; 22:3-18.
6. Carter EM, Davis JG, Raggio CL. Advances in understanding etiology of achondroplasia and review of management. Curr Opin Pediatr. 2007; 19:32-37.
7. Hoover-Fong J, McGready J, Schulze K, Alade AY, Scott CI. A height-for-age growth reference for children with achondroplasia: Expanded applications and comparison with original reference data. Am J Med Genet A. 2017; 173:1226-1230.
8. Posey KL, Hayes E, Haynes R, Hecht JT. Role of TSP-5/COMP in pseudoachondroplasia. Int J Biochem Cell

Biol. 2004; 36:1005-1012.
9. Posey KL, Alcorn JL, Hecht JT. Pseudoachondroplasia/ COMP - Translating from the bench to the bedside. Matrix Biol. 2014; 37:167-173.
10. Unger S, Hecht JT. Pseudoachondroplasia and multiple epiphyseal dysplasia: New etiologic developments. Am J Med Genet. 2001; 106:244-250.
11. Glorieux FH, Pettifor JM. Vitamin D/dietary calcium deficiency rickets and pseudo-vitamin D deficiency rickets. Bonekey Rep. 2014; 3:524.
12. Balsan S, Tieder M. Linear growth in patients with hypophosphatemic vitamin D-resistant rickets: Influence of treatment regimen and parental height. J Pediatr. 1990; 116:365-371.
13. Feng JQ, Ward LM, Liu S, *et al.* Loss of DMP1 causes rickets and osteomalacia and identifies a role for osteocytes in mineral metabolism. Nat Genet. 2006; 38:1310-1315.
14. Lorenz-Depiereux B, Schnabel D, Tiosano D, Hausler G, Strom TM. Loss-of-function ENPP1 mutations cause both generalized arterial calcification of infancy and autosomal-recessive hypophosphatemic rickets. Am J Hum Genet. 2010; 86:267-272.
15. Wagner CL, Greer FR. Prevention of rickets and vitamin D deficiency in infants, children, and adolescents. Pediatrics. 2008; 122:1142-52.
16. Shvack AY, Kuznetsova TG. Lopukhov GA. Three-dimensional non-linear diagnostics of cholangiocarcinoma in patients suffering from intrahepatic cholangiectasis. Actual Aspects of NLS-Diagnostics. 2013; 1:8-12.
17. Ohata Y, Ozono K. Updates on rickets and osteomalacia: Guidelines for diagnosis of rickets and osteomalacia. Clin Calcium. 2013; 23:1421-1428.
18. Kumar CP, Song HR, Lee SH, Suh SW, Oh CW. Thoracic and lumbar pedicle morphometry in achondroplasia. Clin Orthop Relat Res. 2007; 454:180-185.
19. Khan BI, Yost MT, Badkoobehi H, Ain MC. Prevalence of scoliosis and thoracolumbar kyphosis in patients with achondroplasia. Spine Deform. 2016; 4:145-148.
20. McKay SD, Al-Omari A, Tomlinson LA, Dormans JP. Review of cervical spine anomalies in genetic syndromes. Spine (Phila Pa 1976). 2012; 37:E269-277.

Received February 17, 2020; Revised February 25, 2020; Accepted February 28, 2020.

[§]These authors contributed equally to this work.

**Address correspondence to:*
Yanqin Lu and Jinxiang Han, Shandong First Medical University & Shandong Academy of Medical Sciences, 18877 Jingshi Road, Ji'nan, China 250062.
E-mail: yanqinlu@yahoo.com, mls_hanjx@ujn.edu.cn

Brief Report

DOI: 10.5582/irdr.2020.01013

Replication study of four keloid-associated polymorphisms in patients of European descent – a single centre study

Andrzej Dmytrzak[1], Agnieszka Boroń[2], Beata Łoniewska[3], Jeremy S.C. Clark[2], Mariusz Kaczmarczyk[2], Andrzej Ciechanowicz[2,*]

[1] Aesthetic Med, Szczecin, Poland;
[2] Department of Clinical and Molecular Biochemistry, Pomeranian Medical University, Szczecin, Poland;
[3] Department of Neonatal Diseases, Pomeranian Medical University, Szczecin, Poland.

SUMMARY Keloid is defined as a benign dermal fibro-proliferative growth that extends outside the original wound and invades adjacent dermal tissue. Its pathogenesis is complex and much evidence suggests the influence of genetic factors, including the rs873549, rs1511412, rs940187 and rs8032158 polymorphisms associated with keloid risk in Japanese patients. The aim of our study was to investigate possible associations between rs873549, rs1511412, rs940187 and rs8032158 variants and the risk of keloid in Polish patients of European descent. The genetic polymorphisms were identified by sequencing genomic DNA extracted from peripheral blood leukocytes from 86 keloid patients and from newborn cord blood leukocytes from 100 newborns as a control group. No significant differences ($p > 0.05$) in the distributions of rs873549, rs1511412, rs940187 and rs8032158 alleles were found between keloid patients and newborn controls (26.7% *vs*. 25.5%, 9.9% *vs*.7.0%, 19.8% *vs*. 12.5%, and 41.9% *vs*. 33.5%, respectively). Logistic regression with adjustment for gender revealed that only the CC homozygous genotype of rs8032158 polymorphism was significantly more frequent in keloid patients as compared with controls (19.8% *vs*. 11.0%, respectively). Our results suggest that in contrast to Asian populations only the rs8032158 polymorphism at *locus* 15q21.3 is associated with the susceptibility to keloid scarring in patients of European descent.

Keywords association study, genetic polymorphism, Caucasians, keloid

1. Introduction

Keloid is defined as benign proliferative scars that grow beyond the confines of original insults to the skin, invading into adjacent normal tissue. This differentiates keloid from hypertrophic scars, which are raised scars that remain within the boundaries of the inciting cutaneous insult (*1*). The pathogenesis of keloid is complex, and much evidence suggests the influence of genetic factors. The main sources of evidence indicating genetic predisposition to keloid formation are as follows: familial inheritance, ethnic differences in keloid prevalence, and the identification of chromosomal *loci* or SNPs (Single Nucleotide Polymorphisms) for keloid *via* linkage analysis or association studies, respectively (*1,2*).

In 2010 Nakashima *et al*. through a multistage genome-wide association study identified four SNPs, which significantly predisposed to keloid in the Japanese population. The authors reported that the most significant association with keloid was with rs873549 on chromosome 1q41, with rs1511412 and rs940187 in two separate linkage disequilibrium (LD) blocks on chromosome 3q22.3-23, and with rs8032158 on chromosome 15q21.3 (*3*). So far the associations of SNPs on chromosomes: 1q41, 3q22.3-23 and 15q21.3 with keloid have been confirmed in Asian patients (*4-8*) and also that the latter *locus* was also associated with predisposition to keloid in Afro-Americans (*9*). Therefore, this raises the question whether the four SNPs also predispose to keloid formation in patients of European descent. To further address this issue we decided to investigate the possible associations of rs873549, rs1511412, rs940187 and rs8032158 polymorphisms with the risk of keloid in Polish patients.

2. Materials and Methods

2.1. Keloid group and controls

The study group consisted of 86 consecutive patients

with keloid (17 males and 69 females, aged from 18 to 70 years old), who were treated with surgical excision at a cosmetic surgery clinic (Aesthetic Med, Szczecin, Poland). Forty eight patients had been diagnosed with keloid scarring as a postoperative complication from previous surgery; multiple keloid scars were present in 26 patients; and 10 subjects reported the presence of keloid in first degree relatives. The control group consisted of 100 healthy, full-term newborns (52 males and 48 females) randomly chosen from the Newborn DNA Repository at the Pomeranian Medical University in Szczecin. All patients in the study and control groups were Poles of European descent. The study was conducted in accordance with the Declaration of Helsinki (2013) and was approved by bioethics committee at the Pomeranian Medical University in Szczecin. Patients' informed consent for cases and parental informed consent for newborn controls were obtained.

2.2. Genotyping

The rs873549, rs1511412, rs940187 and rs8032158 polymorphisms were identified by sequencing amplicons from genomic DNA (sequences of primers for polymerase chain reaction are available upon request) extracted from peripheral blood leukocytes from keloid patients and from newborn cord blood leukocytes from newborns, as described previously (*10*).

2.3. Statistical analyses

Possible divergence of genotype frequencies from Hardy-Weinberg equilibrium and differences in alleles frequencies between groups were assessed using χ^2 tests. Genotype frequencies between groups were compared by logistic regression with adjustment for gender (note that the controls/cases were not matched for gender) in additive, dominant or recessive modes of inheritance for the risk allele. Calculations were performed using a data analysis software system (Dell Statistica, version 13. Dell Inc. 2016, software.dell.com). A two-tailed $p < 0.05$ was considered statistically significant.

3. Results and Discussion

The rs873549, rs1511412, rs940187 and rs8032158 genotype distributions in the control group conformed to expected Hardy-Weinberg equilibria ($p = 0.793$, p = 0.452, $p = 0.189$ and $p = 0.920$, respectively). No significant differences in the distributions of rs873549, rs1511412, rs940187 and rs8032158 alleles were found between keloid patients and newborn controls (Table 1). Logistic regression with adjustment for gender revealed no significant associations between rs873549, rs1511412, rs940187 or rs8032158 and predisposition to keloid in additive or dominant modes of inheritance for the risk allele (data not shown). There were also no significant associations between rs873549, rs1511412 or rs940187 polymorphisms and keloid risk in recessive mode of inheritance for the risk allele. Only the CC homozygous genotype of rs8032158 polymorphism was significantly more frequent in keloid patients as compared with controls (Table 1). Our results confirm the association of rs8032158 polymorphism at *locus* 15q21.3 with keloid, as well as showing its occurrence in another ethnic group. However, we are fully aware that a major limitation of our study is relatively low statistical power due to small sample size, and further studies might well show associations for the other polymorphisms. Our calculation for rs8032158 in the recessive mode of inheritance (performed with the Genetic Power Calculator; *http://zzz.bwh.harvard.edu/gpc/*) revealed that a minimum of 238 keloid patients would be necessary to achieve 80% statistical power under the assumption of a 5% type I error rate (α), and therefore the discovery of an association was fortuitous but substantial.

The rs8032158 SNP maps to intron 4 of the *NEDD4* (Neural Precursor Cell Expressed, Developmentally Down-Regulated 4) gene encoding a ubiquitin ligase (*3*). In addition, rs8032158 is in linkage disequilibrium with rs2271289 in intron 5 of *NEDD4*, which was revealed to be associated with keloid in two independent studies of Chinese Han (*4,8*). On the other hand, the DNA sequencing of the *NEDD4* region in 94 keloid patients has excluded linkage of rs8032158 with hidden causative mutations (*3*). Using an *in silico* approach (*https://*

Table 1. Association analysis of four SNPs (rs873549, rs1511412, rs940187 and rs8032158) with keloid in Caucasians

SNP[a] (Position)	Allele[b] (1/2)	Cases 1/2	Controls 1/2	p	Cases			Controls			p^c	OR (95% CI)[d]
					11	12	22	11	12	22		
rs873549 (1: 222,271,767)	T/C	126/46	149/51	0.785	52	22	12	56	37	7	0.453	1.48 (0.53-4.13)
rs1511412 (3: 138,713,704)	G/A	155/17	186/14	0.316	69	17	0	86	14	0	0.236	1.65 (0.72-3.80)
rs940187 (3: 138,841,593)	C/T	138/34	175/25	0.056	55	28	3	78	19	3	0.896	1.12 (0.20-6.35)
rs8032158 (15: 56,194,877)	T/C	100/72	133/67	0.096	31	38	17	44	45	11	0.046	2.47 (1.01-6.08)

[a]SNP position was indexed to the NCBI build 37 (GRCh37.p13). [b]Allele 1 and allele 2 were defined as the non-susceptible allele or the risk allele, respectively. [c]p values for logistic regression with adjustment for gender in recessive mode of inheritance for the risk allele. [d]OR (Odds Ratios) and CI (Confidence Intervals) were calculated using the non-susceptible allele as a reference.

snpinfo.niehs.nih.gov/ and *http://www.regulomedb.org/*) we were not able to confirm any direct functional significance of either rs8032158 or rs2271289. It has, however, been suggested that *NEDD4* variants might have reduced expression which in turn may cause upregulation of the Transforming Growth Factor-β (TGF-β) signaling pathway, resulting in enhancement of fibroblast proliferation and keloid formation (*3*).

In conclusion, this study has confirmed that among the rs873549, rs1511412, rs940187 and rs8032158 associations previously associated with keloid in Asian patients, only the latter at *locus* 15q21.3 also predisposes to keloid in patients of European descent.

References

1. Glass DA 2nd. Current understanding of the genetic causes of keloid formation. J Investig Dermatol Symp Proc. 2017; 18:S50-S53.
2. Halim AS, Emami A, Salahshourifar I, Kannan TP. Keloid scarring: understanding the genetic basis, advances, and prospects. Arch Plast Surg. 2012; 39:184-189.
3. Nakashima M, Chung S, Takahashi A, Kamatani N, Kawaguchi T, Tsunoda T, Hosono N, Kubo M, Nakamura Y, Zembutsu H. A genome-wide association study identifies four susceptibility *loci* for keloid in the Japanese population. Nat Genet. 2010; 42:768-772.
4. Zhu F, Wu B, Li P, *et al*. Association study confirmed susceptibility *loci* with keloid in the Chinese Han population. PLoS One. 2013; 8:e62377.
5. Ogawa R, Watanabe A, Than Naing B, Sasaki M, Fujita A, Akaishi S, Hyakusoku H, Shimada T. Associations between keloid severity and single-nucleotide polymorphisms: importance of rs8032158 as a biomarker of keloid severity. J Invest Dermatol. 2014; 134:2041-2043.
6. Lu W, Zheng X, Liu S, Ding M, Xie J, Yao X, Zhang L, Hu B. SNP rs1511412 in FOXL2 gene as a risk factor for keloid by meta analysis. Int J Clin Exp Med. 2015; 8:2766-2771.
7. Lu MZ, Ang QQ, Zhang X, Zhang LF, Yao XH, Lv H, Zheng XD, Lu WS. Genomic risk variants at 3q22.3 are associated with keloids in a Chinese Han population. Am J Transl Res. 2018; 10:554-562.
8. Zhao Y, Liu SL, Xie J, Ding MQ, Lu MZ, Zhang LF, Yao XH, Hu B, Lu WS, Zheng XD. NEDD4 single nucleotide polymorphism rs2271289 is associated with keloids in Chinese Han population. Am J Transl Res. 2016; 8:544-555.
9. Velez Edwards DR, Tsosie KS, Williams SM, Edwards TL, Russell SB. Admixture mapping identifies a *locus* at 15q21.2-22.3 associated with keloid formation in African Americans. Hum Genet. 2014; 133:1513-1523.
10. Bińczak-Kuleta A, Szwed A, Walter MR, Kołban M, Ciechanowicz A, Clark JS. Missense splice variant (g.20746A>G, p.Ile183Val) of interferon gamma receptor 1 (IFNGR1) coincidental with mycobacterial osteomyelitis - a screen of osteoarticular lesions. Bosn J Basic Med Sci. 2016; 16:215-221.

Received February 8, 2020; Revised February 21, 2020; Accepted February 25, 2020.

**Address correspondence to:*
Andrzej Ciechanowicz, Department of Clinical and Molecular Biochemistry, Pomeranian Medical University, ul. Powstancow Wlkp. 72, 70-111 Szczecin, Poland
E-mail: aciech@pum.edu.pl

Released online in J-STAGE as advance publication February 28, 2020.

Brief Report

DOI: 10.5582/irdr.2019.01094

Minor blood group incompatibility due to blood groups other than Rh(D) leading to hemolytic disease of fetus and newborn: a need for routine antibody screening during pregnancy

Anika Agrawal[1], Karamalla Saddam Hussain[2], Ajay Kumar[2,*]

[1] Department of Pediatrics, Maulana Azad Medical College, New Delhi, India;
[2] Department of Neonatology, Maulana Azad Medical College, New Delhi, India.

SUMMARY Minor blood group incompatibility due to blood groups other than Rh(D), although an uncommon cause of neonatal hyperbilirubinemia, has the potential to cause severe hyperbilirubinemia and its sequelae in infants, if left undiagnosed and untreated. Here, we describe clinical presentation, diagnosis and treatment of three cases of minor blood group incompatibility due to anti-E and anti-c antibody. All three neonates presented with pallor, icterus and splenomegaly within the first three days of life. Investigations showed indirect hyperbilirubinemia and a positive direct coombs test. Indirect coombs test was positive in the mothers. There was no setting of ABO or Rh(D) incompatibility in any of the neonates. When tested for minor blood group incompatibility, anti E antibody was found to be responsible for hemolysis and hyperbilirubinemia in the first case, and anti c antibody was found in the second case and third case had both anti c and anti E antibodies. While hyperbilirubinemia improved with intensive phototherapy in the first two cases, the third case required a double volume exchange transfusion. On follow up, bilateral sensorineural hearing loss was seen in one of the patients. All three neonates were otherwise healthy, gaining weight and developmentally normal.

Keywords antibody screening, hemolytic disease of newborn, minor blood group, neonatal hyperbilirubinemia, red cell allo-immunization

1. Introduction

The estimated global prevalence of haemolytic disease of the fetus and newborn (HDFN) due to Rh isoimmunisation is 276/100,000 live births per year (*1*). The prevalence of HDFN for developed counties like United States is estimated to be 3/100,000 to 80/100,000 while in developing regions like Latin America, North Africa/the Middle East, South Asia, sub-Saharan Africa, and Eastern Europe/Central Asia, the prevalence of HDFN due to Rh isoimmunisation is estimated at 252, 278, 385, 386, and 529/100,000 live births, respectively (*1,2*). The frequency of neonatal hemolytic disease and indirect hyperbilirubinemia due to Rh sensitisation has decreased with the widespread use of anti-D gamma globulin. Hence, the contribution of minor blood groups incompatibility other than Rh(D) antigen, such as Kell, c, C, E, e has gradually increased in HDFN (*3,4*). The prevalence of red cell antibodies other than anti-D with the potency to induce HDFN is about 1 in 500 pregnancies (*5*). Anti-c is usually described as the next most common cause of severe HDFN after anti-D (*6*). More and more cases of minor blood group incompatibility are now being diagnosed due to advancements in investigation modalities.

Neonates with minor blood group incompatibility may be asymptomatic or the clinical picture may range from mild anemia, reticulocytosis, neonatal hyperbilirubinemia to fetal hydrops (*4,7*). The clinical presentation, diagnosis and management of three cases of neonatal hyperbilirubinemia due to minor blood group incompatibility and maternal allo-immunisation to anti-E and anti-c antigens is discussed here (Table 1).

2. Patients and Methods

All neonates presenting with icterus were examined for pallor, organomegaly and signs of bilirubin encephalopathy. Investigations including a complete blood count and peripheral smear (for hemolysis, spherocytes, atypical cells and reticulocyte count), serum bilirubin levels, ABO and Rh(D) typing of

Table 1. Result of phenotypic analysis and antibody screening in parents and neonate

Items	Case 1		Case 2		Case 3	
Mother's Blood Group	B+		AB+		A+	
Father's Blood Group	O+		O+		A+	
Baby's Blood Group	O+		B+		A+	
DCT (Baby)	3+		4+		4+	
Antigen detection:	Mother	Father	Mother	Father	Mother	Baby*
D	4+	3+	4+	4+	4+	4+
C	4+	-ve	4+	3+	4+	4+
c	4+	3+	-ve	4+	-ve	4+
E	-ve	3+	4+	4+	-ve	4+
e	4+	2+	4+	4+	4+	-ve
Kell	-ve	-ve	-ve	-ve	-ve	-ve
ICT(Mother)	+ve		+ve		+ve	
Antibodies responsible for hemolysis	Anti E antibody in mother and baby		Anti c antibody in mother and baby		Anti E and anti c antibodies in baby	

*antigen detection in father could not be tested because father was not available for testing.

neonate and mother, direct coombs test and Glucose 6 phosphate dehydrogenase enzyme levels were done on all patients at admission. In all patients with a positive direct coombs test in the absence of ABO or Rh(D) setting, autoimmune and alloimmune causes were looked for including indirect coombs test, phenotypic analysis for minor blood groups (C, c, Kell, E, e), antibody screening and anti-nuclear antibodies.

Treatment including phototheraphy and exchange transfusion was done as per the guidelines; and once the bilirubin was below the cut off and in a decreasing trend, phototherapy was discontinued (*8*). All patients were monitored for rebound hyperbilirubinemia before discharge. After discharge, patients were kept under follow up for hearing screening, developmental assessment (*9*) and head circumference monitoring.

2.1. Case 1

A term 40-week gestation, female baby with birth weight 2,860 g was born to a 29-year-old G2P1L1 mother by an uneventful vaginal delivery in hospital. It was a booked pregnancy with regular antenatal visits and normal antenatal ultrasounds. Breast feeding was initiated within first hour of life and continued thereafter. Baby passed urine and stools on the first day of life and was discharged on second day of life. There was no history of jaundice in the first sibling. Jaundice was first noticed by mother on day 3 of life along with highly colored urine. On examination, the baby had icterus up to abdomen and was feeding well. In the follow up visit on day 5 of life, she had icterus up to palms and soles. The baby was admitted and phototherapy started. On examination, the baby was active, alert and accepting breast feeds well. She had hepatomegaly of 1 cm below costal margin and no splenomegaly. There were no signs of bilirubin encephalopathy. All anthropometric measurements were between 3rd and 10th percentile for her gestational age as per Fenton charts.

Investigations showed baby's hemoglobin of 18.5 g/dL, leucocyte count of 10,600/mm^3, platelet count of 279,000/mm^3 and total serum bilirubin (TSB) of 23.8 mg/dL with a direct component of 0.7 mg/dL. Blood group was O Rh (+), and direct coombs test was positive (+++). Mother and father blood groups were B Rh (+) and O Rh (+) respectively. Glucose 6 phosphate dehydrogenase enzyme levels were normal. Peripheral smear showed normal RBC morphology with no evidence of hemolysis or atypical cells. Phenotype analysis for minor blood group antigens in mother and father showed D(4+), C(4+), c(4+), E(-), e(4+), Kell(-) and D(3+), C(-), c(3+), E(3+), e(2+), Kell(-) respectively. Indirect coombs test was positive in the mother. Antibody screening showed anti-E antibody in the mother and baby. Since antibody screening showed anti-E antibody in the mother and baby, a diagnosis of indirect hyperbilirubinemia due to minor blood group incompatibility as a result of anti-E antibody was established.

The patient received phototherapy for 48 hours and serum bilirubin declined to 13.6mg/dL. On follow up visit, 48 hours after discontinuing phototherapy, there was no rebound hyperbilirubinemia. At 8 weeks follow up, the baby was accepting breast feeds, gaining weight, had normal development and Brainstem Evoked Response Audiometry (BERA) showed normal hearing bilaterally.

2.2. Case 2

A term 38-week gestation, male baby with birth weight 3,500 g was born to a 25-year-old G2P1L0 mother by an uneventful vaginal delivery in hospital. It was a booked pregnancy with regular antenatal visits and normal antenatal ultrasounds. The first baby was a female born at term gestation with no clinical pallor or jaundice and survived for 2 hours after birth. A definite cause of death was not established. Breast feeding was initiated

within the first hour of life. Jaundice was first noticed at life hour 8 with highly colored urine. TSB at 20 hours of life was 23 mg/dL with a direct component of 1.2 mg/dL. At the time of admission at 31 hours of life, baby was active, alert, and accepting breast feeds well. Baby had icterus up to palms and soles, hepatomegaly of 3 cm below costal margin and splenomegaly of 3 cm. There were no signs of bilirubin encephalopathy. All anthropometric measurements were between 50th and 90th percentile for age as per the Fenton charts.

Investigations showed hemoglobin of 10.7 g/dL, leucocyte count of 13,900/mm^3, platelet count of 266,000/mm^3 and total bilirubin of 25.9 mg/dL with a direct component of 1.6 mg/dL at 31 hours of life. Baby's blood group was B Rh (+) and direct coombs test was positive (++++). Mother's and father's blood group were AB Rh (+) and O Rh (+) respectively. Glucose 6 phosphate dehydrogenase enzyme level was normal. Peripheral smear showed hemolysis with a reticulocyte count 3.5%. Phenotype analysis for minor blood group antigens in mother and father showed D(4+), C(4+), c(-), E(4+), e(4+), Kell(-) and D(4+), C(3+), c(4+), E(4+), e(4+), Kell(-) respectively. Indirect coombs test was positive in the mother. Antibody screening showed anti-c antibody in the mother and baby. A diagnosis of indirect hyperbilirubinemia due to minor blood group incompatibility as a result of anti-c antibody was made.

Intensive phototherapy was initiated at 31 hours of life and continued. TSB at 67 hours of life was 22.7 mg/dL with a direct component 2.4 mg/dL. A double volume exchange transfusion was performed at 78 hours of life at a TSB of 25 mg/dL with a direct component of 2.9 mg/dL. Following exchange transfusion, intensive phototherapy was continued and serial TSB values showed a decreasing trend. Phototherapy was discontinued at 103 hours of life at a TSB of 13 mg/dL. There was no rebound hyperbilirubinemia. The baby was accepting breast feeds and gaining weight at discharge. At 8 weeks follow up, the baby was accepting breast feeds, gaining weight, had normal development and BERA showed bilateral sensorineural hearing loss.

2.3. Case 3

A term 38-week gestation, male baby with birth weight 2,920 g was born to a 22-year-old primigravida mother by caesarean delivery for fetal distress. It was a booked pregnancy with regular antenatal visits and normal antenatal ultrasounds. Breast feeding was initiated at 3 hours of life and continued thereafter. Baby passed urine and stools on the first day of life. Jaundice was noticed by mother on the second day of life. The baby was admitted to a peripheral health center and phototherapy was started. The investigations showed a maximum TSB of 25.2 mg/dL with direct fraction of 1.2 mg/dL at 110 hours of life. The blood group of the baby and both the parents was A Rh (+). Direct coombs test of the baby was positive (++++). On the 8th day of life the baby was referred in view of persistent hyperbilirubinemia despite receiving phototherapy. At presentation, the baby had icterus up to palms and soles. The baby was active, alert and accepting breast feeds well. He had hepatomegaly of 1.5 cm below costal margin and spleen was not enlarged. There were no signs of bilirubin encephalopathy. All anthropometric measurements were between 10th and 50th percentile for his gestational age as per Fenton charts.

Investigations showed hemoglobin of 10.2 g/dL, leucocyte count of 9,500/mm^3, platelet count of 318,000/mm^3 and TSB of 23 mg/dL with a direct component of 1.7 mg/dL. Glucose 6 phosphate dehydrogenase enzyme levels were normal. Peripheral smear showed evidence of hemolysis with reticulocyte count of 8.5%. Phenotype analysis for minor blood group antigens in both parents was planned but the father was not available for testing. The mother and baby showed an antigen profile of D(4+), C(4+), c(-), E(-), e(4+), Kell(-) and D(4+), C(4+), c(4+), E(4+), e(-), Kell(-) respectively. Indirect coombs test was positive in the mother. Since antibody screening showed anti-E and anti-c antibodies in the mother and baby, a diagnosis of indirect hyperbilirubinemia due to minor blood group incompatibility as a result of anti-E and anti-c antibodies was considered.

The patient received phototherapy for 70 hours and serum bilirubin declined to 10.1 mg/dL. On follow up visit, 48 hours after discontinuing phototherapy, there was no rebound hyperbilirubinemia. At 8 weeks follow up, the baby was accepting breast feeds, gaining weight, had normal development and BERA showed normal hearing bilaterally.

3. Results and Discussion

HDFN, also known as *erythroblastosis fetalis*, occurs when fetal red blood cells, containing paternally inherited antigens that the mother lacks, cross the placenta and stimulate antibody production. The antibodies return to the fetal circulation and result in hemolysis of fetal RBC. The hemolysis may be subclinical or the clinical presentation may vary from *hydrops fetalis*, anemia with reticulocytosis, or hyperbilirubinemia, requiring phototherapy or even exchange transfusion (*3,4*). Historically, Rh D alloimmunization had been the most common cause of HDFN. The introduction of antenatal and postnatal immuno-prophylaxis with anti-D immunoglobulins has reduced the incidence of Rh D allo-immunisation from 14% to 1-2% worldwide (*7*). Subsequently, ABO incompatibility has emerged as the single largest cause of HDFN. However, 3-5% cases of HDFN are reportedly caused by non-ABO, non-Rh(D) antigens including C, c, E, e, Kell, Duffy, Kidd and other antigen systems (*10*).

There are multiple case reports of minor blood group

Table 2. Guidelines in developed countries recommending routine antibody screening during pregnancy

Countries	Prevalence of red cell antibodies/ alloantibodies other than anti-D (*Ref.*)	Recommendation (*Ref.*)
Netherlands	1.23%/0.32% (*5*)	ABO, Rh(D) and Rh(c) blood group antigen typing and screening for RBC antibodies at the booking visit and again at week 27 (*16*).
United Kingdom	1%/0.3% (*17*)	ABO, Rh(D) and Rh(c) blood group antigen typing and screening for RBC antibodies at the booking visit and again at week 28 (*14*).
Australia & New Zealand	0.73%/0.65% (*18*)	ABO, Rh(D) blood group antigen typing and screening for RBC antibodies at the booking visit (*19*).
United States	0.3-3.4%/0.74% (*20*)	ABO, Rh(D) blood group antigen typing and screening for RBC antibodies at the booking visit (*21*).

incompatibility reported from the Asian subcontinent, including reports from India describing severe hemolytic disease due to anti C and anti E in two Rh D positive women, both detected postnatally (*11*). There are case reports from Korea, Taiwan and China describing hemolytic disease due to anti C anti E, anti M, anti Jk and anti Mi (*12*).

Newborns with evidence of hemolysis including positive direct agglutination test and hyperbilirubinemia where no evidence of Rh and ABO incompatibility is found, as in the three cases discussed above, a possibility of minor blood group incompatibility should be considered. These case reports show that HDFN caused by minor blood group incompatibility other than D antigen, may vary from mild to severe in its presentation. Since Rh(D) positive women are as likely to form alloantibodies as Rh(D) negative women, screening for antibodies during pregnancy is needed (*13*). This brings to attention the necessity of introducing antibody screening for pregnant women as part of antenatal care to look for significant alloantibodies other than antiD. Antenatal antibody screening should be done in all pregnant women irrespective of the Rh (D) antigen status to ensure timely availability of antigen negative blood and reduce effects of severe hyperbilirubinemia on the newborn (*13-15*).

Many developed nations have implemented regular screening of all pregnant women and even have national screening programs (Table 2) (*5,14,16-21*). Although universal screening seems justified, the cost and infrastructure required would be immense. Developing countries and under resourced nations need to consider universal antenatal screening and frame guidelines accordingly.

4. Conclusion

Minor blood group incompatibility other than anti-D remains an underreported and frequently misdiagnosed entity. Its presentation ranges from being asymptomatic to significant hyperbilirubinemia and kernicterus. Antenatal detection of significant antibody titre in the mother can ensure timely management and prevent significant morbidity and mortality in the neonate at risk.

References

1. Bhutani VK, Zipursky A, Blencowe H, *et al*. Neonatal hyperbilirubinemia and Rhesus disease of the newborn: incidence and impairment estimates for 2010 at regional and global levels. Pediatr Res. 2013; 74 Suppl 1:86-100.
2. Geaghan SM. Diagnostic laboratory technologies for the fetus and neonate with isoimmunization. SeminPerinatol. 2011; 35:148-154.
3. Özcan M, Sevinç S, Erkan VB, Yurdugül Y, Sarıcı SÜ. Hyperbilirubinemia due to minor blood group (anti-E) incompatibility in a newborn: a case report. Turk PediatriArs. 2017; 52:162-164.
4. Eder AF. Update on HDFN: new information on long-standing controversies. Immunohematology. 2006; 22:188-195.
5. Koelewijn JM, Vrijkotte TG, van der Schoot CE, Bonsel GJ, de Haas M. Effect of screening for red cell antibodies, other than anti-D, to detect hemolytic disease of the fetus and newborn: a population study in the Netherlands. Transfusion. 2008; 48:941–952.
6. Geoff D, Imelda B. The Rh blood group system. In: Essential guide to blood groups. Blackwell Publishing, Amsterdam, the Netherlands, 2007; pp 33-44.
7. Roberts IA. The changing face of haemolytic disease of the newborn. Early Hum Dev. 2008; 84:515-523.
8. American Academy of Pediatrics Subcommittee on Hyperbilirubinemia. Management of hyperbilirubinemia in the newborn infant 35 or more weeks of gestation. Pediatrics. 2004; 114:297-316.
9. Frankenburg WK, Dodds J, Archer P, Shapiro H, Bresnick B.The Denver II: a major revision and restandardization of the Denver Developmental Screening Test. Pediatrics.1992; 89:91-97.
10. Kornstad L. New cases of irregular blood group antibodies other than anti Rh D in pregnancy: frequency and clinical significance. ActaObstetGynecol Scand. 1983; 62:431-436.
11. Thakral B, Agrawal SK, Dhawan HK, Saluja K, Dutta S, Marwaha N. First report from India of haemolytic disease of the newborn by anti c and anti E in Rh (D) positive mothers. Haematology. 2007; 12:377-380.
12. Wu KH, Chu SL, Chang JG, Shih MC, Peng CT.

Haemolytic disease of the newborn due to maternal irregular antibodies in the Chinese population in Taiwan. Transfus Med. 2003; 13:311-314.
13. Basu S, Kaur R, Kaur G. Hemolytic disease of the fetus and newborn: current trends and perspectives. Asian J Transfus Sci. 2011; 5:3-7.
14. White J, Qureshi H, Massey E, Needs M, Byrne G, Daniels G, Allard S, British Committee for Standards in Haematology. Guideline for blood grouping and red cell antibody testing in pregnancy. Transfus Med. 2016; 26:246-263.
15. Azuonwu O, Nnenna I, Douglass SA, Ntaa BN. Consequences of haemolytic disease of the fetus and newborn (HDFN) and the clinical significance of antibody screening in prenatal diagnosis: a study of multigravidal and primigravidal women in Port Harcourt, Niger Delta. Journal of Clinical and Laboratory Medicine. 2016; doi http://dx.doi.org/10.16966/2572-9578.106
16. Slootweg YM, Koelewijn JM, Van Kamp IL, Van der Bom JG, Oepkes D, De Haas M. Third trimester screening for alloimmunisation in Rh(c) negative pregnant women: evaluation of the Dutch national screening programme. BJOG. 2016; 123:955-963.
17. Smith HM, Shirey RS, Thoman SK, Jackson JB. Prevalence of clinically significant red blood cell alloantibodies in pregnant women at a large tertiary-care facility. Immunohematology. 2013; 29:127-130.
18. Pal M, Williams B. Prevalence of maternal red cell alloimmunisation: a population study from Queensland, Australia. Pathology. 2015; 47:151-155.
19. Guidelines for Blood Grouping & Antibody Screening in the Antenatal and Perinatal Setting. 2nd Edition 2004, Prepared by Scientific Subcommittee of the Australian and New Zealand Society of Blood Transfusion Inc.
20. Moinuddin I, Fletcher C, Millward P. Prevalence and specificity of clinically significant red cell alloantibodies in pregnant women - a study from a tertiary care hospital in Southeast Michigan. J Blood Med. 2019; 10:283-289.
21. ACOG Practice Bulletin No. 192: Management of alloimmunization during pregnancy. Obstet Gynecol. 2018; 131:e82-e90.

Received August 14, 2019; Revised January 4, 2020; Accepted January 11, 2020

*Address correspondence to:
Ajay Kumar, Department of Neonatology, Maulana Azad Medical College, New Delhi110002, India.
E-mail: ajayneonatology@gmail.com

Released online in J-STAGE as advance publication February 4, 2020.

Brief Report

DOI: 10.5582/irdr.2019.01109

Characterization of a novel pathogenic variation c.1237T>G in the FZD4 gene presenting new inheritance from an Iranian individual suffering vitreoretinopathy

Mina Zamani[1,2], Gholamreza Shariati[3,2,*], Tahereh Seifi[1,2], Alireza Sedaghat[4,2], Hamid Galehdari[1,*]

[1] Department of Genetics, Faculty of Sciences, Shahid Chamran University of Ahvaz, Ahvaz, Iran;
[2] Narges Genetics Diagnostic Laboratory, Ahvaz, Iran;
[3] Department of Genetics, Ahvaz Jundishapur University of Medical Sciences, Ahvaz, Iran;
[4] Health Research Institute, Diabetes Research Center, Ahvaz Jundishapur University of Medical Sciences, Ahvaz, Iran.

SUMMARY Whole Exome Sequencing (WES) has been used increasingly in genetic determination of various known and unknown genetic disorders. Various genes are involved in the development of the vascular network of retina. Assessment of a collection of these genes could be provided by WES. Here we used WES for a patient suffering vitreoretinopathy to detect the disease causing variant. Sanger sequencing has been applied for variant verification and allelic segregation. After analysis of WES data we found a new variant c.1237T>G in the *FZD4* locus which causes retinopathy of prematurity and exudative vitreoretinopathy (MIM number: 133780). Sanger sequencing showed this single nucleotide variation inherited as homozygous in the patient and heterozygous in her unaffected parents. Notably, bioinformatics analysis predicted the variant as disease causing and it has not been described yet in home datasets and public SNP databases. *FZD4* mutations are mostly inherited as autosomal dominant traits. Our findings showed the first autosomal recessive inheritance of the FZD4 gene related retinopathy. On the other hand, our data shed light on the significance of an Exome sequencing application as a genetic test to identify and characterize the comprehensive spectrum of genetic variation and classification for patients with retinopathies.

Keywords exome sequencing, FZD4, vitreoretinopathy, autosomal recessive

1. Introduction

Familial retinopathy of prematurity and exudative vitreoretinopathy (MIM number: 133780) are rare disorders with retinal vascular development abnormalities which are inherited as autosomal dominant, autosomal recessive, or X-linked traits. Clinical synopsis is asymmetric and variable (*1*). Although Symptoms of the diseases vary widely from mild signs to blindness, a remarkable hallmark is defective retinal angiogenesis, which causes retinal avascularity and subsequently depending on the ischemic rate causes hyperpermeable blood vessels, revascularization, vitreoretinal traction, retinal folds, and retinal detachment (*2-4*).

Occurring mutations in five genes cause vitreoretinopathy including; NDP, FZD4, LRP5, TSPAN12, and ZNF408 (*1,4-9*). Four of them including *NDP*, *FZD4*, *LRP5*, and *TSPAN12* have a central role in Norrin/Frizzled4 signaling, and show a significant role for this pathway in retinal angiogenesis (*10*). Of these genes, FZD4 mutations are mostly inherited as autosomal dominant traits. This gene belongs to the frizzled gene family (seven-transmembrane domain receptors). They are receptors for Wnt proteins and norrin (NDP) and therefore contribute to vascularization of retina (*1*).

In recent years, next generation sequencing (NGS) has improved our knowledge about genetic and molecular bases of various spectrums of genetic disorders. With a multilateral vision, NGS, which has rapidly progressed has helped us to find out not only new disease causing variations but also new unreported inheritances, symptoms and has shed light on the way of knowing genetic roles (*11-13*).

Here we report a single nucleotide variation in an Iranian patient with retinopathy using Exome sequencing. We suggest that the *FZD4* gene might be causative for both autosomal recessive as well as autosomal dominant vitreoretinopathy.

2. Patients and Methods

2.1. Case report

Patient & her parents were recruited from southwest Iran. The proband was a 20-year-old girl with strabismus, horizontal nystagmus, decreased visual acuity, and retinal defects.

2.2. Peripheral blood samples

10 mL of peripheral blood was withdrawn from each of the enrolled patient and her parents, which were collected in EDTA tubes.

2.3. DNA extraction

Genomic DNA was extracted using the standard salting out protocol. The quality and quantity of the extracted DNA samples were checked by gel electrophoresis and Nano-drop.

2.4. Exome sequencing

We applied whole Exome sequencing for the patient. Sample was subjected to Exome enrichment with the sure select v6 followed by sequencing using the Illumina HiSeq 2000 genome analyzer platform (CNAG).

2.5. Sanger Validation

PCR (Polymerase chain reaction) using primers designed by Oligo 7 with the forward 5-AACTGACTGGCTTGTGCTATG-3 and reverse primer TGATGCCCACCAACAAAGAC-3. The PCR was conducted using Master Mix (Amplicon, Denmark) amplified targeted region of the *FZD4* gene. PCR program was chosen as an initial denaturation at 95°C for 5 min, 35 cycles of 95°C for 30 sec, annealing at 60°C for 30 sec, extension at 72°C for 30 s, and a final extension at 72°C for 5 min.

PCR products have directly been sequenced and analyzed using the ABI Prism 3700 automated genetic analyzer (Applied Biosystems). The results were analyzed with Chromas LITE 2.1.1, and then compared with the reference gene sequence using the CLUSTALW (Kyoto University Bioinformatics Center). Finally, the parent analysis and bi-directional sequencing confirmed the presence of the detected mutation.

2.6. In-silico analysis

There are many and various tools for prediction of pathogenicity of variations in genes coding and non-coding regions. In the present study, we used some of these tools for evaluation of disease causing potentiality of the present insertion variation.

3. Results and Discussion

3.1. Clinical reports for the patient

Patient belonged to Fars ethnicity of Iran and has a retinal disorder. The proband in family was a girl (IV-2, Figure 1) 20 years of age. Parents (III-1 and III-2, Figure 1) were related as first cousins. She was the only affected offspring of healthy parents who showed strabismus, horizontal nystagmus, decreased visual acuity and retinal defects. Left eye had no light perception and is unable to distinguish light from dark (NLP). In right eye vascular changes, aneurysmal telangiectasia, vascular leakage, eczema retinal, and tractional retinal detachment on the nasal side of the retina has been observed (Figure 2).

3.2. Sanger sequencing analysis of genomic amplification

Sanger sequencing validation and segregation check

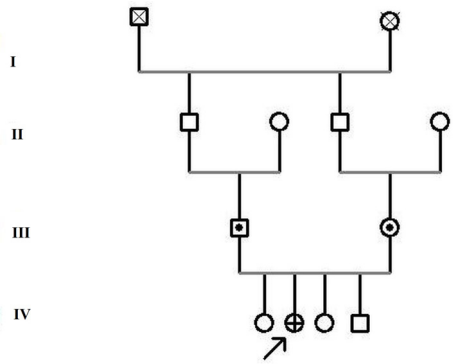

Figure 1. Family pedigree. Healthy father (III-1), healthy mother (III-2), and affected daughter (IV-2) are shown in the pedigree and the inheritance of eye disease seems to be autosomal recessive in the family.

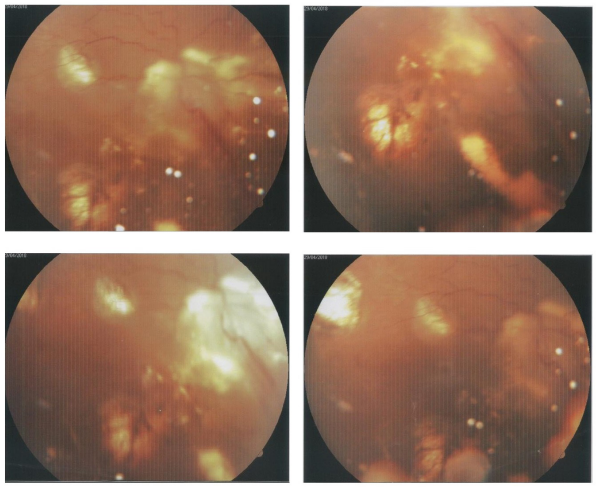

Figure 2. Fundoscopy images. Fundoscopy eyes of patient demonstrating vascular change eczema retinal, tractional retinal detachment.

were used to verify selected variant (Figure 3). Chromatograms (Figure 3) show parents are heterozygous and affected daughter is homozygous for c.1237T>G (according to the genome assembly GRCh37/hg19) in *FZD4*.

3.3. Variant characteristics

Type and predicted pathogenicity of the variation using some pathogenesis evaluation tools are shown in Table 1. The variant was not found in public databases including EXAC and GenmeAD or also in our homemade database, which contains more than 900 exome files.

Figure 4 shows the variant located in second exon of FZD4 transcript, which is present in amino acid 413 of Fzd4 protein. Fzd4 is a transmembrane protein with 509 amino acids, which contains two domains including cd07448 (CRD_FZ4; Cysteine-rich Wnt-binding domain of the frizzled 4 (Fz4) receptor) and cd15038 (7tmF_FZD4; class F frizzled subfamily 4, member of 7-transmembrane G protein-coupled receptors) respectively formed by amino acids 42-167 and amino acids 209-509. The varied amino acid is located in TM helix 5 of cd15038.

The secondary structure of wild-type and mutant protein analysis was done using YASARA version 15.6.21 (*14*). The result showed the content of Fzd4 wild type including 55.5% helix, 4.6% sheet, 7.0% turn, 31.9% coil, 0.9% 3-10 helix and 0.0% pi-helix are the same as mutant one (Figure 5).

Significantly gain of an allosteric site at R417 (Pr = 0.23, $p = 0.02$) and altered trans-membrane protein (Pr =

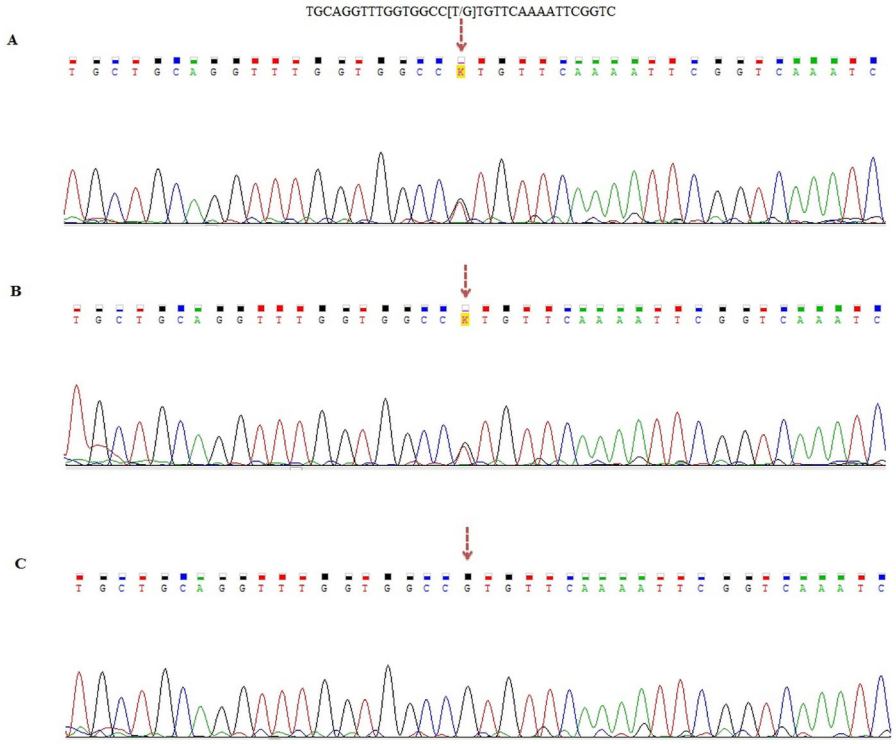

Figure 3. Chromatograms of the affected child and her parents' genome with focusing on the targeted region including the variation. (A), father (III-1 in pedigree); **(B)**, Mother (III-2 in pedigree); and **(C)**, affected daughter (IV-2 in pedigree), Arrows show the location of single nucleotide variation in *FZD4*, c.1237T>G.

Table 1. Location and predicted pathogenicity of the variation

Patient	Gene	Type	Mutation	SIFT	Polyphen2 HDIV	Polyphen2 Hvar
IV-2 (in Figure 1)	*FZD4*	Missense	g.3873T>G c.1237T>G cDNA.1543T>G p.L413V	0.001 Damaging (cut-off = 0.05)	1 Probably Damaging	0.997 Probably Damaging
Mutation Taster	PredictSNP1	PredictSNP2	Proven	MutPred	Stability (I-Mutant v2.0)	Hydrophobicity (Peptide 2.0)
0.9999992 Disease causing	61% Pathogenic	63% Benign	-2.79 Deleterious (cut-off =-2.5)	0.72 Pathgenic	Decrease	No difference

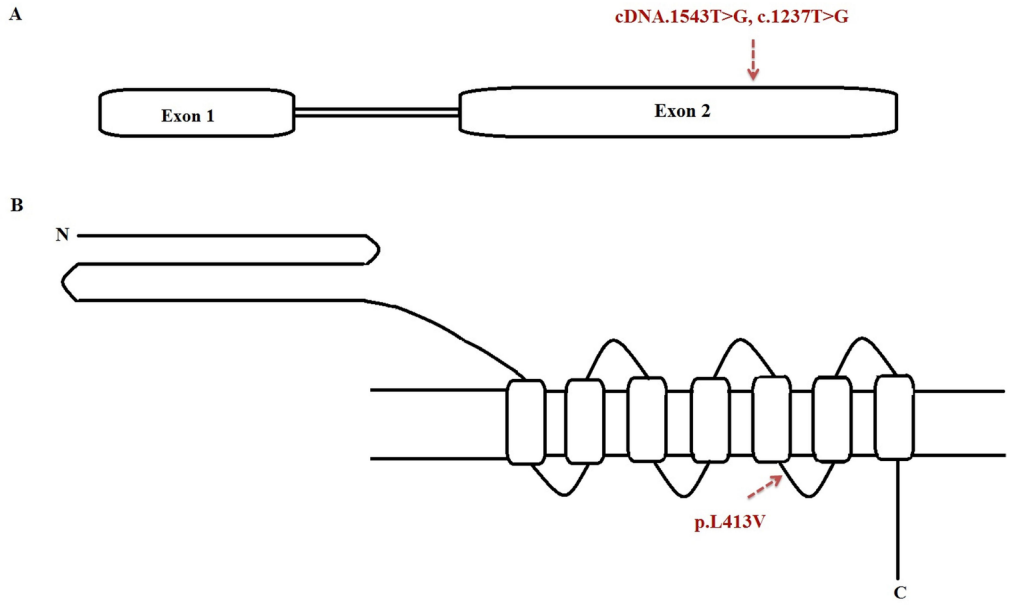

Figure 4. Schematic location of identified variation in (A) transcript and (B) protein of FZD4.

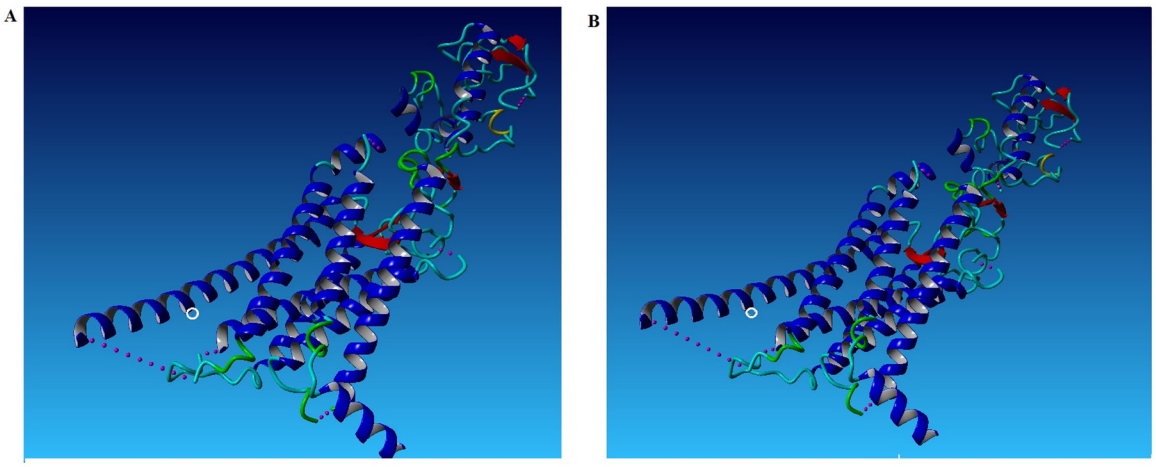

Figure 5. Secondary structure of (A) wild-type and (B) mutant Fzd4. Wight circles show varied amino acid location.

0.01, $p = 0.01$) could be potential effects of the variation according to the MutPred2 molecular mechanism prediction. Peptide 2.0 analysis results showed Hydrophobic: 47.49%, Acidic: 8.57%, Basic: 10.24%, Neutral: 33.71% for both forms.

Vitreoretinopathy is a rare inherited disorder with phenotypic and genotypic variability. Although the main sign of disease is failure of peripheral retinal vascularization, it develops with variable symptoms ranging from asymptotic vascular defects to retinal detachments with blindness. Blood vessel formation developmentally is a remarkable process, which ensures growth and function ranging from cells to the entire organism. Wnt/Frizzled signaling has a central role in the development of the vascular network. To date, six genes have been reported to be a cause for vitreoretinopathy, including LRP5, FZD4, TSPAN12, NDP, ZNF408, and KIF11. LRP5, FZD4, TSPAN12, NDP proteins are members of the Wnt/Norrin signaling pathway, which plays a critical role in eye development and angiogenesis. Mostly, mutations in one of the FZD4, the TSPAN12, the ZNF408, and the KIF11 genes causes autosomal dominant, LRP5 causes autosomal dominant and recessive, and NDP causes X-linked recessive and dominant forms of vitreoretinopathy (*1,2,7,15-22*).

In the present study, a causative genetic mutation in an Iranian family was carried out by Whole Exome sequencing. Followed by data analysis, we identified a novel homozygous single nucleotide variation; c.1237T>G in the *FZD4* gene. Healthy parents were heterozygous for the detected change. To the best of our knowledge according to the OMIM (MIM number: 133780) and review of FZD4 related literature (*4,15,17,20-24*) only autosomal dominant inheritance of vitreoretinopathy caused by mutations of the *FZD4* gene

have reported before. Condo *et al*. reported a 5-month-old baby carrying a homozygous change (p.R417Q) for which both parents harboring the same mutation heterozygously exhibited mild phenotypes, suggesting an autosomal dominant mode of inheritance with variable expressivity (*15*).

The result of in-silico analysis using mutation taster, Polyphen2, SIFT, MutPred2, PredictSNP2, proved this variant is disease causing. In addition, the identified variant is not present in our homemade exome database, which contains 800 samples, or in public SNP databases, including dbSNP, the Exome Aggregation Consortium (ExAC), and the NHLBI GO Exome Sequencing Project (ESP). Peterson *et al*. showed that FZD6 dimerizes and the dimer interface of FZD6 is formed by trans-membrane α-helices four and five (*25*). They demonstrated that some mutations of TM5 decrease affinity between the TM4/5 peptides. These variants located in cytoplasmic domain, very close to TM5 (formed by amino acids 390-410) of Fzd4 (Figure 4) possibly can effect affinity of its dimerization. Although YASARA analysis showed, secondary structure doesn't differ between wild-type and mutant (Figure 5), analysis of molecular mechanism changes underlying the variation by MutPred showed allosteric site at R417 is gained and trans-membrane protein features are altered. Notably variation of R417Q was reported before as a pathogenic allele, rs80358294 (*15,20,26*). So the present identified variation (c.1237T>G or p.L413V, table 1) can indirectly make a partly pathogenic effect by changes in the physicochemical characteristics of neighboring amino acids and total protein.

Finally, we conclude that the new variant c.1237T>G is highly pathogenic with a new autosomal recessive pattern of inheritance first described for vitreoretinopathy. Here by using WES technology we present the unreported inheritance -autosomal recessive- for vitreoretinopathy as the result of mutation in FZD4. The knowledge of this report; emphasizes the potency of exome sequencing acquired data in discovering new aspects of genetic diseases, and provides evidence for the autosomal recessive vitreoretinopathy caused by mutation in the *FZD4* gene of note and should be considered for molecular diagnosis of vitreoretinopathy by clinicians.

Acknowledgements

We would like to express our very great appreciation to the patient and her family. We acknowledge our colleagues from Narges Genetics laboratory, especially Sahar Sedighzadeh and Jawaher Zeighami who helped us for the manuscript revision.

References

1. Gilmour DF. Familial exudative vitreoretinopathy and related retinopathies. Eye (Lond). 2015; 29:1-14.
2. Fei P, Zhu X, Jiang Z, Ma S, Li J, Zhang Q, Zhou Y, Xu Y, Tai Z, Zhang L, Huang L, Yang Z, Zhao P, Zhu X. Identification and functional analysis of novel FZD4 mutations in Han Chinese with familial exudative vitreoretinopathy. Sci Rep. 2015; 5:16120.
3. Criswick VG, Schepens CL. Familial exudative vitreoretinopathy. Am J Ophthalmol. 1969; 68:578-594.
4. Robitaille J, MacDonald ML, Kaykas A, *et al*. Mutant frizzled-4 disrupts retinal angiogenesis in familial exudative vitreoretinopathy. Nat Genet. 2002; 32:326-330.
5. Collin RW, Nikopoulos K, Dona M, *et al*. ZNF408 is mutated in familial exudative vitreoretinopathy and is crucial for the development of zebrafish retinal vasculature. Proc Natl Acad Sci U S A. 2013; 110:9856-9861.
6. Nikopoulos K, Gilissen C, Hoischen A, *et al*. Next-generation sequencing of a 40 Mb linkage interval reveals TSPAN12 mutations in patients with familial exudative vitreoretinopathy. Am J Hum Genet. 2010; 86:240-247.
7. Toomes C, Bottomley HM, Jackson RM, *et al*. Mutations in LRP5 or FZD4 underlie the common familial exudative vitreoretinopathy locus on chromosome 11q. Am J Hum Genet. 2004; 74:721-730.
8. Poulter JA, Ali M, Gilmour DF, *et al*. Mutations in TSPAN12 cause autosomal-dominant familial exudative vitreoretinopathy. Am J Hum Genet. 2016; 98:592.
9. Chen ZY, Battinelli EM, Fielder A, Bundey S, Sims K, Breakefield XO, Craig IW. A mutation in the Norrie disease gene (NDP) associated with X-linked familial exudative vitreoretinopathy. Nat Genet. 1993; 5:180-183.
10. Wang Y, Rattner A, Zhou Y, Williams J, Smallwood PM, Nathans J. Norrin/Frizzled4 signaling in retinal vascular development and blood brain barrier plasticity. Cell. 2012; 151:1332-1344.
11. Gupta S, Chatterjee S, Mukherjee A, Mutsuddi M. Whole exome sequencing: Uncovering causal genetic variants for ocular diseases. Exp Eye Res. 2017; 164:139-150.
12. Stranneheim H, Wedell A. Exome and genome sequencing: a revolution for the discovery and diagnosis of monogenic disorders. J Intern Med. 2016; 279:3-15.
13. Zhu X, Petrovski S, Xie P, *et al*. Whole-exome sequencing in undiagnosed genetic diseases: interpreting 119 trios. Genet Med. 2015; 17:774-781.
14. Krieger E, Vriend G. YASARA View - molecular graphics for all devices – from smartphones to workstations. Bioinformatics. 2014; 30:2981-2982.
15. Kondo H, Hayashi H, Oshima K, Tahira T, Hayashi K. Frizzled 4 gene (FZD4) mutations in patients with familial exudative vitreoretinopathy with variable expressivity. Br J Ophthalmol. 2003; 87:1291-1295.
16. Drenser KA, Dailey W, Vinekar A, Dalal K, Capone A, Jr, Trese MT. Clinical presentation and genetic correlation of patients with mutations affecting the *FZD4* gene. Arch Ophthalmol. 2009; 127:1649-1654.
17. Toomes C, Bottomley HM, Scott S, Mackey DA, Craig JE, Appukuttan B, Stout JT, Flaxel CJ, Zhang K, Black GC, Fryer A, Downey LM, Inglehearn CF. Spectrum and frequency of FZD4 mutations in familial exudative vitreoretinopathy. Invest Ophthalmol Vis Sci.. 2004; 45:2083-2090.
18. Salvo J, Lyubasyuk V, Xu M, Wang H, Wang F, Nguyen D, Wang K, Luo H, Wen C, Shi C, Lin D, Zhang K, Chen R. Next-generation sequencing and novel variant

determination in a cohort of 92 familial exudative vitreoretinopathy patients. Invest Ophthalmol Vis Sci. 2015; 56:1937-1946.
19. Robitaille JM, Zheng B, Wallace K, *et al*. The role of Frizzled-4 mutations in familial exudative vitreoretinopathy and Coats disease. Br J Ophthalmol. 2011; 95:574-579.
20. Qin M, Hayashi H, Oshima K, Tahira T, Hayashi K, Kondo H. Complexity of the genotype-phenotype correlation in familial exudative vitreoretinopathy with mutations in the LRP5 and/or FZD4 genes. Hum mutat. 2005; 26:104-112.
21. MacDonald ML, Goldberg YP, Macfarlane J, Samuels ME, Trese MT, Shastry BS. Genetic variants of frizzled-4 gene in familial exudative vitreoretinopathy and advanced retinopathy of prematurity. Clin Genet. 2005; 67:363-366.
22. Nallathambi J, Shukla D, Rajendran A, Namperumalsamy P, Muthulakshmi R, Sundaresan P. Identification of novel FZD4 mutations in Indian patients with familial exudative vitreoretinopathy. Mol Vis. 2006; 12:1086-1092.
23. Nikopoulos K, Venselaar H, Collin RW, *et al*. Overview of the mutation spectrum in familial exudative vitreoretinopathy and Norrie disease with identification of 21 novel variants in FZD4, LRP5, and NDP. Hum Mutat. 2010; 31:656-666.
24. Yoshida S, Arita R, Yoshida A, Tada H, Emori A, Noda Y, Nakao S, Fujisawa K, Ishibashi T. Novel mutation in *FZD4* gene in a Japanese pedigree with familial exudative vitreoretinopathy. Am J Ophthalmol. 2004; 138:670-671.
25. Petersen J, Wright SC, Rodríguez D, Matricon P, Lahav N, Vromen A, Friedler A, Strömqvist J, Wennmalm S, Carlsson J, Schulte G. Agonist-induced dimer dissociation as a macromolecular step in G protein-coupled receptor signaling. Nat Commun. 2017; 8:226.
26. Kondo H, Qin M, Tahira T, Uchio E, Hayashi K. Severe form of familial exudative vitreoretinopathy caused by homozygous R417Q mutation in frizzled-4 gene. Ophthalmic Genet. 2007; 28:220-223.

Received September 23, 2019; Revised January 7, 2020; Accepted January 17, 2020

**Address correspondence to:*
Hamid Galehdari, Department of Genetics, Faculty of Sciences, Shahid Chamran University of Ahvaz, Ahvaz, Iran.
E-mail: galehdari187@yahoo.com

Gholamreza Shariati, Department of Genetics, Ahvaz Jundishapur University of Medical Sciences, Ahvaz, Iran, and Narges Genetics Diagnostic Laboratory, Ahvaz, Iran.
E-mail: shariatig@yahoo.com

Released online in J-STAGE as advance publication February 4, 2020.

Case Report

DOI: 10.5582/irdr.2020.01007

Nitrous oxide recreational abuse presenting with myeloneuropathy and mimicking Guillain-Barre syndrome

Hussein Algahtani[1,*], Bader Shirah[2], Nawal Abdelghaffar[3], Osamah Abuhawi[3], Abdulrahman Alqahtani[4]

[1] King Abdulaziz Medical City / King Saud bin Abdulaziz University for Health Sciences, Jeddah, Saudi Arabia;
[2] King Abdullah International Medical Research Center / King Saud bin Abdulaziz University for Health Sciences, Jeddah, Saudi Arabia;
[3] Aseer Central Hospital, Abha, Saudi Arabia;
[4] King Khalid University, Abha, Saudi Arabia.

SUMMARY The recreational use of nitrous oxide (N_2O) is increasing in festivals, university parties, clubs, private residences, and parks. The abuse of N_2O has serious complications of the central and peripheral nervous system. In this article, we report a case of a 28-year-old previously healthy man who presented with a three-day history of rapidly progressive leg numbness, tingling, and weakness with gait instability and frequent falls. He had a history of marijuana use and daily inhalation of N_2O (approximately 20 whippets daily over 2-3 years). He was admitted with a presumptive diagnosis of Guillain-Barre syndrome and was started on intravenous immunoglobulin. Three days after admission, paresthesia ascended to the level of nipple line, and his weakness in the lower limb increased significantly. MRI of the cervical spine showed focal non-enhancing lesions extending from C4 to C6. Serum analysis showed low vitamin B12 level, elevated methylmalonic acid, and elevated homocysteine level. Supplemental 1000 μg/day of vitamin B12 intramuscular injections and 15 mg of folic acid tablets were given. The patient showed gradual improvement. This is a rare case of N_2O recreational abuse presenting with myeloneuropathy and mimicking Guillain-Barre syndrome. This case highlights the importance of detailed history and physical examination in patients who arrive at the hospital with clinical features of Guillain-Barre syndrome. This is especially true if there are red flags such as drug abuse or discrepancy between clinical and para-clinical (investigations) parameters. Neuroimaging of the brain and spinal cord might be necessary to score the final diagnosis in such cases.

Keywords nitrous oxide, recreational abuse, myeloneuropathy, Guillain-Barre syndrome

1. Introduction

Nitrous oxide (N_2O), also known as the laughing gas, dinitrogen oxide or dinitrogen monoxide, is a colorless (at room temperature and atmospheric pressure) non-flammable gas with a chemical formula N_2O. Since its discovery, it has been used in the food industry, fuel booster, dissociative anesthesia, and pain control. It has also been used for the treatment of withdrawal of nicotine, opioids, and cocaine (*1*). When used in anesthesia, it is considered a weak anesthetic agent for dental and surgical procedures (*2*).

The recreational use of N_2O is increasing in festivals, university parties, clubs, private residences, and parks. It is the second most popular recreational drug amongst young people affecting 7.6% of youth 16-24 years old in Wales, England annually (*3*). There are no data about the rates of N_2O or inhalant use in Saudi Arabia as evident by a thorough literature review using multiple databases such as Ovid, Medline, EMBASE, ProQuest, Science Direct, Google Scholar, and PubMed. Worldwide, it is the seventh most used drug according to the world drug report 2016 (*4*). It is commonly sold in bulks online presented for use as a whipped cream propellant. It is prepared in prefilled balloons or small pressurized metal canisters which are then transferred into a dispenser (whippets or cracker) (*5*).

In this article, we report a case of nitrous oxide recreational abuse presenting with myeloneuropathy and mimicking Guillain-Barre syndrome.

2. Case Report

A 28-year-old previously healthy man presented

with a three-day history of rapidly progressive leg numbness, tingling, and weakness with gait instability and frequent falls. He denied any history of preceding upper respiratory tract infection, gastroenteritis, or vaccination. There was no history of bowel or bladder dysfunction, head or neck pain, seizures, or memory impairment. There was no past medical history of any endocrine, metabolic, or surgical diseases, and he denied any history of trauma. He was single, high-school-educated with a history of marijuana use and daily inhalation of N_2O. Approximately 20 whippets daily over 2-3 years were used as a means of recreation. No history of other illicit drug use, but he smokes tobacco.

General examination including vital signs was normal. Neurologically, higher mental functions and cranial nerves were normal. He was anxious and depressed. Motor examination showed flaccid bilateral symmetrical upper and lower limb weakness, distal more than proximal with bilateral foot drop. The weakness distally was 2/5 and proximally 4-/5. The tone was reduced in all limbs with reduced pinprick sensation in a patchy distribution with the lower limbs being more involved than the upper limbs. Vibration and joint position sense were impaired bilaterally on the tip of his big toe. Reflexes were +2 in the arm and +1 at the knee with absent ankle jerks and bilateral downgoing toes. Cerebellar examination showed no dysmetria on the finger to nose test, and gait assessment was difficult to assess due to weakness. There was no bulbar weakness or respiratory symptoms.

He was admitted with a presumptive diagnosis of Guillain-Barre syndrome. Laboratory checkup revealed normal complete blood count, renal profile, electrolyte, thyroid function test, and liver function test. Chest x-ray, urinalysis, toxicology screen, and electrocardiogram were normal. Cerebrospinal fluid (CSF) analysis on admission revealed no white blood cells or red blood cells with normal glucose and protein without oligoclonal bands. He was started on intravenous immunoglobulin (IVIG) 400 mg/kg per day for five days.

Three days after admission, paresthesia ascended to the level of nipple line, and reflexes became brisk bilaterally with bilateral upgoing toes (Babinski sign). His weakness in the lower limb increased significantly, and his power was 0/5 distally and proximally. In the upper limbs, his weakness was the same. A repeated CSF analysis ten days after admission revealed again a normal analysis with no albuminocytological dissociation and negative microbiology and cytology. Nerve conduction studies twelve days after admission showed classical axonal length-dependent polyneuropathy. MRI of the cervical spine showed focal non-enhancing lesions extending from C4 to C6 (Figure 1). Serum analysis showed normal folate level at 7 µg/L (normal 2-20 µg/L), low vitamin B12 level at 124 µg/mL (normal 150-800 µg /mL), elevated methylmalonic acid at 3.7 µmol/L (normal 0-0.4 µmol/L), and elevated homocysteine level at 98 (4-20 µmol/L). Supplemental 1000 µg/day of vitamin B12 intramuscular injections and 15 mg of folic acid tablets were given. The patient showed gradual improvement, and six months later, his neurological examination was normal apart from a subtle weakness of foot dorsiflexors (Figure 2).

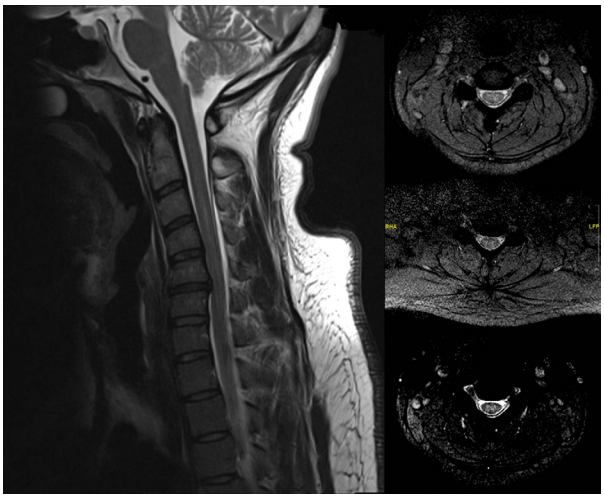

Figure 1. MRI of the cervical spine showing focal non-enhancing lesions extending from C4 to C6.

3. Discussion

In 1793, the English scientist Joseph Priestley was the first to synthesize N_2O gas. In 1799, N_2O was administered to visitors of the pneumatic institute by Sir Humphry Davy. He astutely noted the analgesic effect of the gas and gave it for the first time the term "laughing gas". In the early 1800s, the gas became a popular public entertainment and fashionable addition to British high-society parties due to its euphoric properties (*6*). It also creates a state of depersonalization, derealization, sound distortion, and lightheadedness. The first reported medical use of N_2O was by Horace Wells, an American dentist, who used the gas for his own tooth extraction in 1844 (*7*).

N_2O causes its harmful effect by oxidizing the cobalamin (B12) cobalt atom from its 1+ to 3+ valence state rendering methylcobalamin inactive on a co-factor of methionine synthase. This inhibits the conversion of homocysteine to methionine and 5-methyltetrahydrofolate to tetrahydrofolate. Methionine is necessary for myelin production and to replenish the one carbon donor pool and tetrahydrofolate is necessary for DNA synthesis. In addition, cyanocobalamin is necessary for the conversion of methyl-malonyl CoA to succinyl-coenzyme A (*8*). Accumulation of methyl-malonyl CoA and homocysteine in the serum can be measured by a special laboratory and are used as a surrogate

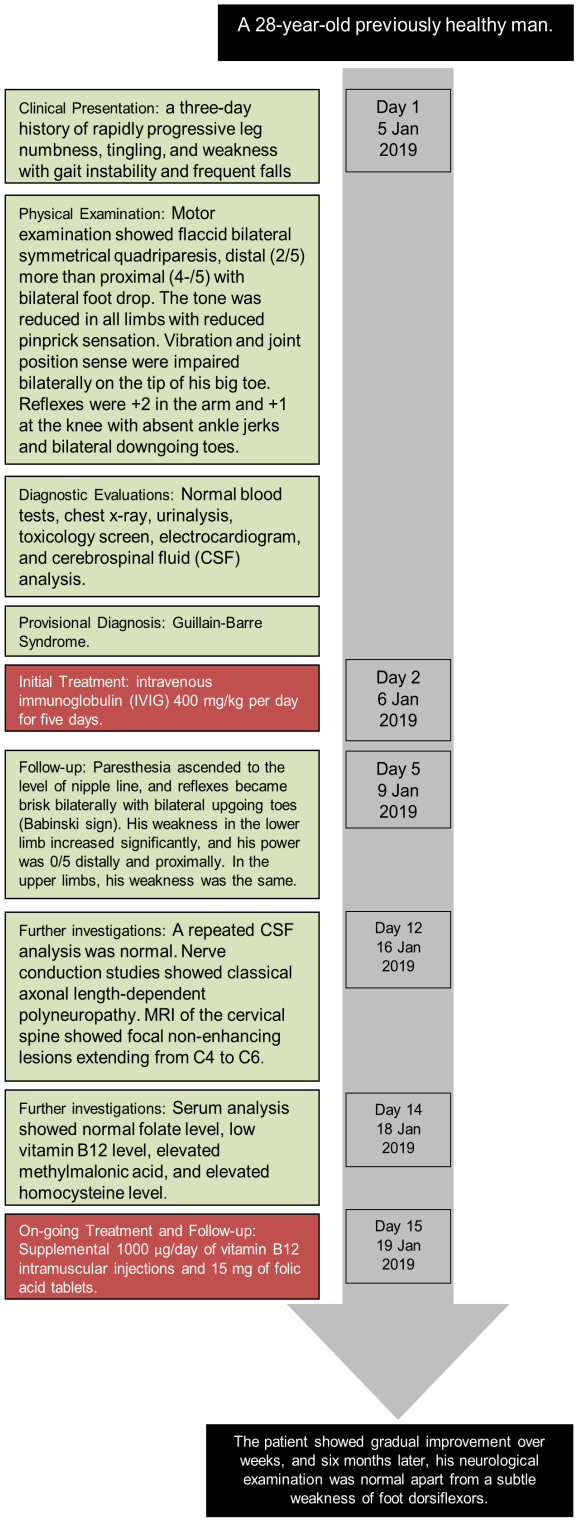

Figure 2. Timeline figure for our case.

marker of vitamin B12 deficiency. Accumulation of methyl-malonate provides abnormal substrates for fatty acids synthesis, and subsequently, these abnormal fatty acids may be incorporated into the myelin sheath. Proper synthesis of succinyl CoA is important as an intermediate in the Krebs cycle (*9*). Other postulated mechanisms of action include a decrease in excitatory neurotransmission throughout the central nervous system via non-competitive glutamate inhibition and acting on a partial mu, kappa and delta opioid receptor agonists modulation dopamine activity and noradrenergic nociceptive pathways (*10*). In our patient, the clinical picture was that of myeloneuropathy with low vitamin B12 and high methylmalonic acid and homocysteine. The positive history of N_2O abuse, presence of clinical features of subacute clinical myeloneuropathy, and biochemical changes have confirmed the diagnosis of N_2O toxicity.

Unfortunately, the gas is also called "legal high" due to easy availability. It has a rapid onset with a peak of around one minute after inhaling and then fading away for 2 minutes. Each canister contains 8 grams of N_2O in a volume of 10 cm3 can be bought for £2. It produces approximately 8 liters of N_2O gas. It has a rapid onset with a peak of around one minute after inhaling and then fading away after 2 minutes (*11*).

The use of N_2O is not as innocent as many people think especially if used in high daily doses (more than ten bulbs) for a prolonged duration. A recent systematic review of the literature by Garakani et al. (*12*) found a total of 72 cases with neurological sequelae to N_2O abuse. They were categorized into four different groups: myeloneuropathy (31 cases), subacute combined degeneration of the spinal cord (17 cases), polyneuropathy (15 cases) and myelopathy (14 cases) (*12*). Nitrous oxide abuse can produce a sense of psychotic and neurological symptoms. Among psychotic symptoms are anxiety, depression, hallucinations, impulsive and aggressive behaviors, manic delusions, and psychosis (*13*). Neurological symptoms include weakness, numbness, ataxia, visual symptoms, falls, and paresthesia, confusion, and forgetfulness (*14*).

A unique finding in our case was the involvement of two different areas in the neuroaxis that are the cervical spinal cord and peripheral nerves. The diagnostic exercise of localization in our case was unique, which was guided by repeated daily history and detailed neurological examination. This was accompanied by timely-ordered investigations. The initial clinical features were suggestive of an acute peripheral neuropathy, which were followed a few days later by clinical features of spinal cord involvement in the cervical segment. Cervical segment involvement was suggested by sensory level, bladder control disturbance, and brisk reflexes. The rapid onset, progressive course, and history of N_2O abuse also guided us to the correct diagnosis.

The neuroradiological changes of N_2O toxicity in the posterior and lateral columns of the spinal cord are those seen in cobalamin deficiency. They include an abnormally high T2 signal intensity that occurs predominantly in the cervical segment of the spinal

cord (*12*).

Treatment is aimed primarily at stopping the exposure and administering B12. There is no standardized B12 regimen, but a commonly accepted plan is 1000 µg intramuscularly for five days and then intermittently until symptoms resolve. An alternative plan is 1000 µg – 2000 µg orally daily for 1-2 weeks and then 500 µg daily for three months (*15*).

Our case report is unique for several reasons. Firstly, although N_2O abuse is common in both developed and developing countries, to date, this is the first case reported from Saudi Arabia as evident by a thorough literature review using multiple databases such as Ovid, Medline, EMBASE, ProQuest, Science Direct, Google Scholar, and PubMed. Secondly, this is the second case of N_2O toxicity presenting as Guillain-Barre syndrome (*16*). Thirdly, our patient was treated aggressively by vitamin B12 injections, folate, and IVIG with an excellent outcome. Finally, our report presents interesting imaging, neurophysiology, and review the important aspects of the topic.

In conclusion, the abuse of N_2O has serious complications of the central and peripheral nervous system. It is a great mimicker, and early diagnosis and treatment are crucial. If the affected patient does not disclose his recreational N_2O abuse or the neurologist fails to inquire about it, diagnosis may be difficult. This case highlights the importance of detailed history and physical examination in patients who arrive at the hospital with clinical features of Guillain-Barre syndrome. This is especially true if there are red flags such as drug abuse or discrepancy between clinical and para-clinical (investigations) parameters. Neuroimaging of the brain and spinal cord might be necessary to score the final diagnosis in such cases.

References

1. Cousaert C, Heylens G, Audenaert K. Laughing gas abuse is no joke. An overview of the implications for psychiatric practice. Clin Neurol Neurosurg. 2013; 115:859-862.
2. Becker DE, Rosenberg M. Nitrous oxide and the inhalation anesthetics. Anesth Prog. 2008; 55:124-130.
3. Mike J. Nitrous Oxide: recreational use, regulation and harm reduction. Drugs Alcohol Today. 2008; 8:22-25.
4. National Survey on Drug Use and Health. Table 1.88B – Specific Hallucinogen, Inhalant, Needle, and Heroin Use in Lifetime, by Age Group: Percentages. 2012–2013. *https://www.samhsa.gov/data/sites/default/files/NSDUH-DetTabs2013.pdf.* (accessed January 21, 2020)
5. Thompson AG, Leite MI, Lunn MP, Bennett DL. Whippits, nitrous oxide and the dangers of legal highs. Pract Neurol. 2015; 15:207-209.
6. Randhawa G, Bodenham A. The increasing recreational use of nitrous oxide: history revisited. Br J Anaesth. 2016; 116:321-324.
7. Weimann J. Toxicity of nitrous oxide. Best Pract Res Clin Anaesthesiol. 2003; 17:47-61.
8. Sanders RD, Weimann J, Maze M. Biologic effects of nitrous oxide: a mechanistic and toxicologic review. Anesthesiology. 2008; 109:707-722.
9. Savage DG, Lindenbaum J, Stabler SP, Allen RH. Sensitivity of serum methylmalonic acid and total homocysteine determinations for diagnosing cobalamin and folate deficiencies. Am J Med. 1994; 96:239-246.
10. Savage S, Ma D. The neurotoxicity of nitrous oxide: the facts and "putative" mechanisms. Brain Sci. 2014; 4:73-90.
11. Garland EL, Howard MO, Perron BE. Nitrous oxide inhalation among adolescents: prevalence, correlates, and co-occurrence with volatile solvent inhalation. J Psychoactive Drugs. 2009; 41:337-347.
12. Garakani A, Jaffe RJ, Savla D, Welch AK, Protin CA, Bryson EO, McDowell DM. Neurologic, psychiatric, and other medical manifestations of nitrous oxide abuse: A systematic review of the case literature. Am J Addict. 2016; 25:358-369.
13. Mancke F, Kaklauskaitė G, Kollmer J, Weiler M. Psychiatric comorbidities in a young man with subacute myelopathy induced by abusive nitrous oxide consumption: a case report. Subst Abuse Rehabil. 2016; 7:155-159.
14. Stockton L, Simonsen C, Seago S. Nitrous oxide-induced vitamin B12 deficiency. Proc (Bayl Univ Med Cent). 2017; 30:171-172.
15. Pugliese RS, Slagle EJ, Oettinger GR, Neuburger KJ, Ambrose TM. Subacute combined degeneration of the spinal cord in a patient abusing nitrous oxide and self-medicating with cyanocobalamin. Am J Health Syst Pharm. 2015; 72:952-957.
16. Tatum WO, Bui DD, Grant EG, Murtagh R. Pseudo-guillain-barre syndrome due to "whippet"-induced myeloneuropathy. J Neuroimaging. 2010; 20:400-401.

Received January 24, 2020; Revised February 10, 2020; Accepted February 14, 2020.

**Address correspondence to:*
Hussein Algahtani, King Abdulaziz Medical City / King Saud bin Abdulaziz University for Health Sciences, P.O. Box: 12723, Jeddah 21483, Saudi Arabia. Contact No.: 00966556633130.
E-mail: halgahtani@hotmail.com

Released online in J-STAGE as advance publication February 18, 2020.

Communication

DOI: 10.5582/irdr.2020.01004

High prevalence of congenital generalized lipodystrophy in Piura, Peru

Nelson David Purizaca-Rosillo[1,2,*], Yamalí Elena Benites-Cóndor[3], Hugo Abarca Barriga[3], Carlos del Águila Villar[3], Miguel Chávez Pastor[3], Littner Franco Palacios[4], Ricardo Olea Zapata[5], James Rejas Parodi[6], Luz Martinez Uceda[7], Felix Chavesta Velásquez[3], John Gamarra Vilela[8], Sebastián Arámbulo Castillo[2,9], Amanda Ávila Reyes[2,9]

[1] Universidad Peruana Cayetano Heredia, Lima, Peru;
[2] Sociedad Científica de Estudiantes de Medicina de la Universidad Nacional de Piura, Perú;
[3] Instituto Nacional de Salud del Niño, Breña, Lima, Peru;
[4] Clínica "Carita Feliz";
[5] Hospital III José Cayetano Heredia, Piura, Peru;
[6] Hospital Jorge Reátegui Delgado, Piura, Peru;
[7] Hospital de la Amistad Peru - Corea Santa Rosa, Piura, Peru;
[8] Hospital de Apoyo Sullana, Piura, Peru;
[9] Professional School of Human Medicine, Faculty of Health Sciences, Universidad Nacional de Piura, Peru.

SUMMARY Congenital generalized lipodystrophy (CGL) is an autosomal recessive rare disease, with a worldwide prevalence of around 1 in every 12 million people. There are several case reports of patients with CGL in Piura, a region in northern Peru; however its regional prevalence is unknown. The objective was to determine the prevalence of CGL in the region of Piura, Peru during the years 2000-2017. A descriptive, observational study was carried out. A search of clinical histories of patients with the diagnosis of CGL attended between 2000 and 2017 in the pediatric and endocrinology services of the reference hospitals of the department of Piura and in the genetic and endocrinology services of the "Instituto Nacional de Salud del Niño". A patient was considered to have CGL if they met the clinical criteria and or if they had a molecular diagnosis, in addition to patients with CGL from the department of Piura reported in previous publications. A total of 23 cases of CGL were found in Piura, the highest prevalence was in 2014 with 1.2 per 100,000 people, and by 2017 the prevalence was 0.86 per 100,000 people. In conclusion, the department of Piura has a high prevalence of CGL.

Keywords congenital generalized lipodystrophy, rare diseases, Peru (Mesh Terms)

1. Introduction

Congenital generalized lipodystrophy (CGL) is an autosomal recessive disease characterized by an almost total absence of adipose tissue from birth, muscular prominence and low levels of leptin. There are 4 molecular subtypes of CGL, based on the genes involved: CGL 1, related to the *AGPAT2* gene, CGL 2 with the *BSCL2* gene, CGL 3 with the *CAV1* gene and CGL 4 with variants in the polymerase I and *PTRF* gene (*1*). Patients with CGL may develop multiple complications, such as insulin resistance that may progress to diabetes mellitus, hepatic steatosis and severe hypertriglyceridemia leading in some cases to cirrhosis and end-stage chronic kidney disease (*2*).

Globally the prevalence of CGL is estimated at 1 in 12 million people (*3*), however, the prevalence varies according to the region under study, for example in Rio Grande Do Norte (RN), Brazil, the prevalence of CGL is 3.23 per 100,000 people (*4*).

In Peru, the first 5 cases of patients with CGL from Piura, a region in northern Peru, were reported in 1999 (*5*). In 2017, a series of 5 cases as well as one other were reported, all from Piura (*6,7*). Although there are multiple reports of CGL from the department of Piura, their prevalence has not been determined. The objective of the study was to estimate the prevalence of CGL and its distribution in the region of Piura, Peru during the years 2000-2017.

2. Methodology

A historical record of patients with a diagnosis of

CGL from the department of Piura was made between the years 2000-2017. A search was made for patients with the diagnosis of CGL between the years 2000-2017 in the services of pediatrics, endocrinology of the reference hospitals of the department of Piura: Hospital III José Cayetano Heredia, Hospital Jorge Reátegui Delgado, Hospital Santa Rosa, Hospital de Apoyo Sullana and also in the services of genetics and pediatric endocrinology of the National Institute of Child Health in Lima, the latter one is considered to be the pediatric reference site in Peru. In addition, patients with CGL from the department of Piura reported in previous publications were included. Patients with CGL were considered if they met the clinical criteria (*8*) and/or if they had molecular diagnosis.

The patients' place of birth, age, sex and current status were recorded and a database was created in *Microsoft Excel* 2017. The annual prevalence was calculated at the departmental and provincial levels, using the annual population reported by the National Institute of Statistics and Information. The study was approved by the Ethics Committee of the National Institute of Child Health, Lima, Peru.

3. Cases of congenital generalized lipodystrophy in Piura

In the initial review, we found a total of 22 patients with a probable diagnosis of CGL and 3 publications with a total of 11 CGL patients (*5-7*). A publication that included 5 patients was excluded because it did not correspond to the study period. Of the 6 patients reported in the other two publications, 3 were not found recorded in clinical histories.

A total of 23 cases of CGL were found, all from the department of Piura, the majority were from the province of Piura (73.9%), they are living (73.9%) and only 34.8% had genetic confirmation (Table 1). All patients had the pathogenic variant homozygote c.213-1336_c.294+1921delinsCA in the *BSCL2* gene.

The highest prevalence of CGL in the department of Piura was in 2014 with 1.2 per 100,000 people, and by 2017 the prevalence was 0.86 per 100,000 people (Table 2). Patients were found in only 3 provinces of the department of Piura: Morropón, Sullana and Piura (Figure 1), and their prevalence by 2017 was 0.6, 1.23 and 1.33 per 100,000 people respectively.

Our study found a high prevalence of CGL (0.86 in 100,000 habitants) in the department of Piura during the year 2017. This prevalence is higher than that reported worldwide, USA, Norway, Lebanon, Portugal (*3,9*), however it is lower than that reported in other regions such as Rio Grande do Norte and Oman, which can reach 3.23 in 100,000 habitants (*4,10*).

The reason for the high prevalence is the founder effect proposed by Purizaca *et al*. (*7*), which described a genetic variant in the *BSCL2* gene associated with type 2 CGL which, to the authors' knowledge, has not been reported in patients outside Piura (*11*). The same pathogenic variant was detected in all the patients in our study who underwent the genetic test; likewise, in patients without genetic confirmation it is assumed that they may have type 2 CGL due to the fact that they share the same clinical and geographic origin.

The department of Piura is divided into 8 provinces and only 3 of them have presented patients with CGL, coming from small agricultural areas that are difficult to access. The authors propose that migration between different agricultural villages in the department of Piura for work, and sometimes precipitated by natural events such as the El Niño phenomenon (*12,13*), may have caused patients carrying the same genetic variant to be found in different provinces due to the movement of groups to areas with better living conditions. The latest verbal reports of patients with and without genetic confirmation from other provinces where no cases had

Table 1. General characteristics of patients with CGL between 2000-2017, Piura, Peru

Variable	*n*	%
Age (median)		6
Age at death (median)		8
Gender		
Male	12	52.2
Female	11	47.8
Province of origin		
Sullana	5	21.7
Morropon	1	4.3
Piura	17	73.9
Current status		
Living	17	73.9
Deceased	6	26.1
Genetic Confirmation		
Yes	8	34.8
No	15	65.2

Table 2. Prevalence of CGL in the department of Piura, 2000-2017

Year	Cases	Prevalence (/100,000)
2000	2	0.12
2001	2	0.12
2002	2	0.12
2003	3	0.18
2004	3	0.18
2005	4	0.24
2006	4	0.23
2007	6	0.35
2008	7	0.40
2009	12	0.68
2010	13	0.73
2011	15	0.84
2012	17	0.94
2013	19	1.05
2014	22	1.20
2015	21	1.14
2016	19	1.03
2017	16	0.86

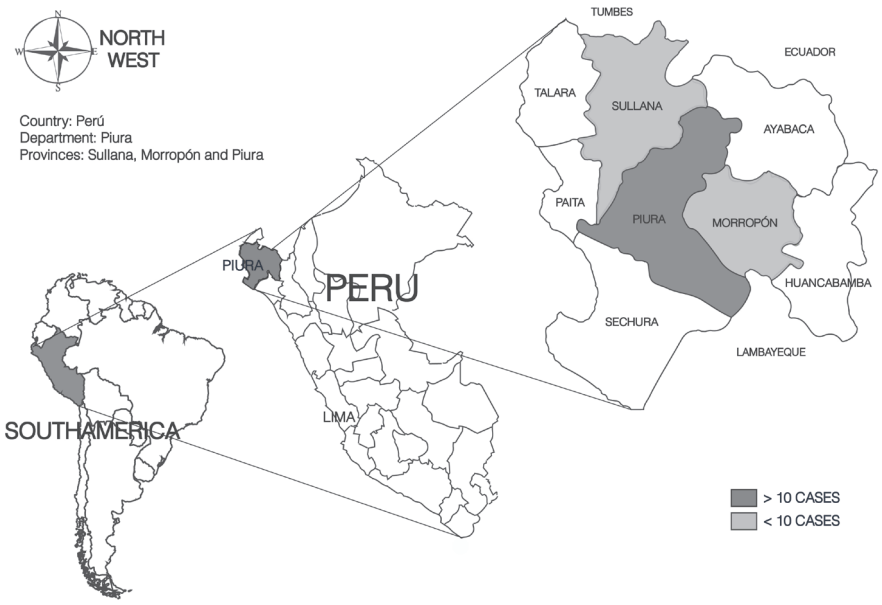

Figure 1. Geographic location of patients with CGL in Piura, Peru.

been registered to reinforce our assumption and oblige us to optimize the active search for them at the regional level. Due to the fact that the first cases were reported in the province of Piura and that this is the one that registers the greatest number of patients, it is assumed that it is where the type 2 CGL index case was presented.

Within the limitations it is necessary to highlight that the prevalence is based on a hospital registry, however, to the knowledge of the authors there are patients with a probable diagnosis of CGL who have not gone to a health center for different reasons such as cultural, economic and geographic, so the actual prevalence could be higher than reported in this study. In conclusion, the department of Piura has a high prevalence of CGL.

References

1. Lightbourne M, Brown RJ. Genetics of lipodystrophy. Endocrinol Metab Clin North Am. 2017; 46:539-554.
2. Akinci B, Onay H, Demir T, *et al*. Natural history of congenital generalized lipodystrophy: A nationwide study from Turkey. J Clin Endocrinol Metab. 2016; 101:2759-2767.
3. Garg A. Acquired and inherited lipodystrophies. N Engl J Med. 2004; 350:1220-1234.
4. de Azevedo Medeiros LB, Cândido Dantas VK, Craveiro Sarmento AS, Agnez-Lima LF, Meireles AL, Xavier Nobre TT, de Lima JG, de Melo Campos JTA. High prevalence of Berardinelli-Seip Congenital Lipodystrophy in Rio Grande do Norte State, Northeast Brazil. Diabetol Metab Syndr. 2017; 9:80.
5. Torres R, Ballona R, Caytano M. Seip Berardinelli Syndrome: Report of 5 cases at the Institute of Child Health (ISN). Folia Dermatol (Peru). 1999; 10:43-47.
6. Gonzalo MM, Estefania CV. Congenital generalized lipodystrophy type 2 in a patient from a high-prevalence area. J Endocr Soc. 2017; 1:1012-1014.
7. Purizaca-Rosillo N, Mori T, Benites-Cóndor Y, Hisama FM, Martin GM, Oshima J. High incidence of BSCL2 intragenic recombinational mutation in Peruvian type 2 Berardinelli- Seip syndrome. Am J Med Genet A. 2017; 173:471-478.
8. Araújo-Vilar D, Santini F. Diagnosis and treatment of lipodystrophy: A step-by-step approach. J Endocrinol Invest. 2019; 42:61-73.
9. Van Maldergem L. Berardinelli-seip congenital lipodystrophy. In: GeneReviews®. 2016. *https://www.ncbi.nlm.nih.gov/books/NBK1212/* (Accessed August 5, 2019)
10. Rajab A, Bappal B, Al-Shaikh H, Al-Khusaibi S, Mohammed AJ. Common autosomal recessive diseases in Oman derived from a hospital-based registry. Community Genet. 2005; 8:27-30.
11. Craveiro Sarmento AS, Ferreira LC, Lima JG, de Azevedo Medeiros LB, Barbosa Cunha PT, Agnez-Lima LF, Galvão Ururahy MA, de Melo Campos JTA. The worldwide mutational landscape of Berardinelli-Seip congenital lipodystrophy. Mutat Res. 2019; 781:30-52.
12. Zapata R. Piura one year after the tragedy: the current situation after the coastal El Niño.Trade. *https://elcomercio.pe/peru/piura-ano-tragedia-situacion-actual-nino-costero-noticia-507536* (accessed March 28, 2019)
13. Bayer AM, Danysh HE, Garvich M, Gonzálvez G, Checkley W, Alvarez M, Gilman RH. An unforgettable event: a qualitative study of the 1997-98 El Niño in northern Peru. Disasters. 2014; 38:351-374.

Received January 14, 2020; Revised February 25, 2020; Accepted February 27, 2020.

Address correspondence to:
Nelson David Purizaca-Rosillo, Universidad Peruana Cayetano Heredia, Av. Honorio Delgado 430, Urb. Ingeniería, S.M.P. Lima, Perú.
E-mail: nelson.purizaca@upch.pe

Letter

DOI: 10.5582/irdr.2020.01009

Multiphasic acute disseminated encephalomyelitis and differential with early onset multiple sclerosis

Arla Cinderella Stokes Brackett[1], Otto Jesus Hernández-Fustes[2,*], Carlos Arteaga Rodríguez[3], Olga Judith Hernandez Fustes[4]

[1] Neurology Service, Hospital San Juan de Dios, Guatemala;
[2] Neurology Department, InNeuro, Curitiba, Brasil;
[3] Neurology Department, Universidad Positivo, Curitiba, Brasil;
[4] Neurophysiology Department, Clínica das Américas, Curitiba, Brasil.

SUMMARY Multiple sclerosis is considered the most frequent demyelinating disorder of the Central Nervous System (CNS) among young adults, yet is very rare before 10 years old. Acute disseminated encephalomyelitis is a monophasic, polysymptomatic disorder that involves the CNS white matter with demyelinating lesions, which usually occurs after systemic viral infections. These two demyelinating diseases can present initially as an acute focal neurological syndrome and they can be difficult to distinguish. We describe a case of a nine-year-old girl that presented initially with dysphonia, gait ataxia, eyelid myokymia and brainstem disturbances. This was her second episode; the first episode was at the age of four years old. She recovered without neurological sequelae. The brain magnetic resonance imaging (MRI) demonstrated multiple demyelinating lesions in the white matter, cortical regions of the frontal lobe, periventricular distribution, internal capsule, corpus callosum and cerebellum. The purpose of the presentation of this case was to highlight the similarities between these two entities, since the clinical picture and neuroimaging are difficult to distinguish, mainly in relation to the first episode.

Keywords multiple Sclerosis, multiphasic acute disseminated encephalomyelitis, childhood

Multiple Sclerosis (MS) is considered the greatest demyelinating disorder in young adults, yet rare before 10 years. The overall incidence of acquired demyelinating syndromes in children and adolescents ranges from 0.6 to 1.66 per 100 000 children per year (*1,2*). Acute disseminated encephalomyelitis (ADEM) is a single-phase, polysymptomatic disorder involving central nervous system blanking, leading to demyelinating lesions secondary to systemic viral infections, often reaching the age of 5 years of age (*3*). For confirmation diagnosis, there is no specific biological marker test or confirmatory test, the MRI being considered the elected exam. Analysis of the cerebrospinal fluid may be useful, showing pleocytosis lymphocytic cells without oligoclonal bands and elevation of albumin. These pathologies may present with a focal neurological syndrome whose differential diagnosis is difficult to distinguish.

We describe a 9-year-old girl with a family health history, that eight days before admission she had gastroenteritis, and on admission presented difficulty walking, dysphonia and dysphagia. Neuro-psychomotor development was normal until that time. At the age of 4, she presented a similar condition accompanied by altered consciousness and coma that was interpreted as viral meningoencephalitis, evolving without sequelae.

Physical examination revealed eyelid myokymia on the right, ataxia, dysphonia, left upper limb monoparesis, left central facial paralysis and involvement of the X and XII cranial nerves.

Current brain MRI revealed multiple demyelinating lesions in the white matter in the frontal and peri-ventricular regions involving the internal capsule, corpus callosum and cerebellum (Figure 1). Cerebrospinal fluid found a slight increase in immunoglobulins (12.7%) and absence of oligoclonal bands. Our patient met the criteria for multiphasic acute disseminated encephalomyelitis (MDEM): *i*) Two clinical events meeting criteria for acute disseminated encephalomyelitis, separated in time by greater than 3 months, and *ii*) No evidence for clinically-silent new lesion formation on MRI between acute disseminated encephalomyelitis episodes (*4*). The patient was medicated with intravenous pulsotherapy of methylprednisolone and acyclovir, obtaining a good

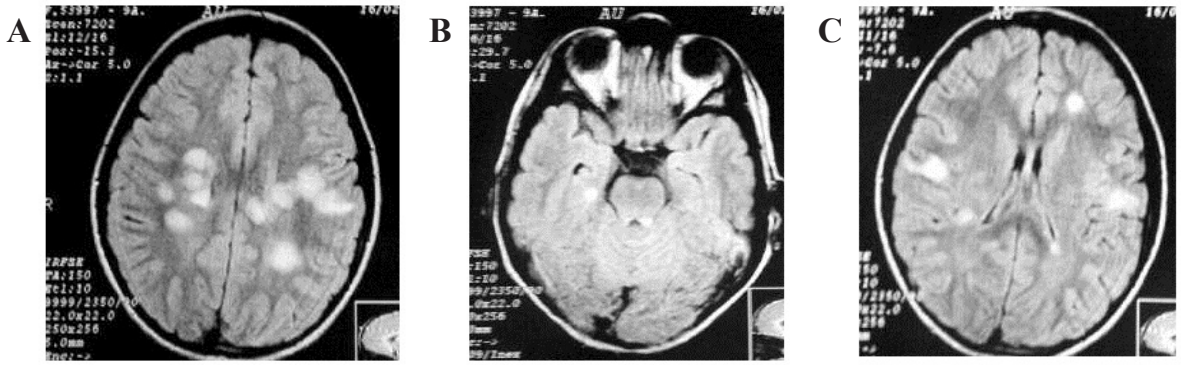

Figure 1. MRI showing multiple nodular, cotton-like images with hyperintense signal at T2 and in the long RT sequence and above all the flair sequence observed in the white matter of the semioval centers, as well as in the cortical regions of the left frontal lobe and suprasilvian regions, some of periventricular distribution in the corpus callosum. Hyperintense images were also observed in the right temporo mesial regions and in the left periaqueductal regions and in the path of the posterior legs of the internal capsules, the left middle cerebellar peduncle and the dentate nuclei of the cerebellum.

recovery in three weeks.

The International Paediatric Multiple Sclerosis Study Group defines ADEM as *i*) a first polyfocal, clinical CNS event with presumed inflammatory demyelinating cause; *ii*) encephalopathy not explained by fever, systemic illness, or postictal symptoms; *iii*) no new clinical and MRI findings emerging 3 months or more after the onset; *iv*) brain MRI is abnormal during the acute (3 mo) phase with diffuse, poorly demarcated, large (> 1-2cm) lesions predominantly involving the cerebral white matter (*5*).

The distinction between ADEM, MDEM or MS has been previously explored with no satisfactory consensus. Historically, ADEM was defined as the initial presentation of disseminated encephalomyelitis and MDEM as the occurrence of new symptoms in the setting of a history of ADEM.

The hallmark of this new category was the occurrence of two clinicoradiographic episodes of disseminated encephalomyelitis separated by at least three months. The clinical findings were defined as being new or a re-emergence of prior symptoms. If the patient sustained three or more episodes, it was classified as having a chronic inflammatory demyelinating disorder (*5*).

Our patient had an interval of five years between the first and the second clinical episode, the time between them can vary from three months to 33 years as reported by Numa *et al*. (*6*).

The presence of antibodies directed against anti-myelin oligodendrocyte protein (MOG) occurs in monophasic demyelinating disorders, particularly, in younger children and patients with ADEM. However, up to 1/3 of these children with MOG-abs will relapse within 2 years. Recent cohorts have suggested that a significant percentage of patients with recurrent optic neuritis, multiphasic demyelinating encephalomyelitis, ADEM associated with optic neuritis and neuromyelitis optica spectrum disorders have MOG-abs (*7,8*).

A diagnosis of MS can be confirmed by the presence of recurrent clinical demyelinating events and/or MRI evidence for new lesions involving different regions of the CNS. Implementation of the 2010 revised McDonald criteria may allow for diagnosis to be made at the time of the first demyelinating syndrome if imaging demonstrates silent lesions in two of the four regions typical for MS, at least one of which enhances with gadolinium. When criteria are not met at the time of the first event, new clinical attacks and/or serial imaging demonstrating accrual of lesions are needed to confirm the diagnosis of MS (*9*).

The purpose of the presentation of this case was to highlight the similarities between these two entities, since the clinical picture and neuroimaging are difficult to distinguish, mainly in relation to the first episode. Considering that 25% of cases with ADEM evolve to MS, evolutionary studies of neuroimaging are recommended.

Acknowledgements

In memory of Dr. Arla Cinderella Stokes Brackett, first author of this work, who left us early, for sharing her kindness and work with patients and with us during the three years of her residence, THANK YOU.

References

1. Waldman A, Ghezzi A, Bar-Or A, Mikaeloff Y, Tardieu M, Banwell B. Multiple sclerosis in children: an update on clinical diagnosis, therapeutic strategies, and research. Lancet Neurol. 2014; 13:936-348.
2. Sánchez-Calderón M, de Santos T, Martín S, Angulo T, Careaga J, Campos-Castelló J. Esclerosis múltiple en la infancia: nuestra experiencia y revisión de la literatura. Rev Neurol. 1998; 27:237-241.
3. Tenembaum S, Chitnis T, Ness J, Hahn JS; International Pediatric MS Study Group. Acute disseminated encephalomyelitis. Neurol. 2007; 68:S23-S36.
4. Banwell B, Ghezzi A, Bar-Or A, Mikaeloff Y, Tardieu

M. Multiple sclerosis in children: clinical diagnosis, therapeutic strategies, and future directions. Lancet Neurol. 2007; 6:887-902.
5. Krupp LB, Tardieu M, Amato MP, Banwell B, Chitnis T, Dale RC, Ghezzi A, Hintzen R, Kornberg A, Pohl D, Rostasy K, Tenembaum S, Wassmer E; International Pediatric Multiple Sclerosis Study Group. International Pediatric Multiple Sclerosis Study Group criteria for pediatric multiple sclerosis and immune-mediated central nervous system demyelinating disorders: revisions to the 2007 definitions. Mult Scler. 2013; 19:1261-1267.
6. Numa S, Kasai T, Kondo T, Kushimura Y, Kimura A, Takahashi H, Morita K, Tanaka A, Noto Y, Ohara T, Nakagawa M, Mizuno T. An adult case of anti-myelin oligodendrocyte glycoprotein (MOG) antibody-associated multiphasic acute disseminated encephalomyelitis at 33-year intervals. Intern Med. 2016; 55:699-702.
7. Hacohen Y, Banwell B. Treatment approaches for MOG-Ab-associated demyelination in children. Curr Treat Options Neurol. 2019; 21:2.
8. Hacohen Y, Mankad K, Chong WK, Barkhof F, Vincent A, Lim M, Wassmer E, Ciccarelli O, Hemingway C. Diagnostic algorithm for relapsing acquired demyelinating syndromes in children. Neurology. 2017; 89:269-278.
9. Yeshokumar AK, Narula S, Banwell B. Pediatric multiple sclerosis. Curr Opin Neurol. 2017; 30:216-221.

Received January 28, 2020; Revised February 22, 2020; Accepted February 26, 2020.

**Address correspondence to:*
Otto Jesus Hernández-Fustes, Neurology Department, InNeuro, Av. Marechal Floriano Peixoto 170, sl. 1509, Centro, Curitiba 80020-090, Brasil.
E-mail: otto.fustes@hc.ufpr.br

IRDR
Intractable & Rare Diseases Research

Guide for Authors

1. Scope of Articles

Intractable & Rare Diseases Research is an international peer-reviewed journal. Intractable & Rare Diseases Research devotes to publishing the latest and most significant research in intractable and rare diseases. Articles cover all aspects of intractable and rare diseases research such as molecular biology, genetics, clinical diagnosis, prevention and treatment, epidemiology, health economics, health management, medical care system, and social science in order to encourage cooperation and exchange among scientists and clinical researchers.

2. Submission Types

Original Articles should be well-documented, novel, and significant to the field as a whole. An Original Article should be arranged into the following sections: Title page, Abstract, Introduction, Materials and Methods, Results, Discussion, Acknowledgments, and References. Original articles should not exceed 5,000 words in length (excluding references) and should be limited to a maximum of 50 references. Articles may contain a maximum of 10 figures and/or tables.

Brief Reports definitively documenting either experimental results or informative clinical observations will be considered for publication in this category. Brief Reports are not intended for publication of incomplete or preliminary findings. Brief Reports should not exceed 3,000 words in length (excluding references) and should be limited to a maximum of 4 figures and/or tables and 30 references. A Brief Report contains the same sections as an Original Article, but the Results and Discussion sections should be combined.

Reviews should present a full and up-to-date account of recent developments within an area of research. Normally, reviews should not exceed 8,000 words in length (excluding references) and should be limited to a maximum of 100 references. Mini reviews are also accepted.

Policy Forum articles discuss research and policy issues in areas related to life science such as public health, the medical care system, and social science and may address governmental issues at district, national, and international levels of discourse. Policy Forum articles should not exceed 2,000 words in length (excluding references).

Case Reports should be detailed reports of the symptoms, signs, diagnosis, treatment, and follow-up of an individual patient. Case reports may contain a demographic profile of the patient but usually describe an unusual or novel occurrence. Unreported or unusual side effects or adverse interactions involving medications will also be considered. Case Reports should not exceed 3,000 words in length (excluding references).

News articles should report the latest events in health sciences and medical research from around the world. News should not exceed 500 words in length.

Letters should present considered opinions in response to articles published in Intractable & Rare Diseases Research in the last 6 months or issues of general interest. Letters should not exceed 800 words in length and may contain a maximum of 10 references.

3. Editorial Policies

Ethics: Intractable & Rare Diseases Research requires that authors of reports of investigations in humans or animals indicate that those studies were formally approved by a relevant ethics committee or review board.

Conflict of Interest: All authors are required to disclose any actual or potential conflict of interest including financial interests or relationships with other people or organizations that might raise questions of bias in the work reported. If no conflict of interest exists for each author, please state "There is no conflict of interest to disclose".

Submission Declaration: When a manuscript is considered for submission to Intractable & Rare Diseases Research, the authors should confirm that 1) no part of this manuscript is currently under consideration for publication elsewhere; 2) this manuscript does not contain the same information in whole or in part as manuscripts that have been published, accepted, or are under review elsewhere, except in the form of an abstract, a letter to the editor, or part of a published lecture or academic thesis; 3) authorization for publication has been obtained from the authors' employer or institution; and 4) all contributing authors have agreed to submit this manuscript.

Cover Letter: The manuscript must be accompanied by a cover letter signed by the corresponding author on behalf of all authors. The letter should indicate the basic findings of the work and their significance. The letter should also include a statement affirming that all authors concur with the submission and that the material submitted for publication has not been published previously or is not under consideration for publication elsewhere. The cover letter should be submitted in PDF format. For example of Cover Letter, please visit http://www.irdrjournal.com/downcentre.php (Download Centre).

Copyright: A signed JOURNAL PUBLISHING AGREEMENT (JPA) form must be provided by post, fax, or as a scanned file before acceptance of the article. Only forms with a hand-written signature are accepted. This copyright will ensure the widest possible dissemination of information. A form facilitating transfer of copyright can be downloaded by clicking the appropriate link and can be returned to the e-mail address or fax number noted on the form (Please visit Download Centre). Please note that your manuscript will not proceed to the next step in publication until the JPA Form is received. In addition, if excerpts from other copyrighted works are included, the author(s) must obtain written permission from the copyright owners and credit the source(s) in the article.

Suggested Reviewers: A list of up to 3 reviewers who are qualified to assess the scientific merit of the study is welcomed. Reviewer information including names, affiliations, addresses, and e-mail should be provided at the same time the manuscript is submitted online. Please do not suggest reviewers with known conflicts of interest, including participants or anyone with a stake in the proposed research; anyone from the same institution; former students, advisors, or research collaborators (within the last three years); or close personal contacts. Please note that the Editor-in-Chief may accept one or more of the proposed reviewers or may request a review by other qualified persons.

Language Editing: Manuscripts prepared by authors whose native language is not English should have their work proofread by a native English speaker before submission. If not, this might delay the publication of your manuscript in Intractable & Rare Diseases Research.

The Editing Support Organization can provide English proofreading, Japanese-English translation, and Chinese-English translation services to authors who want to publish in Intractable & Rare Diseases Research and need assistance before submitting a manuscript. Authors can visit this organization directly at http://www.iacmhr.com/iac-eso/support.php?lang=en. IAC-ESO was established to facilitate manuscript preparation by researchers whose native language is not English and to help edit works intended for international academic journals.

4. Manuscript Preparation

Manuscripts should be written in clear, grammatically correct English and submitted as a Microsoft Word file in a single-column format. Manuscripts must be paginated and typed in 12-point Times New Roman font with 24-point line spacing. Please do not embed figures in the text. Abbreviations should be used as little as possible and should be explained at first mention unless the term is a well-known abbreviation (*e.g.* DNA). Single words should not be abbreviated.

Title page: The title page must include 1) the title of the paper (Please note the title should be short, informative, and contain the major key words); 2) full name(s) and affiliation(s) of the author(s), 3) abbreviated names of the author(s), 4) full name, mailing address, telephone/fax numbers, and e-mail address of the corresponding author; and 5) conflicts of interest (if you have an actual or potential conflict of interest to disclose, it must be included as a footnote on the title page of the

manuscript; if no conflict of interest exists for each author, please state "There is no conflict of interest to disclose"). Please visit Download Centre and refer to the title page of the manuscript sample.

Abstract: The abstract should briefly state the purpose of the study, methods, main findings, and conclusions. For article types including Original Article, Brief Report, Review, Policy Forum, and Case Report, a one-paragraph abstract consisting of no more than 250 words must be included in the manuscript. For News and Letters, a brief summary of main content in 150 words or fewer should be included in the manuscript. Abbreviations must be kept to a minimum and non-standard abbreviations explained in brackets at first mention. References should be avoided in the abstract. Key words or phrases that do not occur in the title should be included in the Abstract page.

Introduction: The introduction should be a concise statement of the basis for the study and its scientific context.

Materials and Methods: The description should be brief but with sufficient detail to enable others to reproduce the experiments. Procedures that have been published previously should not be described in detail but appropriate references should simply be cited. Only new and significant modifications of previously published procedures require complete description. Names of products and manufacturers with their locations (city and state/country) should be given and sources of animals and cell lines should always be indicated. All clinical investigations must have been conducted in accordance with Declaration of Helsinki principles. All human and animal studies must have been approved by the appropriate institutional review board(s) and a specific declaration of approval must be made within this section.

Results: The description of the experimental results should be succinct but in sufficient detail to allow the experiments to be analyzed and interpreted by an independent reader. If necessary, subheadings may be used for an orderly presentation. All figures and tables must be referred to in the text.

Discussion: The data should be interpreted concisely without repeating material already presented in the Results section. Speculation is permissible, but it must be well-founded, and discussion of the wider implications of the findings is encouraged. Conclusions derived from the study should be included in this section.

Acknowledgments: All funding sources should be credited in the Acknowledgments section. In addition, people who contributed to the work but who do not meet the criteria for authors should be listed along with their contributions.

References: References should be numbered in the order in which they appear in the text. Citing of unpublished results, personal communications, conference abstracts, and theses in the reference list is not recommended but these sources may be mentioned in the text. In the reference list, cite the names of all authors when there are fifteen or fewer authors; if there are sixteen or more authors, list the first three followed by *et al*. Names of journals should be abbreviated in the style used in PubMed. Authors are responsible for the accuracy of the references. Examples are given below:

Example 1 (Sample journal reference):
Inagaki Y, Tang W, Zhang L, Du GH, Xu WF, Kokudo N. Novel aminopeptidase N (APN/CD13) inhibitor 24F can suppress invasion of hepatocellular carcinoma cells as well as angiogenesis. Biosci Trends. 2010; 4:56-60.

Example 2 (Sample journal reference with more than 15 authors):
Darby S, Hill D, Auvinen A, *et al*. Radon in homes and risk of lung cancer: Collaborative analysis of individual data from 13 European case-control studies. BMJ. 2005; 330:223.

Example 3 (Sample book reference):
Shalev AY. Post-traumatic stress disorder: Diagnosis, history and life course. In: Post-traumatic Stress Disorder, Diagnosis, Management and Treatment (Nutt DJ, Davidson JR, Zohar J, eds.). Martin Dunitz, London, UK, 2000; pp. 1-15.

Example 4 (Sample web page reference):
World Health Organization. The World Health Report 2008 – primary health care: Now more than ever. *http://www.who.int/whr/2008/whr08_en.pdf* (accessed September 23, 2010).

Tables: All tables should be prepared in Microsoft Word or Excel and should be arranged at the end of the manuscript after the References section. Please note that tables should not in image format. All tables should have a concise title and should be numbered consecutively with Arabic numerals. If necessary, additional information should be given below the table.

Figure Legend: The figure legend should be typed on a separate page of the main manuscript and should include a short title and explanation. The legend should be concise but comprehensive and should be understood without referring to the text. Symbols used in figures must be explained.

Figure Preparation: All figures should be clear and cited in numerical order in the text. Figures must fit a one- or two-column format on the journal page: 8.3 cm (3.3 in.) wide for a single column, 17.3 cm (6.8 in.) wide for a double column; maximum height: 24.0 cm (9.5 in.). Please make sure that artwork files are in an acceptable format (TIFF or JPEG) at minimum resolution (600 dpi for illustrations, graphs, and annotated artwork, and 300 dpi for micrographs and photographs). Please provide all figures as separate files. Please note that low-resolution images are one of the leading causes of article resubmission and schedule delays. All color figures will be reproduced in full color in the online edition of the journal at no cost to authors.

Units and Symbols: Units and symbols conforming to the International System of Units (SI) should be used for physicochemical quantities. Solidus notation (*e.g.* mg/kg, mg/mL, mol/mm^2/min) should be used. Please refer to the SI Guide www.bipm.org/en/si/ for standard units.

Supplemental data: Supplemental data might be useful for supporting and enhancing your scientific research and Intractable & Rare Diseases Research accepts the submission of these materials which will be only published online alongside the electronic version of your article. Supplemental files (figures, tables, and other text materials) should be prepared according to the above guidelines, numbered in Arabic numerals (*e.g.*, Figure S1, Figure S2, and Table S1, Table S2) and referred to in the text. All figures and tables should have titles and legends. All figure legends, tables and supplemental text materials should be placed at the end of the paper. Please note all of these supplemental data should be provided at the time of initial submission and note that the editors reserve the right to limit the size and length of Supplemental Data.

5. Submission Checklist

The Submission Checklist will be useful during the final checking of a manuscript prior to sending it to Intractable & Rare Diseases Research for review. Please visit Download Centre and download the Submission Checklist file.

6. Online submission

Manuscripts should be submitted to Intractable & Rare Diseases Research online at http://www.irdrjournal.com. The manuscript file should be smaller than 5 MB in size. If for any reason you are unable to submit a file online, please contact the Editorial Office by e-mail at office@irdrjournal.com

7. Accepted manuscripts

Proofs: Galley proofs in PDF format will be sent to the corresponding author *via* e-mail. Corrections must be returned to the editor (office@irdrjournal.com) within 3 working days.

Offprints: Authors will be provided with electronic offprints of their article. Paper offprints can be ordered at prices quoted on the order form that accompanies the proofs.

Page Charge: No page charges will be levied to authord for the publication of their article except for reprints.

(As of February 2013)

Editorial and Head Office:

Pearl City Koishikawa 603
2-4-5 Kasuga, Bunkyo-ku
Tokyo 112-0003, Japan
Tel: +81-3-5840-9968
Fax: +81-3-5840-9969
E-mail: office@irdrjournal.com